NATIONAL CENTER FOR EARTHQUAKE ENGINEERING RESEARCH

ISSN 1088-3800

Seismic Resistance of Bridge Piers Based on Damage Avoidance Design

by

J.B. Mander and C-T. Cheng

Technical Report NCEER-97-0014

December 10, 1997

This research was conducted at the University at Buffalo, State University of New York and was supported by the Federal Highway Administration under contract number DTFH61-92-C-00112.

NOTICE

This report was prepared by the University at Buffalo, State University of New York as a result of research sponsored by the National Center for Earthquake Engineering Research (NCEER) through a contract from the Federal Highway Administration. Neither NCEER, associates of NCEER, its sponsors, the University at Buffalo, State University of New York nor any person acting on their behalf:

a. makes any warranty, express or implied, with respect to the use of any information, apparatus, method, or process disclosed in this report or that such use may not infringe upon privately owned rights; or

b. assumes any liabilities of whatsoever kind with respect to the use of, or the damage resulting from the use of, any information, apparatus, method, or process disclosed in this report.

Any opinions, findings, and conclusions or recommendations expressed in this publication are those of the author(s) and do not necessarily reflect the views of NCEER or the Federal Highway Administration.

NATIONAL CENTER FOR EARTHQUAKE ENGINEERING RESEARCH
Headquartered at the State University of New York at Buffalo

Seismic Resistance of Bridge Piers Based on Damage Avoidance Design

by

John B. Mander and Chin-Tung Cheng

Publication Date: December 10, 1997
Submittal Date: February 7, 1997

Technical Report NCEER-97-0014

NCEER Task Number 112-D-5.1 and 5.2

FHWA Contract Number DTFH61-92-C-00112

1 Associate Professor, Department of Civil, Structural and Environmental Engineering, State University of New York at Buffalo
2 Research Assistant, Department of Civil, Structural and Environmental Engineering, State University of New York at Buffalo

NATIONAL CENTER FOR EARTHQUAKE ENGINEERING RESEARCH
State University of New York at Buffalo
Red Jacket Quadrangle, Buffalo, NY 14261

PREFACE

The National Center for Earthquake Engineering Research (NCEER) was established in 1986 to develop and disseminate new knowledge about earthquakes, earthquake-resistant design and seismic hazard mitigation procedures to minimize loss of life and property. The emphasis of the Center is on eastern and central United States *structures*, and *lifelines* throughout the country that may be exposed to any level of earthquake hazard.

NCEER's research is conducted under one of four Projects: the Building Project, the Nonstructural Components Project, and the Lifelines Project, all three of which are principally supported by the National Science Foundation, and the Highway Project which is primarily sponsored by the Federal Highway Administration.

The research and implementation plan in years six through ten (1991-1996) for the Building, Nonstructural Components, and Lifelines Projects comprises four interdependent elements, as shown in the figure below. Element I, Basic Research, is carried out to support projects in the Applied Research area. Element II, Applied Research, is the major focus of work for years six through ten for these three projects. Demonstration Projects under Element III have been planned to support the Applied Research projects and include individual case studies and regional studies. Element IV, Implementation, will result from activity in the Applied Research projects, and from Demonstration Projects.

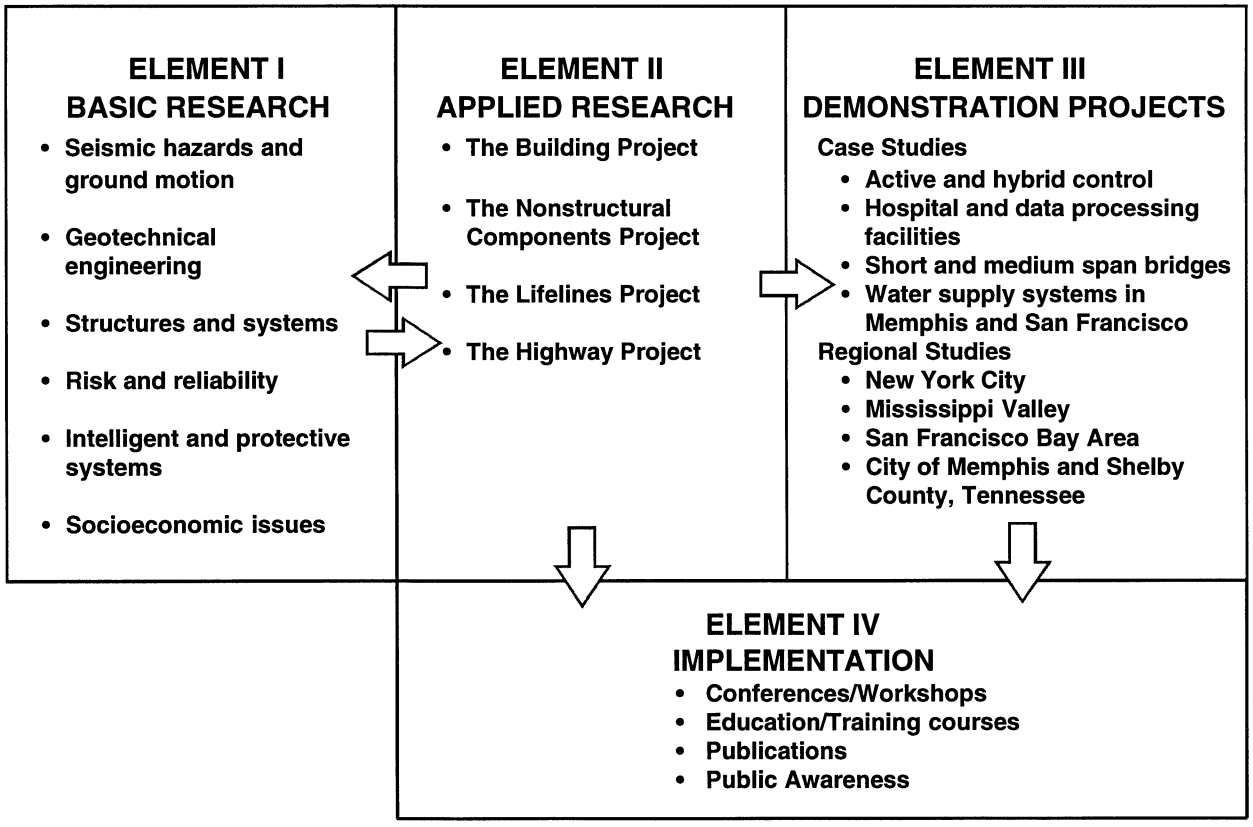

Research under the **Highway Project** develops retrofit and evaluation methodologies for existing bridges and other highway structures (including tunnels, retaining structures, slopes, culverts, and pavements), and develops improved seismic design criteria and procedures for bridges and other highway structures. Specifically, tasks are being conducted to: (1) assess the vulnerability of highway systems and structures; (2) develop concepts for retrofitting vulnerable highway structures and components; (3) develop improved design and analysis methodologies for bridges, tunnels, and retaining structures, with particular emphasis on soil-structure interaction mechanisms and their influence on structural response; and (4) review and improve seismic design and performance criteria for new highway systems and structures.

Highway Project research focuses on one of two distinct areas: the development of improved design criteria and philosophies for new or future highway construction, and the development of improved analysis and retrofitting methodologies for existing highway systems and structures. The research discussed in this report is a result of work conducted under the new highway construction project, and was performed within Tasks 112-D-5.1, "Capacity Detailing of Columns, Walls and Piers for Ductility and Shear" and 112-D-5.2, "Capacity Detailing of Members to Ensure Elastic Behavior" of the project as shown in the flowchart.

The research reported herein had two primary objectives. The first objective was to develop improved seismic detailing requirements for the design of bridge columns, walls and piers. It entailed analytical modeling of cyclic energy absorption capacity and validation by experimental testing of various concepts and parameters. The second objective was to develop seismic design and capacity detailing recommendations for portions of bridge substructures that do not participate as primary energy dissipation elements.

This report presents a new design paradigm called Damage Avoidance Design (DAD) for bridge piers. Recommendations are provided for construction of bridge piers based on modular (precast) beam and column elements that are free to rock under large lateral loads. Damage is avoided by using special detailing at the connections. The DAD approach is compatible with other similar approaches used for seismic evaluation and design of isolated bridge structures and the emerging displacement-based design philosophy.

SEISMIC VULNERABILITY OF NEW HIGHWAY CONSTRUCTION
FHWA Contract DTFH61-92-C-00112

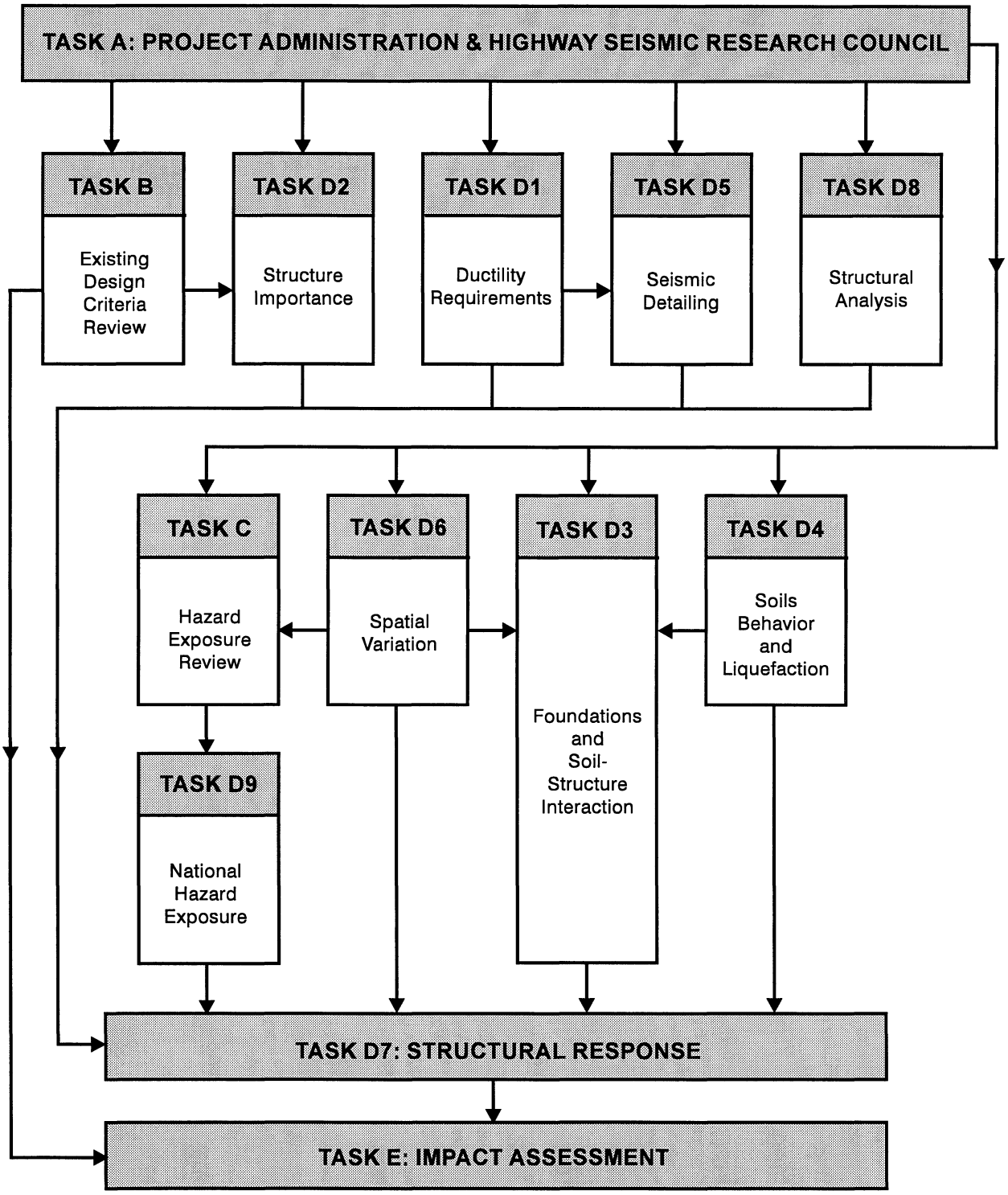

ABSTRACT

Current seismic resistant design practice is based on economic (limited strength) and life safety (large displacement capacity) considerations. The seismic design philosophy that seeks to achieve these objectives is based on ductile detailing of plastic hinge regions. Unfortunately, the hysteretic energy that is dissipated in hinge zones causes damage that is generally not possible to repair. After a large earthquake, even though life-safety may have been maintained, extensive damage may have leave the structure unserviceable. The research reported as part of this investigation is concerned with developing a new paradigm called *Damage Avoidance Design (DAD)*. Construction of bridges piers is based on modular (precast) beam and column elements that are free to rock under large lateral loads. Damage is avoided by special detailing of the connections. If desired, the lateral strength can be enhanced by using supplementary unbonded prestressing tendons. Due to the use of specially detailed steel-steel interfaces, the columns are expected to behave in a bilinear fashion with neither damage nor degradation in strength and stiffness.

A generalized displacement-based seismic design methodology is proposed for bridge structures with rocking piers. Damping is assessed based on the energy radiated (lost) on each impact. For a given pushover curve and effective viscous damping, the expected seismic displacement may be predicted by comparing it to the elastic design spectra (demand). To validate the proposed design philosophy, the seismic performance of a near full-size precast concrete rocking column substructure was investigated. Under large lateral (rocking) displacements, no damage to either the concrete column, connection or foundation was observed. The strength and stiffness was observed to remain the same after many cycles of loading. A complete force-deformation model for the rocking column accounting for: structural flexibility (pre-rocking), rigid body kinematics (post-rocking) and the prestressing action of the tendons is proposed. Good agreement between the predictive theory and the experimentally observed force-deformation results was demonstrated.

ACKNOWLEDGEMENTS

This research was carried out in the Department of Civil Engineering at the State University of New York at Buffalo.

Financial support is gratefully acknowledged from the National Center for Engineering Earthquake Research through contract with the Federal Highway Administration on Seismic Vulnerability of New Highway Construction (FHWA Contract DTFH61-92-00112).

Testing of the column specimens was undertaken with the assistance of technicians Messrs Cizdziel, Pattarroyo, Pitman and Walch of the Department of Civil Engineering Seismic Research Laboratory is gratefully acknowledged.

The authors would also like to recognize the contributions from Dr. Joel From, Post Doctoral Research Associate, and Sandy Sheard, Research Assistant, for constructing the full size test specimen. Without their help this part of the project would not have been possible.

TABLE OF CONTENTS

TABLE OF CONTENTS (cont.)

LIST OF ILLUSTRATIONS

LIST OF ILLUSTRATIONS (cont.)

LIST OF TABLES

SECTION 1
INTRODUCTION

1.1 Research Motivation

Bridge structures are important entities of the civil infrastructure system. In the event of an earthquake, highway systems serve as lifelines that are required to link important facilities such as hospitals, schools, fire stations and civil defense centers, etc. It is important that the integrity of the highway system be protected. Even after a very strong earthquake, it is desirable that the highway system continue to function without disruption. However, current state-of-the-practice does not meet this demanding standard of post-earthquake serviceability, but rather only attempts to maintain life-safety.

For bridge structures, the most common form of seismic resistant construction is based on *Ductile Design*. Reinforced concrete bridge piers are designed for ductility, whereby in an earthquake the seismic energy is dissipated in plastic hinge zones that occur at the ends of the bridge columns. The intention of this design approach is to enforce a ductile mechanism to form without permitting the structure to collapse. However, damage to the hinge zones and the resulting permanent lateral displacements that follow a large earthquake may be so severe that it is necessary to either rebuild or replace that part of the bridge substructure. Oftentimes the bridge itself needs to be rebuilt. Therefore, irreparable damage to structures is inevitable under this design philosophy in a strong earthquake.

An alternative form of seismic resistant design to the more traditional ductile design philosophy is *Seismic Isolation*. This design approach has been used increasingly over the last two decades. The reason for its appeal is that an isolated structure can survive an earthquake without incurring damage to the main structural components. Energy is generally dissipated through mechanical dissipating devices such as lead cores within lead-rubber bearings, via friction in sliding bearings, or with special supplemental mechanical energy dissipating devices

such as steel, viscous or viscoelastic dampers. Perhaps the major disincentive for using this design philosophy is that large horizontal displacements need to be accommodated in the bearing system. It is conceivable that under a maximum credible earthquake, particularly with near-field (fling) effects, the provided design displacement can be exceeded. The bearings can thus fail, resulting in unseating of the deck. Therefore, even seismically isolated structures may be damaged in a maximum strong earthquake.

1.2 Research Needs

From the foregoing discussion, together with the large body of anecdotal evidence that has arisen from recent earthquakes such as Loma Prieta (1989), Northridge (1994) and Kobe (1995), it is evident that there is a need to design more robust bridge structures that avoid damage in order to maintain post-earthquake serviceability. It therefore follows that there is a need for new design philosophies that have the attributes of the present ductile design (that is limited displacement plus energy dissipation) and isolation design (that is the absence of damage under service-like excitation). In other words, new types of bridge pier designs and forms of construction are needed that can avoid damage entirely.

1.3 Research Objectives

The principal objective of this research is to explore new seismic design paradigms and new construction methodologies that permit large displacements while avoiding seismically-induced damage. To achieve this objective, a new design methodology called *Damage Avoidance Design* (DAD) is proposed. In the design of ductile bridge piers, the seismic deformations are accommodated by the plastic hinges through the yielding of steel and deterioration of concrete which implies inevitable damage. However, if the longitudinal column steel is made discontinuous at the beam-column interface, column rocking is allowed. Using special detailing, damage may be avoided and large seismic deformations may be accommodated. Energy is dissipated through radiation damping.

In this study the proposed new design concepts are first developed from a theoretical perspective, and then validated through experimentation on near full-sized column tests. Analytical models are also proposed and simplified design theories advanced.

1.4 Literature Review of Previous Related Work

1.4.1 Existing Rocking Structures

It is relatively rare to find structures that have been designed to rock on their foundations. Two state-of-the-practice examples may be found in New Zealand: the South Rangitikei Railway Bridge, and an industrial chimney at the Christchurch Airport (Skinner et al., 1993). Both structures were designed by the same firm of consulting engineers.

The South Rangitikei Rail Bridge is the largest concrete bridge in the southern hemisphere. The bridge is a tall (72 m) structure with twin hollow column piers supporting a single cell box girder. The box girder, which consists of 58 m continuous deck spans, is designed to carry a single narrow-gauge railway track for Coopers E-40 loading. The columns were designed to be hollow as a weight saving measure; an important consideration in seismic design. Torsional beam mechanical energy dissipating devices are installed at the foot of each column as the bridge piers step from one column leg to the other (Cormack, 1988). Subsequent research by Priestley et al. (1978) showed that such devices may not be needed as the rocking piers dissipate considerable energy when each leg slams onto the foundation. Nevertheless, the mechanical energy dissipators are intended to restrain uplift as well as attenuate the number of rocking cycles.

The Industrial Chimney at the Christchurch Airport is a slender structure that is really only designed to support its self-weight and lateral (wind and/or seismic) loading. Yielding metal uplift restrainers are installed at the base to inhibit overturning (Skinner et al., 1979).

1.4.2 Seismic Analysis of Rocking Columns

The subject of rocking structures is not new and dates back to the early work of Housner (1963). However, that work and much of the work that followed by the other researchers such as Priestley et al. (1978), Meek (1978), Aslam et al. (1980), MacManus et al. (1983), Yim et al. (1980), Psycharis and Jennings (1983), Shenton and Jones (1990, 1992), Kadakal (1994), Priestley et al. (1996), Iyengar and Roy (1996), and Lin and Yim (1996), investigated the seismic response of rigid block systems. Meek (1978) introduced aspects of structural flexibility coupled with rocking structures, while Aslam et al. (1980) considered the influence of prestress that provided some resistance in anchoring a rigid structure to the ground to increase its rocking resistance.

In their recently published monograph, Priestley et al. (1996) describes the behavior and design of rocking bridge piers. However, they do not integrate the three interacting aspects of rocking, structural flexibility and prestressing into their design formulations.

1.4.3 Seismic Detailing of Precast/Prestressed Unbonded Post-tensioned (Rocking) Connections

An innovative rocking beam-to-column connection was proposed by Priestley and Tao (1993) and tested by Priestley and MacRae (1996). The beams were designed to rock at the column interface during seismic loading. The precast beam-column joint connection consisted of post-tensioned partially unbonded tendons to reduce the shear demand on the joint area and special spiral confinement at the beam plastic hinge regions to provide higher compressive concrete strength for rocking toe (beam corner). Test results showed that the connection absorbed less energy than regular ductile connection due to rocking. However, the specimens performed well at large lateral displacements and suffered much less damage than a regular ductile design. Nevertheless, extensive cracking was observed in the joint region together with concrete cover spalling at the beam ends. Although it was evident that performance was superior to conventional ductile design, damage still occurred. Moreover, the expected bilinear

performance was not obtained. From this research, it is evident that improvements are needed in detailing of the rocking toe region. Better detailing is required to mitigate the high contact point forces in order to avoid damage.

1.5 What Then is Particularly New in this Study?

As mentioned previously, this research explores the use of a new structural design and construction philosophy——*Damage Avoidance Design (DAD)*. This proposed design methodology permits large displacements while avoiding seismically-induced damage. The basic design philosophy is to disconnect the longitudinal steel at the cap beam-column interface and allow the columns to rock on both the pile cap and/or pier cap. As the longitudinal reinforcement is discontinuous, low cycle fatigue is prevented and damage to the concrete avoided——the structure can accommodate large seismic displacements through rocking behavior without inducing damage.

A similar idea of rocking behavior in the precast concrete beam-to-column joints for building frames has been proposed by Priestley and Tao (1993) and validated by Priestley and MacRae (1996). However, they were unsuccessful in completely avoiding damage due to some deficient detailing. Improved detailing is adopted herein that ensures that the structure behaves in a bilinear elastic manner without inducing any damage under seismic loads. Under this design approach, neither stiffness degradation nor post-earthquake residual displacements are expected.

1.6 Scope and Organization of Report

Following this introductory section, the concept development of the DAD philosophy is discussed and design methodology proposed in section 2. Next, design examples are given in section 3. Section 4 presents the experimental performance of a near full-sized rocking column. Section 5 presents the results of experimental and theoretical force-displacement modeling. In Section 6 conclusions from this study and recommendations for future research are presented. Finally, references are given in Section 7.

SECTION 2
CONCEPT DEVELOPMENT AND DAMAGE AVOIDANCE DESIGN THEORY

2.1 INTRODUCTION

This section explores a new seismic design paradigm called *Damage Avoidance Design (DAD)*. The principal features of this design scenario are presented schematically in terms of their construction in figure 2-1. The intent of this method of construction is to not only maintain life safety in a strong earthquake, but also to avoid damage with the primary objective of maintaining post-earthquake serviceability. To achieve this objective, large seismically-induced deformations must be accommodated.

This section first describes the concept development and design features of the proposed *DAD* philosophy. This is followed by close scrutiny of some of the apparent concerns regarding this approach to seismic design. The remainder of the section describes the underlying theory and design strategies for bridge systems with rocking piers. Although the subject of rocking structures is not new, dating back to the early work of Housner (1963), much of the work that followed was aimed at investigating the seismic response of *rigid* rocking block systems. Although Meek (1978) introduced aspects of structural flexibility coupled with rocking structures, and Aslam et al. (1980) considered the influence of prestress that provided some resistance in anchoring a rigid structure to the ground to increase its rocking resistance, neither investigator specifically addressed issues pertaining to bridge structures. Only recently did Priestley et al. (1996) describe in their monograph the behavior and design of rocking bridge piers. However, Priestley et al. did not integrate the inter-related aspects of rocking, structural flexibility and prestressing in their design recommendations. This section attempts to address these issues and to present unified analysis and design procedures.

For design purposes, the expected bilinear cyclic force-deformation behavior can be used in simplified monotonic form to assess displacement demands under design ground motions. To

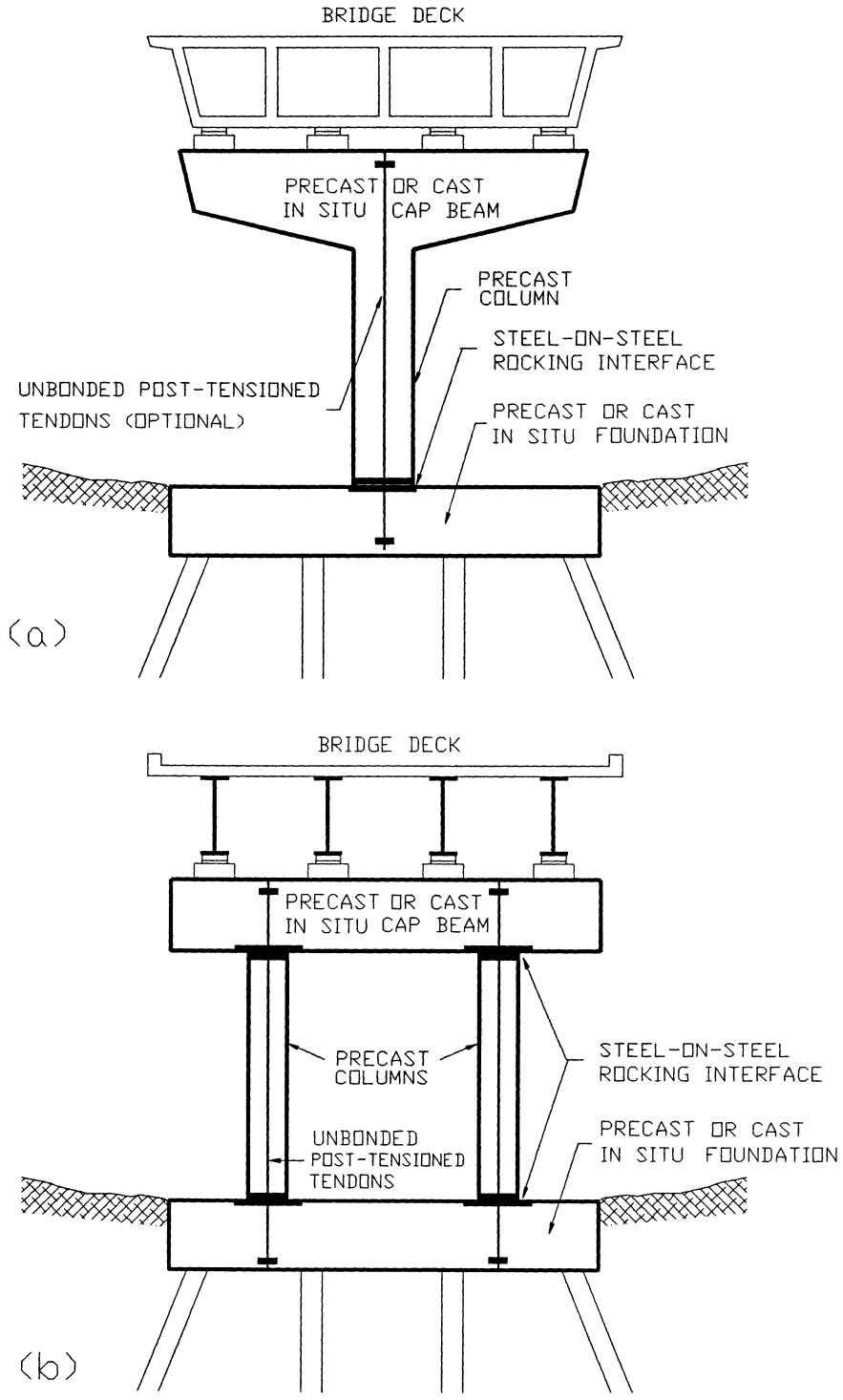

Figure 2-1 Salient construction details of the proposed new approach to seismic design of bridge piers.

achieve this the rocking amplitude and the associated energy radiated (lost) on impact is converted into an equivalent viscous damping factor. By comparing the push-over capacity with the appropriate damped seismic design elastic (demand) spectra, the structure's maximum force and displacement can be determined. This proposed energy-based design approach is compatible with similar approaches used for seismic evaluation and design of isolated bridge structures (Buckle and Friedland, 1995), and the emerging displacement based design philosophy (Kowalsky et al., 1995, and Priestley 1996). Finally, the theory is compared with the classical rigid rocking block theory of Housner (1963).

2.2 Design Features and Concept Development

As shown in figure 2-1, the main features of this design methodology can be summarized as follows:

(i) The longitudinal reinforcement of the columns is terminated at the beam-column interface to enable the columns to rock on cap/foundation beam surfaces without inducing damage.

(ii) Central post-tensioned steel tendons inside the columns may be provided to increase the lateral resistance. If the tendons remain unbonded they can serve as large displacement restraint devices and prevent complete overturning (toppling) in very large earthquakes.

(iii) A steel-steel rocking interface is provided at the foot of the column and foundation/cap beam. This is designed to accommodate the high contact point forces at the rocking toe during uplift of the columns.

(iv) Although not a requirement, the structures can be factory precast to maintain quality and shorten the construction time-frame. This feature is considered to be particularly attractive where construction is seasonal and curtailed during the

wintertime. Constructional economics are likely to outweigh the added cost of special detailing and post-tensioning.

The use of post-tensioned tendons for precast concrete beam-column connections has been investigated previously by several researchers such as Blakeley and Park (1971), Park and Thompson (1977), Nishiyama et al. (1991), Priestley and Tao (1993), Stone et al. (1995), and Priestley and MacRae (1996). Early research by Park and Thompson (1977) found that a central prestressing tendon at mid-depth of the beam passing through the column was effective in enhancing the joint core shear strength. Nishiyama et al. (1991) concluded that a reasonable amount of prestressing force ($0.06f_c'A_g$) ameliorated the performance of beam-column joint assemblages. However, extensive cracks developed at the joint regions and cover concrete spalling was observed at beam corners in these tests. To circumvent the problem, Stone et al. (1995) and Bull et al. (1995) used steel angles to protect beam corners from concrete crushing during cyclic loading. Although test results showed that the cover concrete spalling was prevented, cracks still occurred within the beam-column joint and beam face. To overcome this disadvantage, a new technique with a steel-steel rocking interface is proposed herein so that high contact point forces at the rocking toe can be accommodated and thus no damage will be induced.

Figure 2-2 shows schematically the hysteretic behavior of a two-column bridge pier designed by the proposed DAD concept. The precast columns are expected to rock on the pile cap or foundation beam surface to accommodate large seismically induced deformations. The lateral forces are resisted by the vertical dead load at pier top and the post-tensioned steel inside the columns. Under small earthquakes, the ground excitations may be resisted by the linear elastic strength with no uplift. Under strong earthquakes, the whole system is expected to behave in a bilinear elastic fashion without inducing any damage to either the column or foundation. Because of linear elastic behavior, the columns are self-centering with no residual drift expected after the ground excitation has abated.

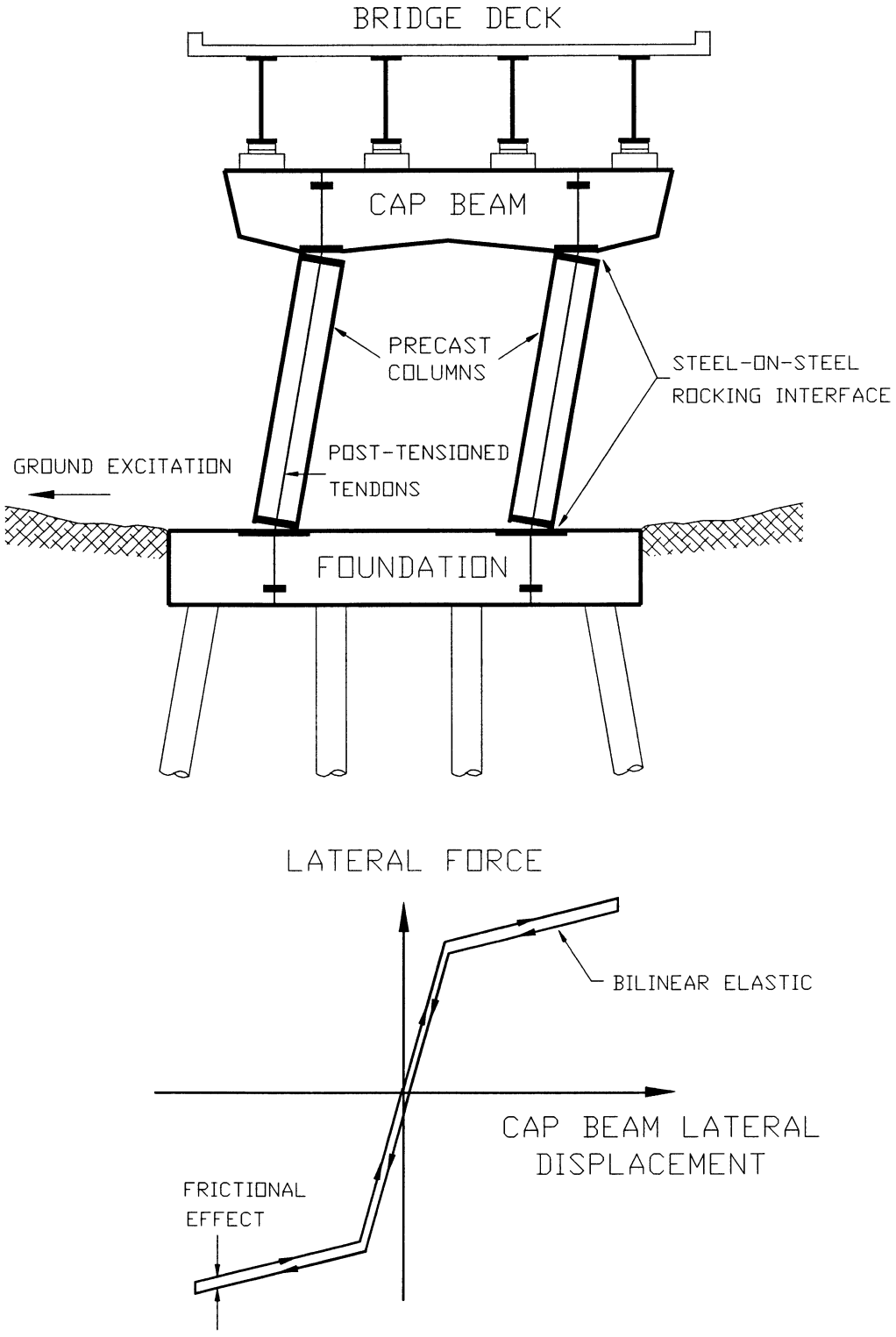

Figure 2-2 Hysteretic behavior and energy dissipation that form the basis of Damage Avoidance Design (DAD) concept.

2.3 DESIGN CONCERNS

Three concerns may be raised for this new design:

The first concern: How is ductility provided by the rocking columns under ground excitation? It should be noted that the conventional notion of ductility is strictly irrelevant with rocking piers —— it is post-uplift displacement capacity which is of concern. With the possibility of vertical vibration during earthquake, the gravity load and the corresponding lateral resistance of columns may be reduced. Additionally, overturning (toppling) of rocking piers must be prevented to ensure life-safety. Therefore, the presence of the post-tensioned steel may be provided to ensure adequate restraint in both the axial and lateral directions. Aslam et al. (1980) studied the earthquake response of a rigid block with a central prestressing rod (prestressed up to 0.4 of block weight) under strong earthquake (Pacoima Dam S16E) excitation. The analysis showed that the block did overturn without the vertical restraint; whereas it did not with the restraint, indicating the efficacy of the vertical restraint.

The second concern: How is energy dissipation accommodated by the rocking piers? Because of the inherent bilinear elastic behavior and due to the absence of damage, no hysteretic energy absorption can be expected. Instead, energy dissipation occurs on impact (radiated damping) as the energy associated with the vertical component of the moment of momentum is lost on each half-cycle (Housner, 1963). Further energy dissipation can be provided, if desired, by use of supplementary mechanical energy dissipation devices and/or yielding tendons. The latter will be theoretically discussed in the following subsection.

The third concern: What is the expected dynamic performance of a bridge with rocking piers under seismic excitations? The rocking response of a rigid block on elastic foundation has been investigated by many authors such as Housner (1963), Aslam et al. (1980), Shenton and Jones (1990, 1992), Kadakal (1994), Iyengar and Roy (1996), and Lin and Yim (1996). It is well known that the rocking response is highly nonlinear without a discrete natural frequency. Rocking response can be very sensitive to small parameter variations and excitation details (Lin

and Yim, 1996). Shenton and Jones (1990, 1992) have shown that taller blocks with a high coefficient of friction are more susceptible to pure rocking motion, and that shorter blocks with a low coefficient of friction are more vulnerable to pure sliding. Kadakal (1994) studied three parameters governing the equation of motion: equivalent circular frequency of the block, its slenderness ratio r_{sl} (defined as the vertical distance divided by horizontal distance between the center of the gravity and the point of rotation) and the coefficient of restitution e for measuring the energy loss during each impact. He found that with the decreasing e, the energy loss increases.

Priestley and Tao (1993) studied the dynamic performance of precast post-tensioned concrete frames with partially unbonded tendons. Beams were expected to rock on column surfaces during seismic loading. Extensive dynamic inelastic analysis showed that displacement of a bilinear elastic system with partially bonded tendons are larger than those of an idealized hysteretic system (fully bonded tendons, representative monolithic reinforced concrete connection), but not by a substantial margin. They also showed that the ground motion chosen had much more influence on displacements than did the type of hysteresis loop.

The dynamic performance of a flexible rocking bridge piers with respect to energy dissipation and radiated damping will be discussed theoretically in the following subsection.

2.4 Lateral Strength Capacity and Behavior of Rocking Bridge Piers

2.4.1 Pier Stiffness

Figure 2-3 shows a two-column bridge pier designed with rocking columns. The columns have a half width b in the mid height region, a semi-base width b_t at the top of columns and b_b at the bottom of columns, over a clear height between rocking interfaces of H_c.

If it is assumed that the columns are tall and slender, then the coefficient of friction should be sufficiently large so that there will be no sliding between the columns and the cap or

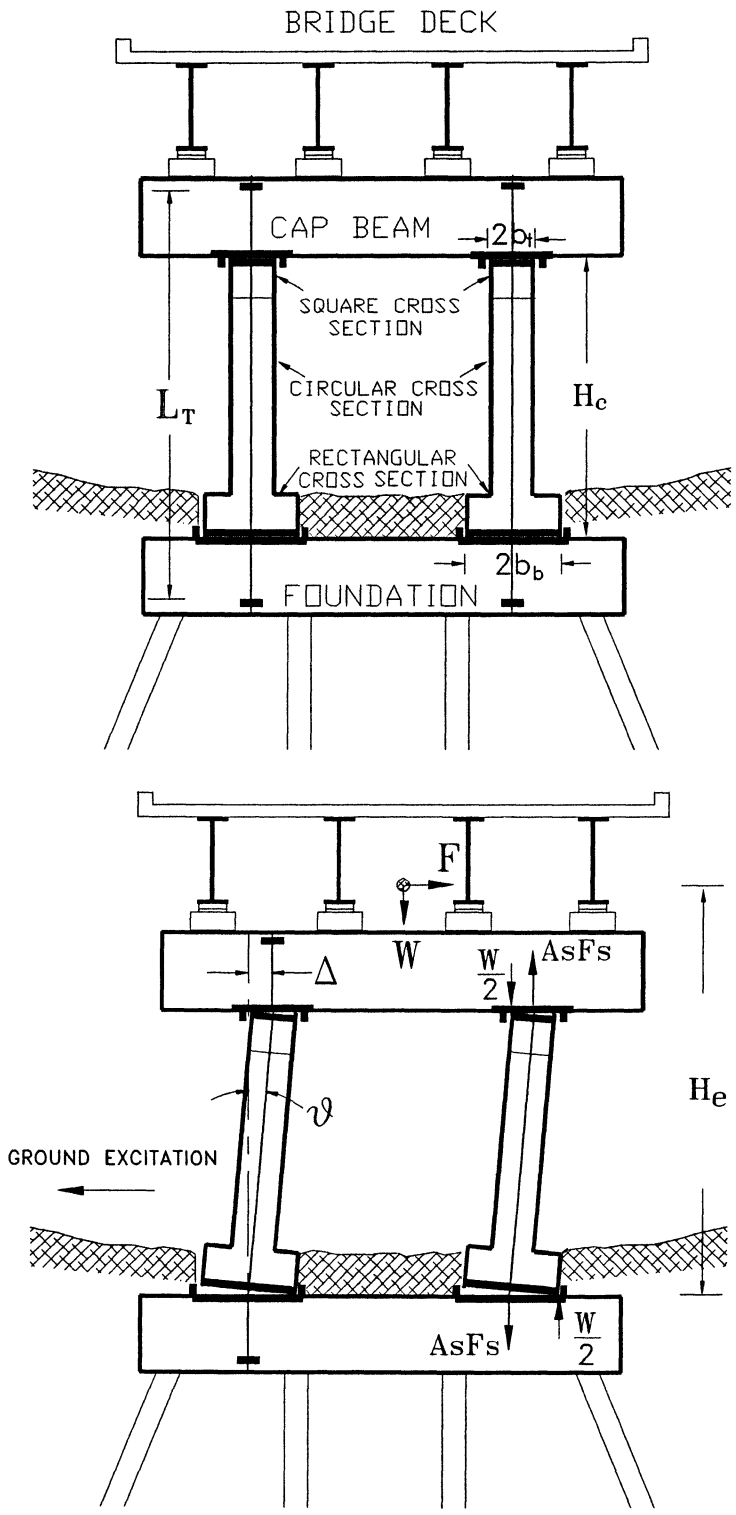

Figure 2-3 Rocking column pier bent.

foundation beams. However, this assumption is only important if no supplementary prestressing is to be used. It is expected that pintles or shear keys could be used in the connection detailing to inhibited sliding. If the rocking columns are reinforced with supplementary prestressing (central tendons), the tensile force in the tendons acts like a spring trying to restrain the rocking motion of the columns. The further the columns rock, the greater the tendons are stressed. For small angle rocking the tendons will remain elastic at all times. If tendons are post-tensioned, the tensile force can be calculated as

$$F_s = A_s f_s = E_s A_s \left[\frac{(b_t\theta + b_b\theta)}{L_T} + \varepsilon_0 \right] \leq A_s f_y \tag{2-1}$$

where E_s = Young's modulus of prestressed tendons, A_s = area of tendons, f_y = yield stress of tendons, L_T = length of unbonded prestressing tendons, θ = column drift angle due to rocking and ε_0 = strain in post-tensioned tendons due to initial prestress (if any). If the angular stiffness of tendons with respect to the rocking toe is assumed

$$K_s = E_s A_s \left(\frac{b_b + b_t}{L_T} \right) \tag{2-2}$$

the tendon force becomes

$$F_s = K_s \left(\theta + \frac{L_T}{b_b + b_t} \varepsilon_0 \right) \tag{2-3}$$

2.4.2 Base Shear Capacity, C_c

The lateral resistance of rocking bridge piers is provided by the combination of gravity load and the prestressing force in the tendons. Under seismic excitations, the rocking columns will behave in a bilinear elastic manner. The first elastic range (pre-rocking) is governed by the structural flexibility of rocking columns. The second elastic range (post-rocking) is governed by rigid body kinematics of the rocking mechanism.

Prior to uplift, the columns possess fixed-fixed ends and deform elastically. Therefore, the pre-rocking base shear capacity of the system can be obtained from the elastic flexural stiffness of each column as

$$K_c = n_c \frac{12 E_c I_{eff}}{H_c^3} \tag{2-4}$$

where n_c = number of the columns, H_c = column height and $E_c I_{eff}$ = effective flexural rigidity of the columns which may be assumed as $0.5 E_c I_g$ for reinforced concrete columns and $0.7 E_c I_g$ for prestressed columns (Priestley et al., 1996). Therefore, the pre-rocking elastic force-deformation relations can be simply expressed as

$$C_c = \frac{F}{W} = \frac{K_c \Delta}{W} \tag{2-5}$$

where F = lateral force of rocking columns needed to push a displacement Δ at the center of the gravity and W = total tributary weight carry by the pier.

After uplift of the columns, the cap beam and superstructure move parallel to the ground without rotation, the rotation of columns can be calculated as

$$\theta = \frac{\Delta}{H_c} \tag{2-6}$$

The lateral force at this stage is resisted by the axial load at the pier top and the tendons inside the columns. The post-rocking base shear capacity can be obtained by considering the free body diagram of the pier as shown in figure 2-3 and equating the overturning and resisting moments at the rocking toe, that is

$$\begin{aligned} C_c = \frac{F}{W} &= \frac{b_t + b_b - \Delta}{H_c} + n_c \frac{K_s}{W} \frac{(b_t + b_b)}{H_c} \left(\frac{\Delta}{H_c} + \frac{L_T}{b_b + b_t} \varepsilon_0 \right) \\ &\leq \frac{b_b + b_t - \Delta}{H_c} + n_c \frac{A_s f_y (b_b + b_t)}{W H_c} \end{aligned} \tag{2-7}$$

The first term on the right hand side represents the resistance provided by the gravity load and

the second term by the supplementary prestressing which will reach an upper limit when the tendons yield. If a ratio of the stiffness of tendons with respect to gravity load is defined as

$$r_s = \frac{n_c K_s L_T}{W(b_b + b_t)} \tag{2-8}$$

By rearranging the terms in equation (2-7)

$$\begin{aligned} C_c &= \frac{b_b + b_t}{H_c}\left[1 + r_s \varepsilon_0 - \left(\frac{H_c}{b_b + b_t} - r_s \frac{(b_b + b_t)}{L_T}\right)\theta\right] \\ &\leq \frac{b_b + b_t}{H_c}\left(1 + r_s \varepsilon_y - \frac{H_c \theta}{b_b + b_t}\right) \end{aligned} \tag{2-9}$$

where $\theta = \Delta / H_c$. If tendons are just slack ($\varepsilon_0 = 0$), then

$$C_c = \frac{b_b + b_t}{H_c}\left[1 - \left(\frac{H_c}{b_b + b_t} - r_s \frac{b_b + b_t}{L_T}\right)\theta\right] \tag{2-10}$$

If the bridge columns are not reinforced with tendons, then lateral resistance is provided by the gravity load only, thus:

$$C_c = \frac{b_b + b_t}{H_c} - \theta \tag{2-11}$$

2.4.3 Dynamic Response

The energy dissipation of a rocking bridge pier primarily comes from the impact between the column and the foundation beam (Housner, 1963). If the impact is assumed to be inelastic (that is no bounce), the reduction of kinetic energy during impact is found by equating the moment of momentum prior to and after impact. Before impact, the deck and cap beam travel in rigid body motion without rotation with a translational velocity which have a downward component as shown in figure 2-4(a). The columns have angular velocity and translational velocity at its rotation centroid.

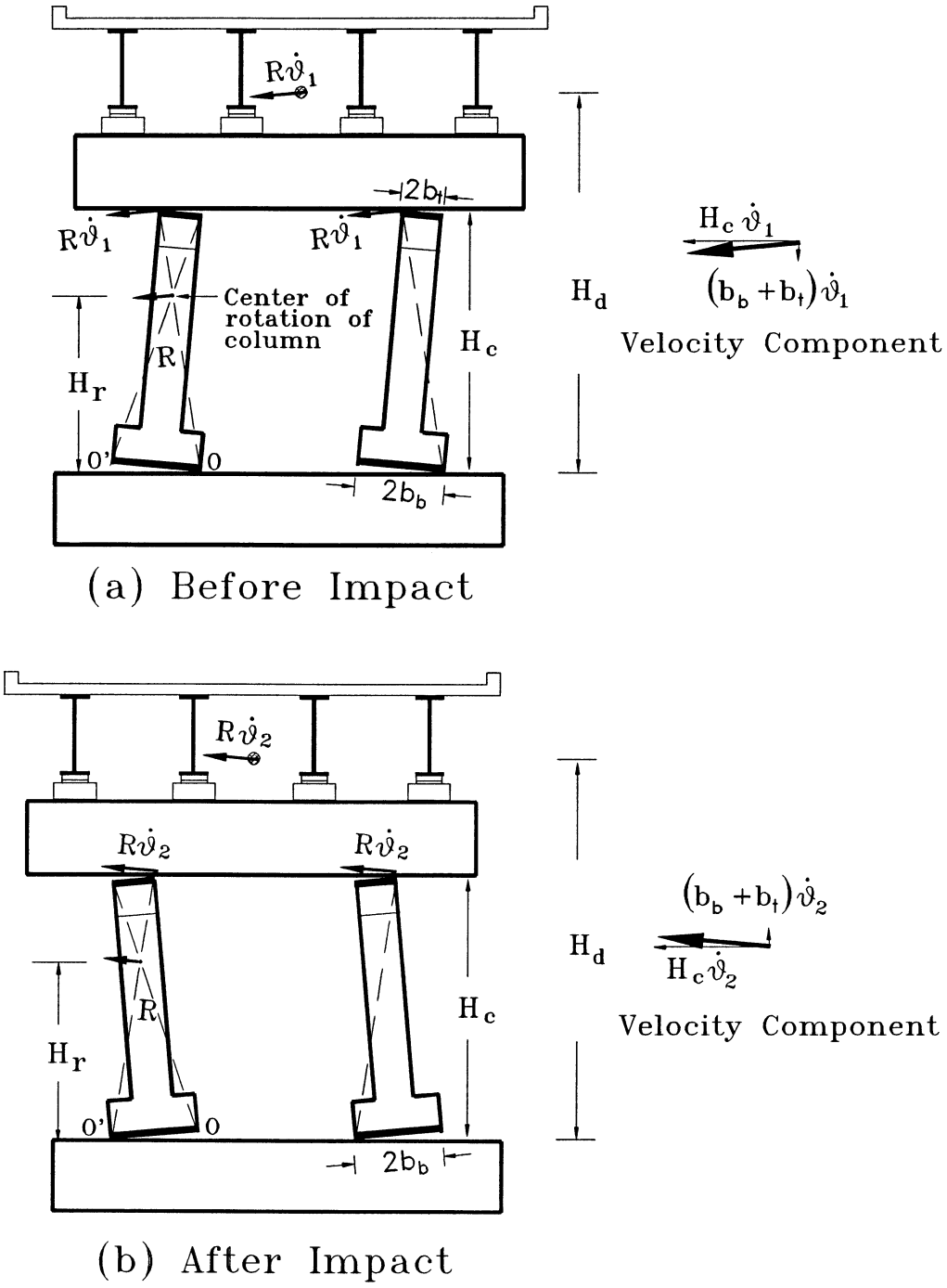

Figure 2-4 Schematic graphs showing velocity of bridge deck and columns prior and after impact.

Before Impact: The moment of momentum of the bridge pier with respect to rocking toe O' can be calculated as

$$IP_{bf} = n_c\left[m_c\left((r_x^2 + r_y^2) + (H_r^2 - b_b^2)\right)\right]\dot{\theta}_1 + m_d\left[H_c^2 - (b_b + b_t)(b_b - b_t)\right]\dot{\theta}_1 \tag{2-12}$$

where m_c and H_r are respectively the mass and the elevation of rotation center for columns, r_x and r_y are the radius of gyration about the centroid in X and Y axes for columns, m_d = the mass of bridge deck including cap beam, n_c = number of columns, and $\dot{\theta}_1$ = angular velocity with respect to rocking toe before impact. If moment of inertia of column and bridge deck is respectively defined as

$$I_c = n_c m_c\left((r_x^2 + r_y^2) + (H_r^2 + b_b^2)\right) \tag{2-13}$$

and

$$I_d = m_d\left(H_c^2 + (b_b + b_t)^2\right) = m_d R^2 \tag{2-14}$$

Thus the total mass moment of inertia of the bridge pier is

$$I_{pier} = I_c + I_d \tag{2-15}$$

and equation (2-12) can be rearranged as

$$\begin{aligned} IP_{bf} &= n_c\left[I_c - 2m_c b_b^2\right]\dot{\theta}_1 + \left[I_d - 2m_d b_b (b_b + b_t)\right]\dot{\theta}_1 \\ &= I_{pier}\left[1 - \frac{2n_c m_c b_b^2 + 2m_d b_b (b_b + b_t)}{I_{pier}}\right]\dot{\theta}_1 \end{aligned} \tag{2-16}$$

After impact: the bridge deck and cap beam travel in rigid body motion without rotation with a translational velocity which has an upward vertical component as shown in figure 2-4(b). Therefore, the moment of momentum with respect to rocking toe O' after impact is given by

$$IP_{af} = n_c\left[m_c\left((r_x^2 + r_y^2) + (H_r^2 + b_b^2)\right)\right]\dot{\theta}_2 + m_d\left[H_c^2 + (b_b + b_t)^2\right]\dot{\theta}_2 \tag{2-17}$$

where $\dot{\theta}_2$ = angular velocity with respect to rocking toe after impact. Rearranging the terms of above equation gives

$$IP_{af} = (n_c I_c + I_d)\dot{\theta}_2 = I_{pier}\dot{\theta}_2 \tag{2-18}$$

By equating the moment of momentum prior to the impact in equation (2-16) and after the impact in equation (2-18), the kinetic energy reduction factor can be defined as

$$r = \frac{\frac{1}{2}I_{pier}\dot{\theta}_1^2}{\frac{1}{2}I_{pier}\dot{\theta}_2^2} = \left(\frac{\dot{\theta}_2}{\dot{\theta}_1}\right)^2 = \left(1 - \frac{2n_c m_c b_b^2 + 2m_d b_b (b_b + b_t)}{I_{pier}}\right)^2 \tag{2-19}$$

2.4.4 Equivalent Damping Ratio, ξ

An energy approach is adopted herein to assess the effective viscous damping factor of a rocking pier system. Using this energy approach, damping can be found from the energy absorbed and dissipated on each half-cycle. Considering <u>one</u> impact per half-cycle, the equivalent viscous damping factor of the pier system is given by

$$\xi = \frac{\delta E}{\pi F \Delta} \tag{2-20}$$

where F = uplift force, Δ = displacement amplitude, and δE = dissipated/radiated energy. Energy dissipation is analyzed as follows:

<u>Tendons that do not yield</u>: If the columns restrained by central post-tensioned tendons tilt a <u>small</u> angle θ, and assuming tendons do not yield during rocking, its potential energy will be restored in the change of the elevation of centroid due to rocking and in the strain energy of tendons which will be the trapezoidal area beneath the stress-strain curve of steel as shown in figure 2-5, that is

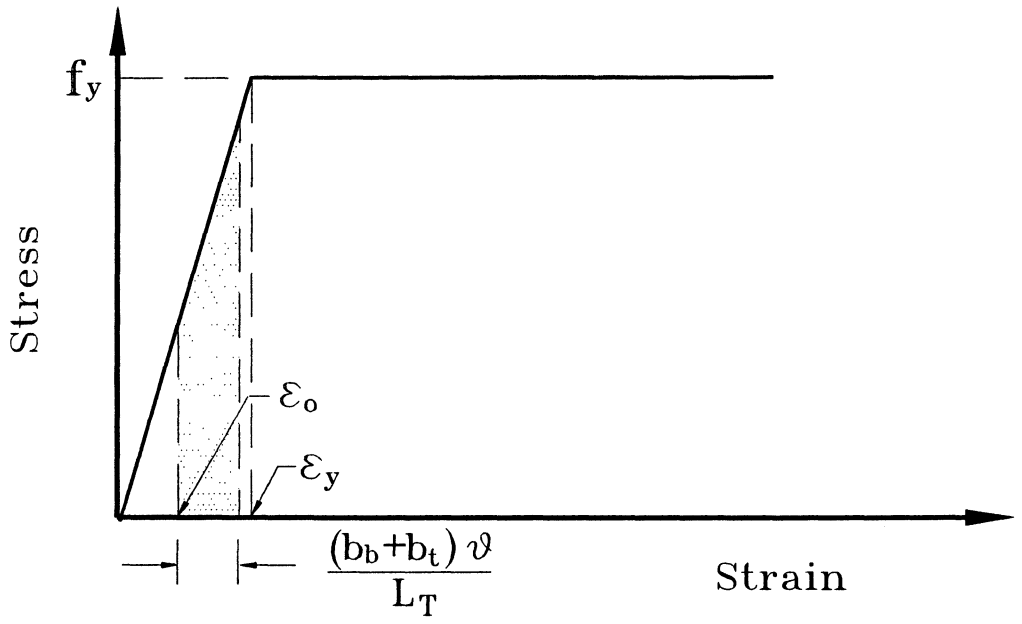

(a) The tendons do not yield

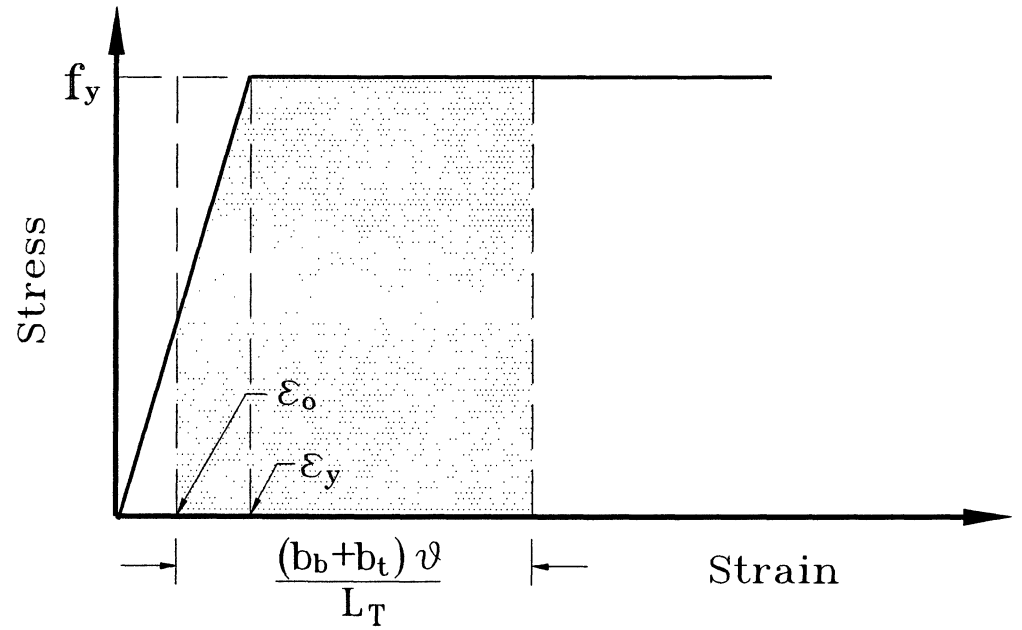

(b) The tendons yield

Figure 2-5 Strain energy stored beneath the stress-strain curve of the tendons.

$$E_p = W(b_b + b_t)\sin\theta + n_c\frac{1}{2}\left[E_s A_s \varepsilon_o + E_s A_s\left(\frac{(b_b + b_t)\theta}{L_T} + \varepsilon_o\right)\right](b_b + b_t)\theta$$

$$\approx W(b_b + b_t)\theta + n_c\left(\frac{1}{2}K_s(b_b + b_t)\theta^2 + K_s L_T \varepsilon_o \theta\right) \qquad \text{(2-21a)}$$

$$= W(b_b + b_t)\theta\left[1 + r_s\left(\frac{(b_b + b_t)\theta}{2L_T} + \varepsilon_o\right)\right]$$

Yielding Tendons: If the tendons yield during rocking, potential energy will be

$$E_p = W(b_b + b_t)\sin\theta + n_c\left[E_s A_s \varepsilon_y (b_b + b_t)\theta - \frac{1}{2}E_s A_s L_T(\varepsilon_y - \varepsilon_o)^2\right]$$

$$\approx W(b_b + b_t)\theta + n_c K_s L_T\left[\varepsilon_y\theta - \frac{1}{2}\frac{L_T}{b_b + b_t}(\varepsilon_y - \varepsilon_o)^2\right] \qquad \text{(2-21b)}$$

$$= W(b_b + b_t)\left[\theta + r_s\left(\varepsilon_y\theta - \frac{L_T}{2(b_b + b_t)}(\varepsilon_y - \varepsilon_o)^2\right)\right]$$

Energy Loss: The energy lost due to impact is

$$\delta E = E_p(1 - r) \qquad \text{(2-22)}$$

Therefore, if the tendons do not yield, substituting equations (2-9) and (2-22) into (2-20) and converting rotation to displacement, radiated damping ratio of the bridge is given by

$$\xi = \frac{(1 - r)}{\pi}\frac{\left[1 + r_s\left(\frac{(b_b + b_t)\theta}{2L_T} + \varepsilon_0\right)\right]}{\left[1 + r_s\varepsilon_0 - \left(\frac{H_c}{b_b + b_t} - r_s\frac{b_b + b_t}{L_T}\right)\theta\right]} \qquad \text{(2-23a)}$$

If the tendons yield, radiated damping is given by

$$\xi = \frac{(1-r)}{\pi}\frac{\left[\theta + r_s\left(\varepsilon_y\theta - \frac{L_T}{2(b_b+b_t)}(\varepsilon_y-\varepsilon_o)^2\right)\right]}{\left(1 + r_s\varepsilon_y - \frac{H_c\theta}{(b_b+b_t)}\right)\theta} \qquad \text{(2-23b)}$$

If the tendons are initially snug (with no initial prestress, $\varepsilon_0 = 0$) and do not yielded during rocking, then above equation can be simplified as

$$\xi = \frac{(1-r)}{\pi}\frac{\left(1 + r_s\frac{(b_b+b_t)\theta}{2L_T}\right)}{\left[1 - \left(\frac{H_c}{b_b+b_t} - r_s\frac{b_b+b_t}{L_T}\right)\theta\right]} \qquad \text{(2-24a)}$$

If the tendons yield, then

$$\xi = \frac{(1-r)}{\pi}\frac{\left[\theta + r_s\varepsilon_y\left(\theta - \frac{L_T}{2(b_b+b_t)}\varepsilon_y\right)\right]}{\left(1 + r_s\varepsilon_y - \frac{H_c\theta}{b_b+b_t}\right)\theta} \qquad \text{(2-24b)}$$

If bridge columns do not possess prestressing tendons, then

$$\xi = \frac{(1-r)}{\pi}\frac{(b_b+b_t)}{(b_b+b_t-H_c\theta)} \qquad \text{(2-25)}$$

2.5 Elastic Spectral Demand

In the publication ATC-33, the Applied Technology Council (ATC, 1995) proposed a modification of the elastic response spectra for high viscously damped systems as shown in figure 2-6. This method was also recommended by Constantinou et al. (1996). In this figure, A is the peak ground acceleration and S represents code recommended soil-type factor. Base shear reduction factors due to high damping are also presented in the figure. By using a regression analysis, the reduction factor for short and long period ranges can be expressed in terms of damping ratio as follows:

Damping Ratio (% Of Critical)	Factor Bs for Short-Period	Factor Bl for Long-Period
< 2	0.8	0.8
5	1.0	1.0
10	1.3	1.2
20	1.8	1.5
30	2.3	1.7
40	2.7	1.9
> 50	3.0	2.0

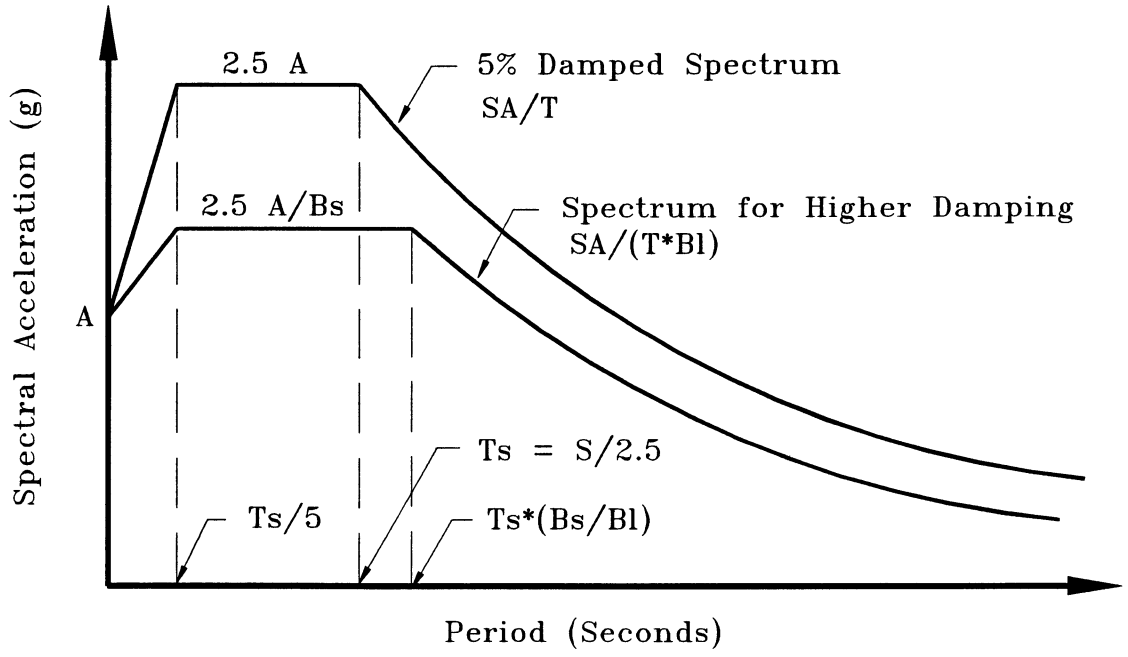

Figure 2-6 Modification of elastic response spectrum for high damping (Applied Technology Council, 1995).

damping ratio as follows:

$$B_s = \left(\frac{\xi}{0.05}\right)^{0.5} \tag{2-26}$$

and

$$B_1 = \left(\frac{\xi}{0.05}\right)^{0.3} \tag{2-27}$$

The base shear demand for "short" period structures in presence of high damping is given by

$$C_d = 2.5\frac{A}{B_s} \tag{2-28}$$

Similarly, for "long" period structures with high damping the base shear demand is given by

$$C_d = \frac{SA}{TB_1} \tag{2-29}$$

From the well-known inter-relationship between spectral acceleration and spectral displacement the latter can be obtained from

$$S_d = \Delta_{max} = \frac{C_d g T^2}{4\pi^2} \tag{2-30}$$

By plotting the base shear demand (C_d obtained from equations (2-28) and (2-29)) against the spectral displacement (S_d from equation (2-30)) it is possible to obtain the force-displacement demand spectra for a given design earthquake motion.

2.6 Analysis of Lateral Force Capacity vs. Demand

Because the seismic demand can be directly expressed in terms of a set of lateral force-displacement relationship, it is possible to compare this demand with the structure's lateral force-displacement (pushover) capacity.

The maximum displacement capacity (Δ_c) that exists just prior to topping of the pier system can be obtained from equation (2-7) as follows

$$\Delta_c = (b_b + b_t)\left(1 + \frac{n_c F_{pu}}{W}\right) \tag{2-31}$$

where $F_{up} = A_s f_y$ = maximum prestressing force in the tendons of one column, n_c = number of columns in the pier bent, and the other system parameters as defined previously.

By comparing capacity with demand if is possible to form a *displacement C/D* ratio as follows

$$r_\Delta = \frac{\Delta_c}{\Delta_{max}} \tag{2-32}$$

where Δ_{max} = maximum response displacement demand for a given peak ground acceleration ratio, A. Note that the above C/D ratio r_Δ is a *factor of safety* against pier toppling.

An algorithm for determining the ratio A for a given Δ_{max} is presented below.

Step 1. Assume a maximum response displacement, Δ_{max}.

Step 2. Based on this response displacement, calculate the effective damping (ξ_{eff}) using the appropriate equation from (2-23) to (2-25).

Step 3. Based on the maximum displacement, calculate base shear capacity (C_c) using the appropriate equation from (2-9) to (2-11).

Step 4. Calculate natural period using equation (2-30)

Step 5. By equating base shear capacity with the demand calculate the required peak ground acceleration to induce maximum displacement demand using either equation (2-28) or (2-29).

If the intersection of initial stiffness of bridge prior rocking and elastic demand with 5% viscous damping is defined as elastic base shear demand (C_d^e), the *force reduction factor* is given by

$$R_\mu = \frac{C_d^e}{C_c} \tag{2-33}$$

2.7 Comparison of Rocking Theory for Flexible Piers with Housner's Rocking Rigid Block Theory

It should be emphasized that the foregoing theoretical development is intended for flexible rocking bridge piers that may also be post-tensioned down to their foundations. If a very stiff (or rigid) structure is assumed without post-tensioning then the theory should converge to a rocking rigid block analysis. Therefore, it is of interest to compare the proposed theory with the original rocking rigid block theory of Housner (1963). This comparison is considered important as he used a different approach to assess damping than the energy-based approach developed herein.

This subsection first describes Housner's rocking block theory and then goes on to compare lateral strength and damping factors with the theory advanced herein.

2.7.1 Rigid Block Theory of Housner (1963)

Housner (1963) assumed that for a tall and slender rocking block the coefficient of friction between the block and foundation was sufficiently large to inhibit base sliding. Figure 2-7 presents the properties of a rocking rigid block where W = weight, I_o = mass moment of inertia about the rocking toe (point o), h = height to the center of gravity above the base and b = semi-base width of the block. The line from point o to center of gravity makes an angle α with the vertical face of the block and can be found from $\alpha = \tan^{-1} b/h$. Under dynamic excitation the rocking angle of the block from the vertical is defined as θ.

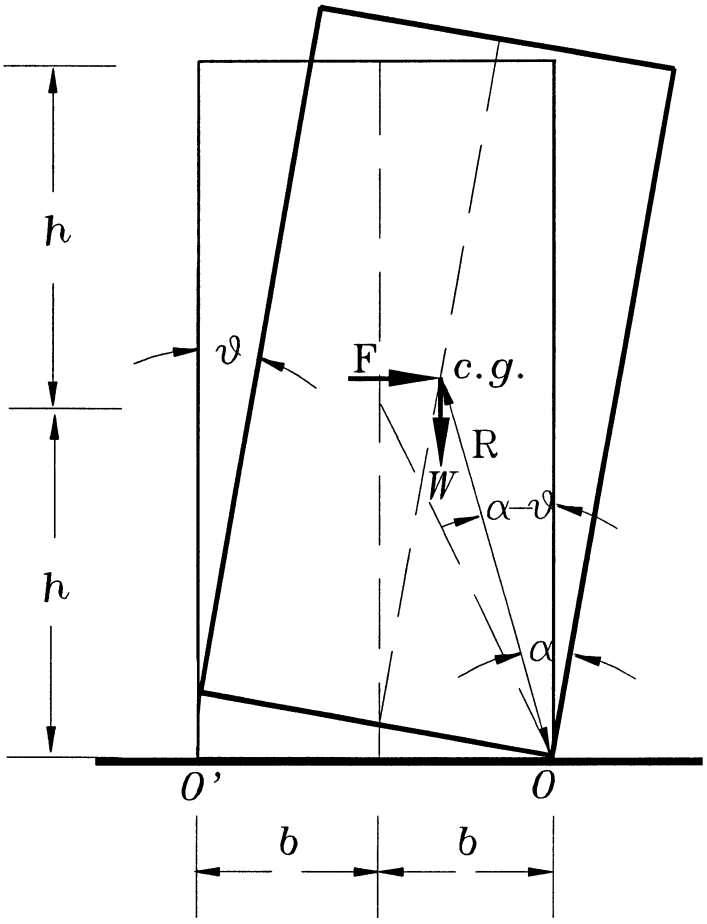

Figure 2-7 Rigid rocking block on rigid foundation.

The equation of motion obtained from the force equilibrium applied to the block is given by

$$I_o\ddot{\theta} = -WR\sin(\alpha - \theta) \tag{2-34}$$

where $R = \sqrt{b^2 + h^2}$ and $I_o = \frac{4}{3}mR^2$ in which m = mass of the block. For tall/slender block having an angle α less than 20° ($h/b > 2.75$), the equation may be written as

$$I_o\ddot{\theta} - WR\theta = -WR\alpha \tag{2-35}$$

This equation, subjected to the initial conditions $\theta = \theta_o$ and $\dot{\theta} = 0$ at $t = 0$, has the solution

$$\theta = \alpha - (\alpha - \theta_o)\cosh pt \tag{2-36}$$

where $p = \sqrt{\frac{WR}{I_o}}$

If each impact is assumed to be completely inelastic (that is no bouncing occurs), the reduction of kinetic energy during impact is given by

$$r = \left(\frac{\frac{1}{2}I_o\dot{\theta}_2^2}{\frac{1}{2}I_o\dot{\theta}_1^2}\right) = \left(\frac{\dot{\theta}_2}{\dot{\theta}_1}\right)^2 \tag{2-37}$$

where $\dot{\theta}_1$ and $\dot{\theta}_2$ are the angular velocity prior and after the impact. By equating the moment of momentum about the rocking toe (point o') prior and after the impact, the factor r is given by

$$r = \left(1 - \frac{2mb^2}{I_o}\right)^2 \tag{2-38}$$

where $I_o = \frac{4}{3}mR^2$ =moment of inertia with respect to rocking toe O.

By relating this r factor with the angular velocity in equation (2-36), the displacement ratio, φ ($\varphi = \frac{\theta}{\alpha} = \frac{\Delta}{b}$), after n-th impact can be derived as

$$\varphi_n = 1 - \sqrt{1 - r^n[1 - (1 - \varphi_o)^2]} \tag{2-39}$$

where Δ = lateral displacement at the gravity center of the block.

Natural Period: The rocking period can be obtained by defining the block fall from $\theta = \theta_o$ to $\theta = 0$ in a time $t = \frac{T}{4}$, then

$$T = \frac{4}{p}\cosh^{-1}\left(\frac{1}{1 - \varphi_o}\right) = \frac{4}{p}\ln\frac{1 + \sqrt{1 - (1 - \varphi_o)^2}}{1 - \varphi_o} \tag{2-40}$$

Base Shear Capacity: From the aforementioned elastic response spectral relationship given in equation (2-30) the base shear capacity is given by

$$C_c = \frac{S_a}{g} = \frac{4\pi^2}{T^2}\frac{\Delta_{max}}{g} \tag{2-41}$$

where S_a = spectral acceleration and Δ_{max} = spectral displacement. By substituting equation (2-40) into (2-41), the base shear capacity can be expressed as

$$C_c = \frac{\pi^2 mR}{4I_o}\frac{b\varphi_o}{\left(\ln\frac{1 + \sqrt{1 - (1 - \varphi_o)^2}}{1 - \varphi_o}\right)^2} \tag{2-42}$$

Equivalent Damping Ratio: Based on Housner's early work, Priestley et al. (1996) expressed the effective damping ratio by assuming that the initial displacement φ_o decays logarithmically to φ_n after the n-th impact:

$$\xi = \frac{\ln\left(\frac{\varphi_o}{\varphi_n}\right)}{n\pi} \tag{2-43}$$

Considering only the first impact ($n = 1$) and then substituting equation (2-39) into (2-43), the effective viscous damping is expressed as

$$\xi = \frac{1}{\pi} \ln \left(\frac{\varphi_o}{1 - \sqrt{1 - r[1 - (1 - \varphi_o)^2]}} \right) \tag{2-44}$$

2.7.2 Comparison

To compare the difference between the two approaches, two concrete blocks, one with $b=1\ m$, $h=4\ m$ and the other $b=1\ m$, $h=8\ m$, are considered. The unit weight of concrete block is assumed to be 23 kN/m^3.

The lateral resistance of a rocking block cab be found by considering the exact geometry shown in figure 2-7. Equating the lateral overturning moment with the self-weight stabilizing moment about the rocking toe gives,

$$F\ R \cos(\alpha - \theta) = W\ R \sin(\alpha - \theta) \tag{2-45}$$

Thus an "exact" solution accounting for large angles can be found from

$$C_c = \frac{F}{W} = \tan(\alpha - \theta) \tag{2-46}$$

The lateral deflection is given by

$$\varphi = \frac{\Delta}{b} = \frac{h}{b} \sin\theta \cos\theta + \sin^2\theta \tag{2-47}$$

Based on a small angle theory pushover analysis, the base shear capacity for a rigid rocking block can be derived in a similar fashion to the general theory given in section 2.4.1. This results in

$$C_c = \frac{F}{W} = \frac{b - \Delta}{h} \tag{2-48}$$

The base shear capacity with respect to the normalized displacement ($\varphi = \frac{\Delta}{b} = \frac{\theta}{\alpha}$) calculated from the "exact" pushover analysis (equation (2-46)) and the small angle theory pushover analysis (equation (2-48)) are compared with Housner's theoretical prediction (equation (2-42)) in figure 2-8.

It is evident that there are systematic differences between the approaches. Housner's approach also has some simplifying assumptions associated with small angle theory. This leads to an underestimate of the uplift capacity and an overestimate of the resistance at large displacements (when $\Delta > 0.5b$). This is attributed to the highly nonlinear dynamic characteristics of the rigid rocking block which was used as an indirect way of assessing the lateral strength.

Based on small angle pushover analysis, damping ratio for a rocking block considering radiated energy loss due to impact can be expressed as

$$\xi = \frac{1 - r}{\pi\left(1 - \frac{\Delta}{b}\right)} \qquad \textbf{(2-49)}$$

where r = reduction factor of kinetic energy as defined in equation (2-38). The effective viscous damping with respect to the displacement amplitude from both approaches (equations (2-44) and (2-49)) is presented in figure 2-9.

As shown in figure 2-9, the difference in damping ratio calculated from both approaches is quite small for small angle rocking. However, as the tilting angle (displacement) increases ($\Delta > 0.5b$), damping assessed by pushover analysis is apparently excessive. This deviation results from the small angle rotation assumption in the estimation of radiated energy loss due to impact as derived in equation (2-21). By comparing figure 2-9, it is noted that this deviation will be reduced for slender block. Notwithstanding the above remarks, it should be remembered that Housner's approach is also inexact owing to the abovementioned errors inherent in determining the lateral displacements.

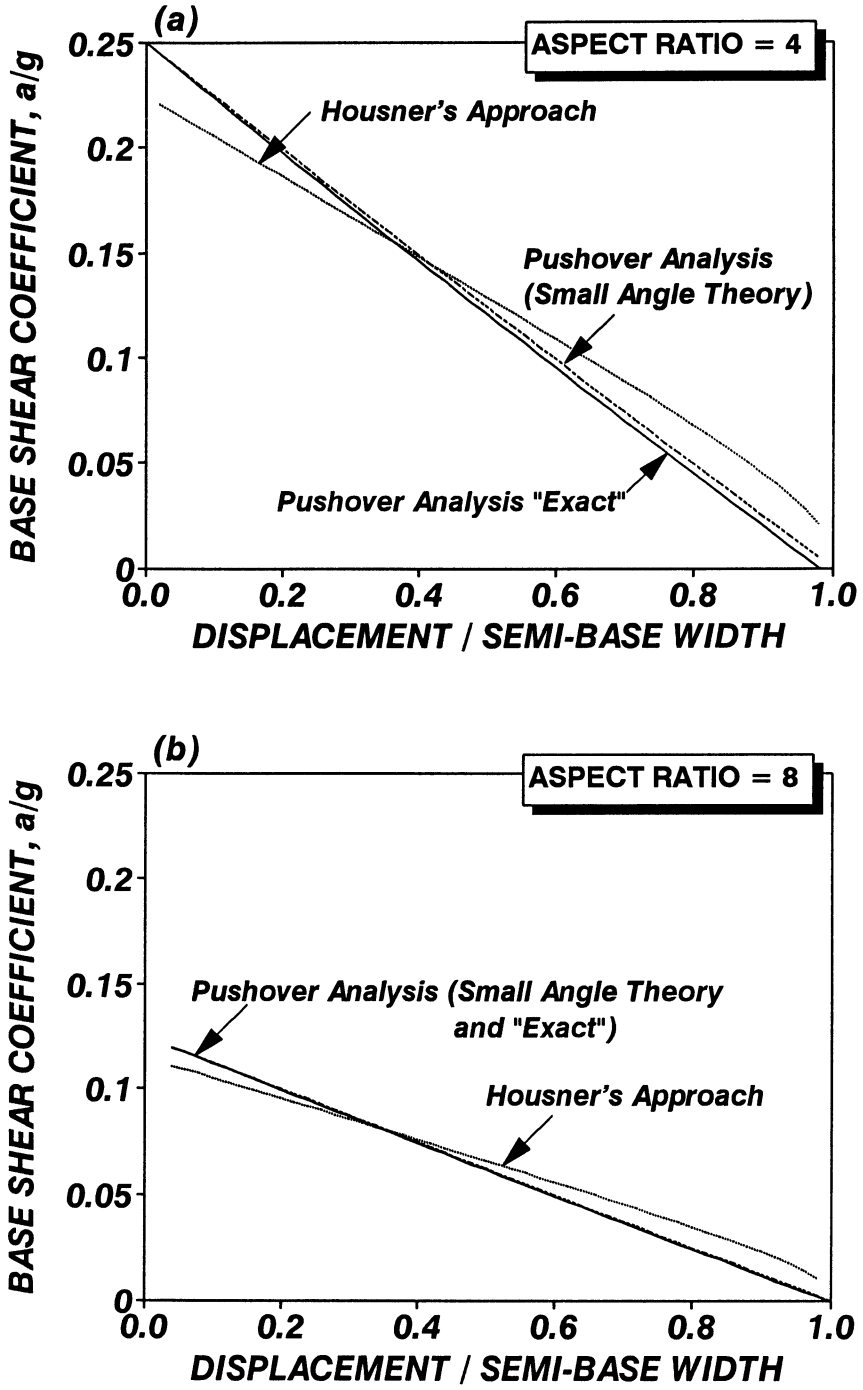

Figure 2-8 Comparison of base shear capacity between pushover analysis and Housner's approach for rigid rocking block with aspect ratios of 4 and 8.

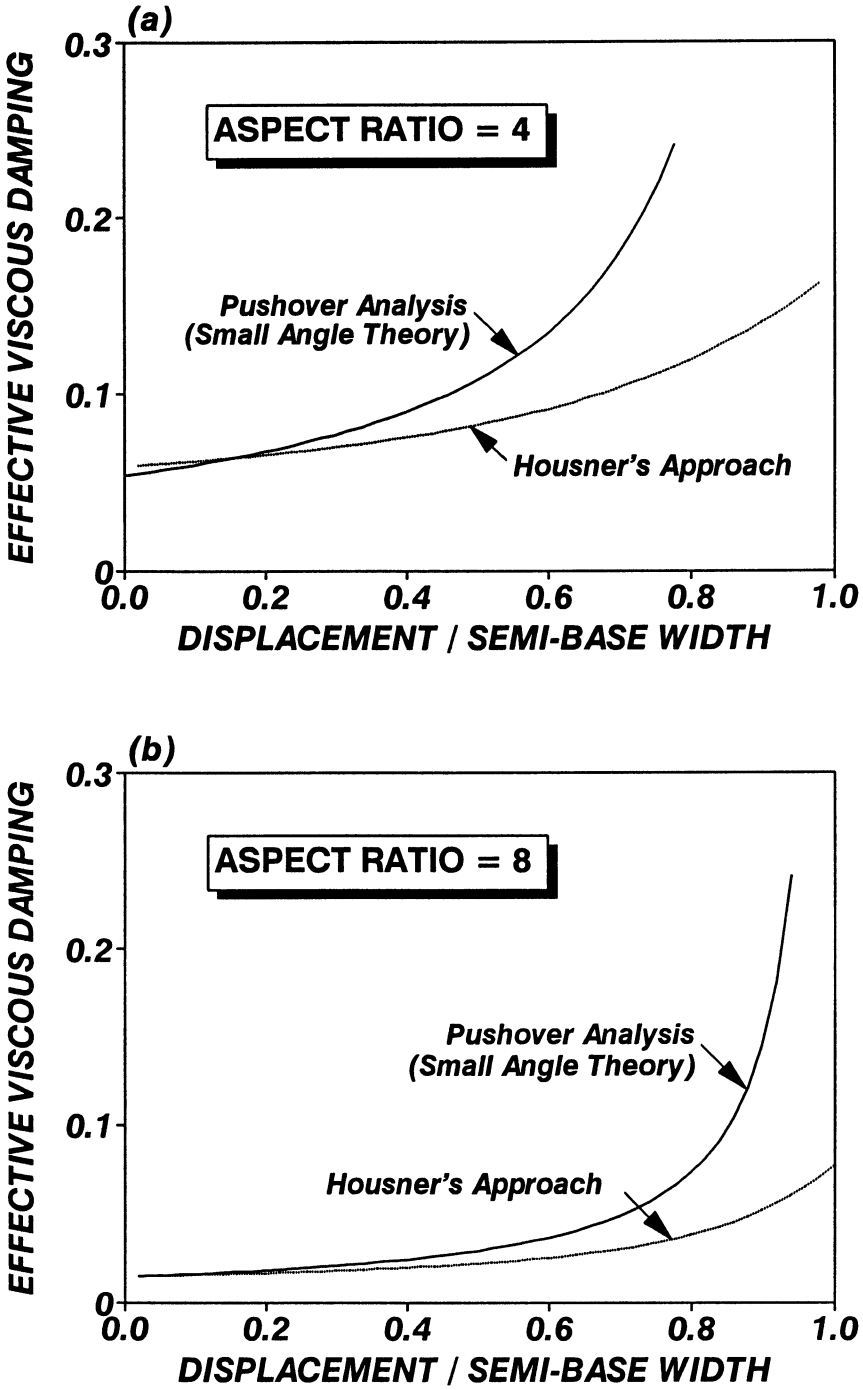

Figure 2-9 Comparison of effective viscous damping between pushover analysis and Housner's approach for rigid rocking block with aspect ratios of 4 and 8.

Overall, the response of the block from simple push over analysis is compatible with the classical theory proposed by Housner (1963) providing the rocking angles remain small. Therefore, it is suggested that either theory could be used provided $\Delta < 0.5b$.

2.8 SUMMARY

In this section, a new design philosophy referred as *Damage Avoidance Design* (DAD) is explored. The intent of this methodology is to not only maintain life safety in a strong earthquake, but also to avoid damage, while accommodating large seismically-induced deformations. The main features of this design methodology are (i) longitudinal reinforcement of columns is disconnected at beam-column interface to allow the columns to rock on cap/foundation beam surface without inducing damage, (ii) central post-tensioning tendons inside the columns may be provided to increase the lateral resistance, and/or to ensure there is sufficient post-uplift displacement capability, (iii) a steel-on-steel rocking interface is designed to accommodate high contact pressure at rocking toe during uplifting of the columns, and (iv) the structures can be precast to ensure high quality and shorten the construction time-frame.

A complete cyclic loading analysis procedure is proposed which can be simplified for design procedures to give a bi-linear push over force-deformation capacity. Furthermore, the rocking amplitude and the associated energy radiated (lost) on impact is converted into an equivalent viscous damping constant. By comparing the push over capacity with the appropriate damped seismic design elastic (demand) spectra, the structure's maximum force and displacement can be determined. This proposed design approach is compatible with similar approaches used for seismic evaluation and design of isolated bridge structures (Buckle and Friedland, 1995), and the emerging displacement based design philosophy (Kowalsky et al., 1995, and Priestley 1996). It is shown that the proposed seismic displacement theory collapses to the classical rigid rocking block theory of Housner (1963). Differences between the approach advanced herein for flexible structures and the Housner solution for rigid rocking structures can be attributed to the errors arising from assuming small angle displacement theory holds throughout. As toppling is approached, this assumption is clearly in error. However, if response displacement are

by a factor of safety such that $r_{\Delta} \geq 2$ (that is $\Delta < 0.5b$), then small displacement theory provides sufficient accuracy.

SECTION 3
ILLUSTRATIVE DAMAGE AVOIDANCE DESIGN EXAMPLE

3.1 INTRODUCTION

In this section, an illustrative example based on the Damage Avoidance Design theory described in the previous section is presented. This example first illustrates the preliminary design procedure. Secondly, several solutions based on different construction strategies are given. Next, the seismic response of the various solutions are evaluated in terms of displacement capacity vs. demand. Finally, design details for rocking columns are presented.

3.2 DESIGN PROBLEM

Consider part of a "long" multiple-span concrete slab on steel girder bridge. Each span is 40 m in length and the deck is 12.5 m wide. The soffit of the superstructure is to be8 m above ground level. Design a rocking pier bent to be fixed to a rigid piled foundation. For simplicity, assume the effective deck weight (girders + concrete deck + guard rails) to be 7 kPa.

The following assumptions can be made:

- Bridge is located in SPC D such that the peak ground acceleration coefficient is A = 0.6.
- Soil type factor S = 1.0.
- Unit weight of reinforced concrete = 23.5 kN/m^3.
- f_c' = 40 MPa.
- For prestressing bars, assume f_{su} = 1100 MPa (Grade 160 ksi).

3.3 Design Solutions

Tributary gravity weight $W_y = 40 \times 12.5 \times 7 = 3500\ kN$

Transverse inertia weight $W_x = W_y = 3.5\ MN$

$\therefore$ seismic mass of deck $= m_d = W_x/g = 3500/9.81 = 356.8\ t$

Structural Geometry:

- Adopt two columns spaced $8\ m$ apart—each column with a total height of $7\ m$.
- Assume each column carries a gravity load of $0.1 f_c' A_g$
  Then the required area of each column is

$$A_g > \frac{W_y/2}{0.1 f_c'} = \frac{3.5/2}{0.1 \times 40} = 0.438\ m^2 \Rightarrow D > 747\ mm$$

Adopt a circular cross section with a diameter $D = 800\ mm$ and height of $5\ m$.

Cross area of each column $A_g = \frac{\pi}{4} D^2 = \frac{\pi}{4} 0.8^2 = 0.502\ m^2$

$$\therefore \frac{P}{f_c' A_g} = \frac{3.5/2}{0.1 \times 0.502} = 0.087$$ —— satisfactory.

- Try using the square cross section at the top end with a width of $0.8\ m$ and at the bottom end with a width of $2.4\ m$ as shown in figure 3-1. This base width will be evaluated by this design procedure.

Dynamic Properties:

- Mass of each column m_c is

$$m_c = \left(2.4 \times 2.4 \times 1 + 0.8 \times 0.8 \times 1 + \frac{\pi}{4} \times 0.8^2 \times 5 \right) \times 2.4 = 21.4\ t$$

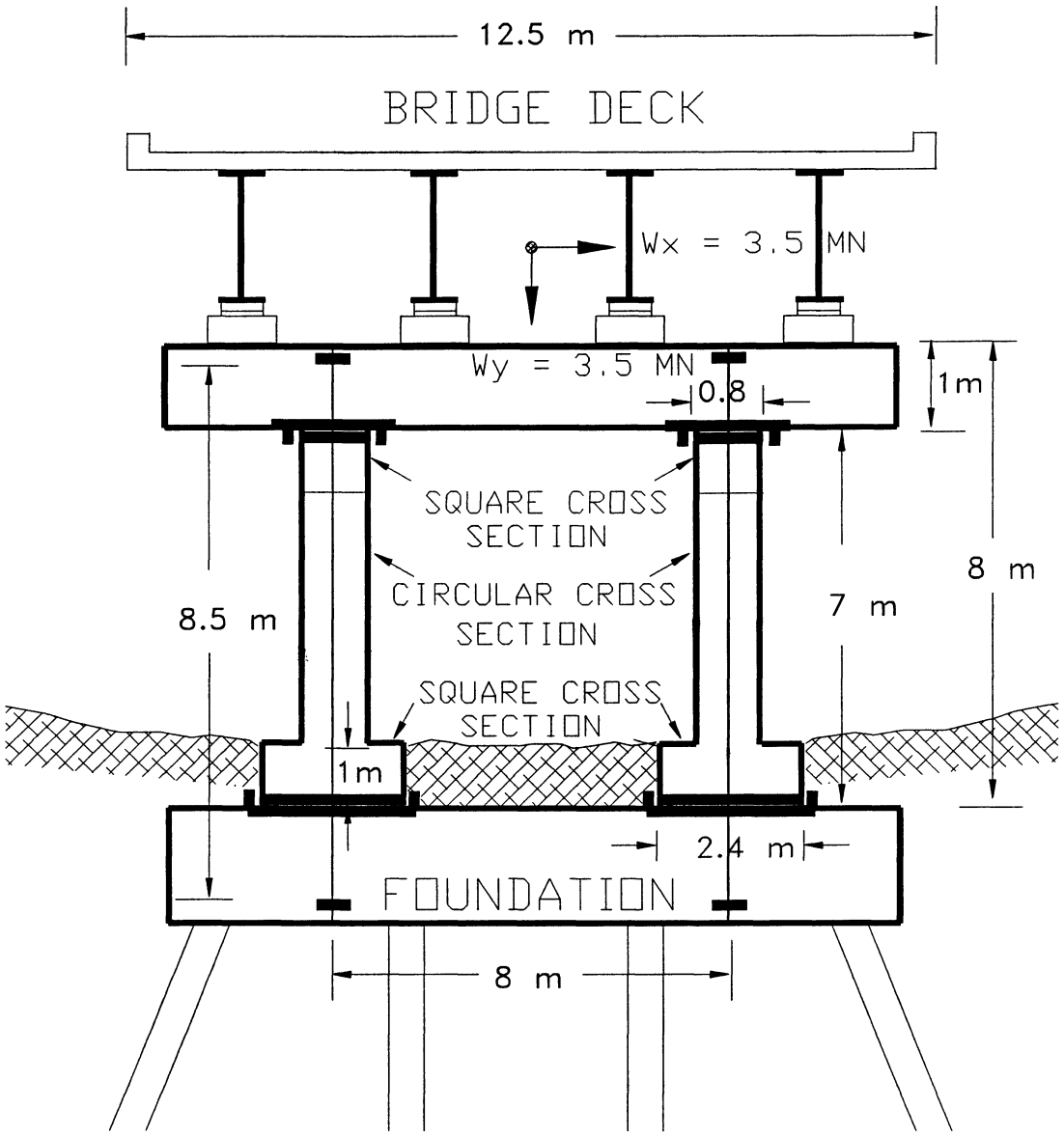

Figure 3-1 Bridge with I shape rocking piers.

Adopt cap beam dimension of (1 m high, 2 m wide and 12 m long) the mass of the cap beam is

$$m_b = 12 \times 2 \times 1 \times 2.4 = 57.6 \ t$$

The total tributary seismic mass is given by

$$m = 2m_c + m_b + m_d = 42.8 + 57.6 + 356.8 = 457.2 \ t$$

- The critical overturning angle for columns is given by

$$\alpha = \tan^{-1}\left(\frac{b_b + b_t}{H_c}\right) = \tan^{-1}\left(\frac{1.6}{7}\right) = 12.9°$$

- When columns uplift, the distance from top rocking toe to the diagonal bottom toe is

$$R = \sqrt{(b_b + b_t)^2 + H_c^2} = \sqrt{1.6^2 + 7^2} = 7.4 \ m$$

- The moment of inertia about the rocking toe, I_o, is calculated as

$$I_{pier} = \sum_{J=1}^{3} n_c\left(m_{cI}(r_{xI}^2 + r_{yI}^2) + m_{cI}R_I^2\right) + (m_b + m_d)R^2$$

where m_{cI} = ith component of mass in T-shape columns, r_{xI} and r_{yI} are the radius of gyration in X and Y axes for ith component, and R_I = distance from centroid of ith component to the rocking toe.

$$I_{pier} = 2\left[13.8\left(\frac{1}{12}(2.4^2 + 1^2) + (1.2^2 + 0.5^2)\right) + 1.54\left(\frac{1}{12}(0.8^2 + 1^2) + (1.2^2 + 6.5^2)\right)\right]$$

$$+ 2\left[6.03\left(\frac{1}{12}(3 \times 0.4^2 + 5^2) + (1.2^2 + 3.5^2)\right)\right] + (57.6 + 356.8)7.4^2$$

$$= 23080 \ t\text{-}m^2$$

- The kinetic energy reduction factor is

$$r = \left(1 - \frac{2 n_c m_c b_b^2 + 2(m_b + m_d) b_b (b_b + b_t)}{I_{pier}}\right)^2$$

$$r = \left(1 - \frac{2 \times 2 \times 21.4 \times 1.2^2 + 2 \times 414.4 \times 1.2 \times 1.6}{23080}\right)^2 = 0.857$$

- Lateral stiffness of pier bent prior to rocking is

$$K_c = n_c \frac{12 E_c I_{eff}}{h_c^3}$$

where n_c = number of columns, h_c = column height above the bottom rocking base measured to be $6\ m$ and E_c = Young's modulus of concrete can be calculated as $E_c = 4700\sqrt{40\ (MPa)} = 30000\ MPa$, thus

$$K_c = 2\frac{12 \times (30 \times 10^6) \times (\pi \times 0.8^4 \times 0.5/64)}{6^3} = 33565\ kN/m$$

- The pre-rocking natural period for the elastic structure is

$$T_e = 2\pi\sqrt{\frac{m}{K_c}} = 2\pi\sqrt{\frac{457.2}{33565}} = 0.73\ sec$$

- Based on conventional design elastic demand

$$C_d = \frac{1.2\,SA}{T^{2/3}} < 2.5A$$

therefore,

$$C_d = \frac{1.2 \times 1 \times 0.6}{0.73^{2/3}} = 0.89 < 2.5 \times 0.6 = 1.5$$

if $R = 5$ then required uplift capacity should be

$$C_c = \frac{C_d}{R} = \frac{0.89}{5} = 0.18$$

- Now check the rocking base widths

$$C_c = \frac{b_b + b_t}{H_c} - \theta$$

therefore,

$$b_b > (C_c + \theta)H_c - b_t$$

- Assume a design column drift of 0.05

$$b_b > (0.18 + 0.05)7 - 0.4 = 1.2$$

Adopt $b_b = 1.2\ m$

Solution Scheme I: No prestressing

- Assume a response displacement of $\Delta_{max} = 0.5\Delta_c = 0.5(b_b + b_t) = 0.5 \times 1.6 = 0.8\ m$.

$$\theta = \frac{\Delta_{max}}{H_c} = \frac{0.8}{7} = 0.114\ rad$$

- Based on this displacement, the effective damping from equation (2-25) is

$$\xi = \frac{1}{\pi}\left[\frac{1 - r}{1 - \frac{H_c\theta}{b_b + b_t}}\right] = \frac{1}{\pi}\left[\frac{1 - 0.857}{1 - \frac{0.8}{1.6}}\right] = 0.091 = 9.1\%$$

- From equation (2-11) the base shear capacity is

$$C_c = \frac{b_b + b_t}{H_c} - \theta = \frac{1.6}{7} - 0.114 = 0.114$$

- From equation (2-30) the effective (rocking) period of the structure is

$$T = 2\pi\sqrt{\frac{\Delta}{C_c\, g}} = 2\pi\sqrt{\frac{0.8}{0.114 \times 9.81}} = 5.31 \text{ sec}$$

- From equation (2-29) the required peak ground acceleration can be found

$$C_d = C_c = 0.114 = \frac{A}{5.31\left(\frac{0.139}{0.05}\right)^{0.3}}$$

solving $A = 0.72$.
The relation among base shear capacity, damping ratio and displacement under this peak ground excitation is plotted in figure 3-2.

- Displacement capacity will be the sum of semi-base width at top and bottom of column. The displacement capacity/demand ratio is

$$r_\Delta = \frac{\Delta_c}{\Delta_{max}} = \frac{1.6}{0.8} = 2.0$$

- The elastic base shear demand can be calculated as

$$C_d^e = \frac{SA}{T_e} = \frac{0.72}{0.73} = 0.99$$

therefore, the force reduction factor is

$$R_\mu = \frac{C_d^e}{C_c} = \frac{0.99}{0.114} = 8.7$$

- This procedure is repeated by changing the maximum displacement to obtain

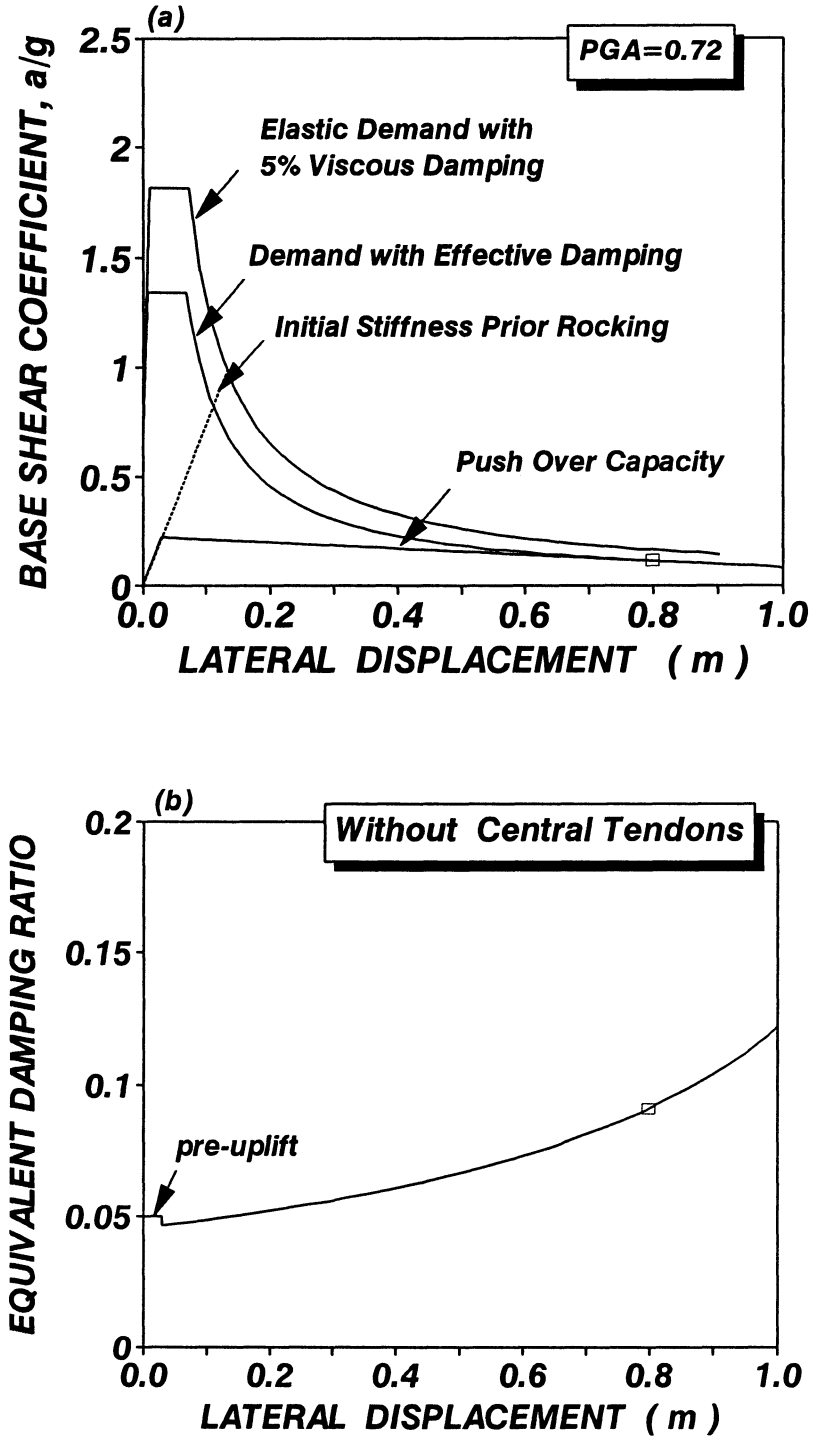

Figure 3-2. Variation of (a) base shear capacity and (b) equivalent damping with lateral displacement for the illustrative bridge pier example without tendon reinforcement under 9.872 g ground excitiation.

the corresponding peak ground acceleration.

Solution Scheme II: With slack central tendons

- Assumed each column is centrally reinforced with two 25 *mm* diameter high strength threadbars ($A_s = 0.001\,m^2$, $f_{su} = 1100\,MPa$ and $f_y = 0.75 f_{su} = 0.75 \times 1100 = 825\,MPa$) which are anchored into cap or foundation beams through a depth of 0.75 *m*.

- The tendons are assumed to be just slack.
  The anchorage length, L_T, for the high strength threadbar is thus designed to be 8.5 *m*. Then, tendons will have an angular stiffness with respect to the rocking toe as

$$K = E_s A_s \frac{b_b + b_t}{L_t} = 2000000 \times 0.001 \times \frac{1.6}{8.5} \times 1000 = 38140\ kN/rad$$

- Tendon stiffness ratio with respect to gravity load, r_s, is given by

$$r_s = \frac{n_c K_s L_T}{W(b_b + b_t)} = \frac{2 \times 38140 \times 8.5}{457.2 \times 9.81 \times 1.6} = 90.35$$

- Yield drift angle for tendons is given by

$$\theta_y = \frac{A_s f_y}{K_s} = \frac{0.001 \times 825 \times 1000}{38140} = 0.022$$

- Yield displacement for tendons at the center of gravity is

$$\Delta_y = \theta_y H_c = 0.022 \times 7 = 0.154\ m$$

- Assume a maximum response displacement of 0.8 *m*.

$$\theta = \frac{0.8}{7} = 0.114 \ rad$$

- Because the maximum displacement is greater than the yield displacement, tendons yield during ground shaking.
  Based on this displacement, the effective viscous damping can be calculated from equation (2-24b),

$$\xi = \frac{\left[0.114 + 90.35 \times 0.0041\left(0.114 - \frac{8.5}{2 \times 1.6}0.0041\right)\right](1 - 0.782)}{\pi\left[1 + 90.35 \times 0.0041 - \frac{0.8}{1.6}\right]0.114} = 0.07 = 7\%$$

- From equation (2-7) the base shear capacity is

$$C_c = \frac{b_b + b_t}{H_c}\left[1 - \left(\frac{H_c}{b_b + b_t} - r_s \frac{b_b + b_t}{L_T}\right)\theta\right] \le \frac{b_b + b_t}{H_c}\left[1 + r_s \varepsilon_y - \frac{H_c \theta}{b_b + b_t}\right]$$

$$= \frac{1.6}{7}\left[1 - \left(\frac{7}{1.6} - 90.35 \frac{1.6}{8.5}\right)0.114\right] \le \frac{1.6}{7}\left[1 + 90.35 \times 0.0041 - \frac{0.8}{1.6}\right]$$

$$= 0.557 \le 0.199$$

$$\therefore \ C_c = 0.199$$

- Using equation (2-30) the effective natural period of the structure

$$T = 2\pi\sqrt{\frac{\Delta}{C_c \, g}} = 2\pi\sqrt{\frac{0.8}{0.199 \times 9.81}} = 4.02 \ sec$$

- Solve for the required peak ground acceleration from equation (2-29),

$$C_d = C_c = 0.199 = \frac{A}{4.02\left(\frac{0.0695}{0.05}\right)^{0.3}}$$

$\therefore\ A = 0.88.$

The relation among base shear capacity, damping ratio and displacement under this peak ground excitation is plotted in figure 3-3.

- Based on equation (2-31), calculate the displacement capacity

$$\Delta_c = (b_b + b_t)\left(1 + \frac{n_c A_s f_y}{W}\right) = 1.6\left(1 + \frac{2 \times 0.001 \times 825 \times 1000}{457.2 \times 9.81}\right) = 2.19$$

Therefore, displacement capacity/demand ratio is

$$r_\Delta = \frac{\Delta_c}{\Delta_{max}} = \frac{2.19}{0.8} = 2.74$$

- The elastic base shear demand can be determined from

$$C_d^e = \frac{SA}{T} = \frac{0.88}{0.73} = 1.21$$

- The force reduction factor is given by

$$\mathcal{R}_\mu = \frac{C_d^e}{C_c} = \frac{1.21}{0.199} = 6.1$$

- This procedure is repeated by changing the maximum displacement to obtain its corresponding peak ground acceleration.

Solution Scheme III: With post-tensioned central tendons

- Assume each column is centrally reinforced with two 25 *mm* diameter high strength threadbars (f_y = 825 *MPa*) which are post-tensioned up to two-

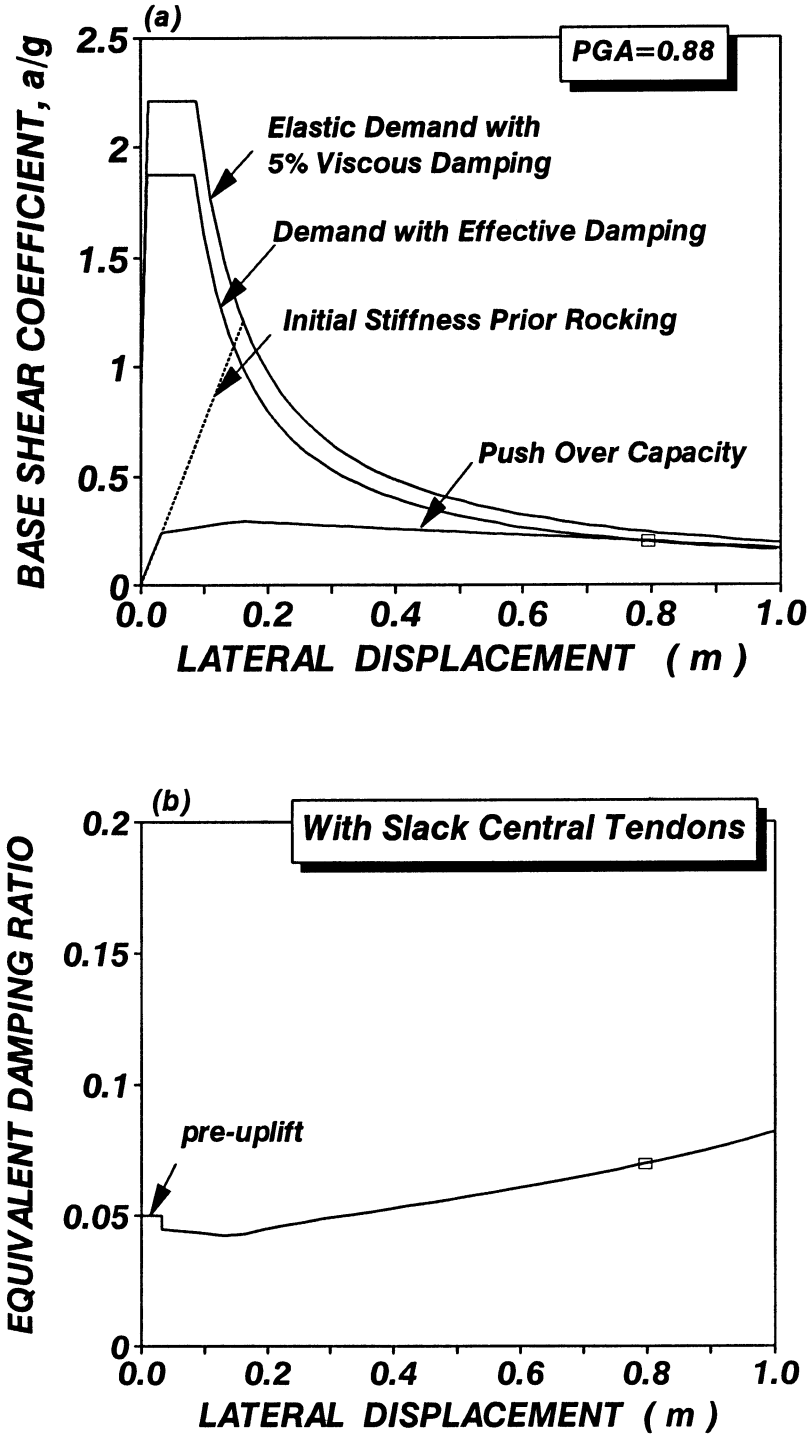

Figure 3-3 Variation of (a) base shear capacity and (b) equivalent damping with lateral displacement for the illustrative bridge pier example centrally reinforced with two slack tendons under $0.88\,g$ ground excitation.

third the yield strain ($\varepsilon_o = \frac{2}{3}\varepsilon_y$).

- Yield drift angle for the tendons is thus given by

$$\theta_y = \frac{1}{3}\frac{A_s f_y}{K_s} = \frac{0.001 \times 825 \times 1000}{3 \times 38140} = 0.0073 = 0.73\%$$

- Yield displacement for tendons at the gravity center is

$$\Delta_y = \theta_y H_c = 0.0073 \times 7 = 0.051\, m$$

- Assume a maximum response displacement of $0.8\, m$.

$$\theta = \frac{0.8}{7} = 0.114\ rad$$

- Because the maximum displacement is greater than the yield displacement tendons yield during ground shaking.
Based on this displacement, the effective viscous damping can be calculated from equation (2-23b),

$$\xi = \frac{\left[0.114 + 90.35\left(0.0041 \times 0.114 - \frac{8.5}{21.6}\left(0.0041 - \frac{2}{3}\,0.0041\right)^2\right)\right](1 - 0.782)}{\pi\left[1 + 90.35 \times 0.0041 - \frac{0.8}{1.6}\right]0.114}$$

$$= 0.0715 = 7.2\%$$

- Calculate the base shear capacity, C_c, from equation (2-7),

$$C_c = \frac{b_b + b_t}{H_c}\left[1 + r_s\varepsilon_o - \left(\frac{H_c}{b_b + b_t} - r_s\frac{b_b + b_t}{L_T}\right)\theta\right] \le \frac{b_b + b_t}{H_c}\left[1 + r_s\varepsilon_y - \frac{H_c\theta}{b_b + b_t}\right]$$

$$= \frac{1.6}{7}\left[1 + 90.35 \times 0.0027 - \left(\frac{7}{1.6} - 90.35\frac{1.6}{8.5}\right)0.114\right] \le \frac{1.6}{7}\left[1 + 90.35 \times 0.0041 - \frac{0.8}{1.6}\right]$$

$$= 0.614 \le 0.199$$

$$\therefore \quad C_c = 0.199$$

- The effective period of damped structure from equation (2-30) is

$$T = 2\pi\sqrt{\frac{\Delta}{C_c\, g}} = 2\pi\sqrt{\frac{0.8}{0.199 \times 9.81}} = 4.02 \text{ sec}$$

- Based on equation (2-29), the required peak ground acceleration is

$$C_d = C_c = 0.199 = \frac{A}{4.02\left(\frac{0.0715}{0.05}\right)^{0.3}}$$

Solving $A = 0.89$.
The relation among base shear capacity, damping ratio and displacement under this ground excitation is plotted in figure 3-4.

- Based on equation (2-31), calculate the displacement capacity

$$\Delta_c = (b_b + b_t)\left(1 + \frac{n_c A_s f_y}{W}\right) = 1.6\left(1 + \frac{2 \times 0.001 \times 825 \times 1000}{457.2 \times 9.81}\right) = 2.19$$

Therefore, displacement capacity/demand ratio is

$$r_\Delta = \frac{2.19}{0.8} = 2.74$$

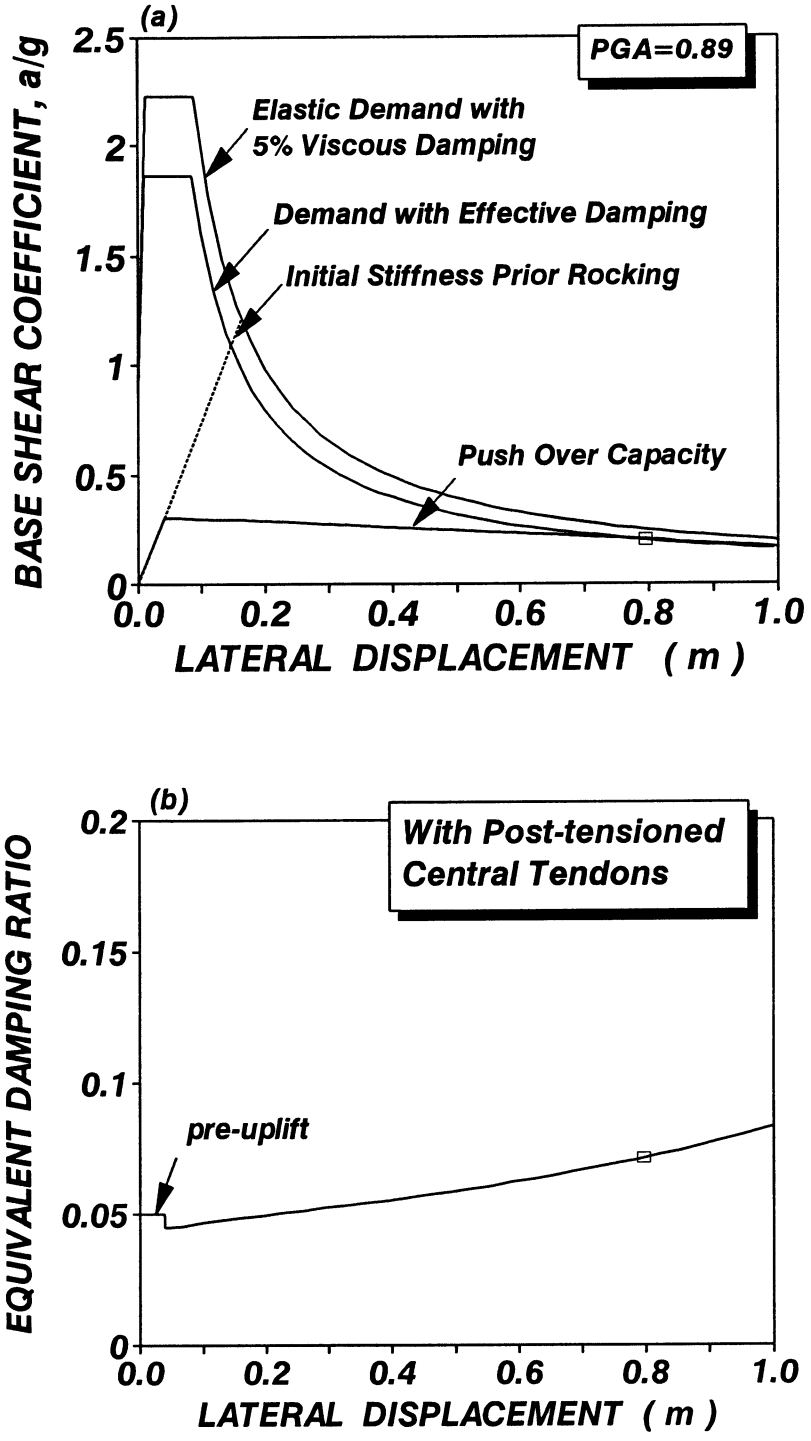

Figure 3-4 Variation of (a) base shear capacity and (b) equivalent damping with lateral displacement for the illustrative bridge pier example centrally reinforced with two post-tensioned tendons under 0.89 g ground excitation.

- The elastic base shear demand can be calculated as

$$C_d^e = \frac{SA}{T} = \frac{0.89}{0.73} = 1.22$$

Force reduction factor is given by

$$R_\mu = \frac{C_d^e}{C_c} = \frac{1.22}{0.199} = 6.1$$

- This procedure is repeated by changing the maximum displacement to obtain its corresponding peak ground acceleration.

Discussion of Results:

Lateral Displacement:

Lateral displacement with respect to peak ground acceleration for the three solution schemes is plotted in figure 3-5(a). Figure 3-5(b) presents the base shear capacity versus peak ground acceleration. As shown in figure 3-5(a), the restraint of central tendons effectively reduces the lateral displacements of rocking piers. The post-tensioned forces which stiffen the structure further reduce the lateral displacements especially for peak ground acceleration less than 0.4 g. This beneficial effect also induces the enhancement of base shear capacity as shown in figure 3-5(b).

Therefore, it is concluded that the restraint of tendons has an effect equivalent physically increasing the base width so that lateral displacement is reduced and base shear capacity is raised. Moreover, the post-tensioned force further helps in stiffening the structure to reduce the displacements and enhance base shear capacity for low to moderate intensity ground shaking (less than 0.4 g)

Displacement Capacity/Demand Ratio.

The capacity/demand evaluation for various solution schemes is plotted in figure 3-6. Figure 3-6(a) shows the effect of different tendon applications on the displacement capacity/demand ratio and force reduction factor. For comparison, a case where the rocking piers centrally reinforced with three post-tensioned tendons is also analyzed and plotted in the figure. The amount of central tendons

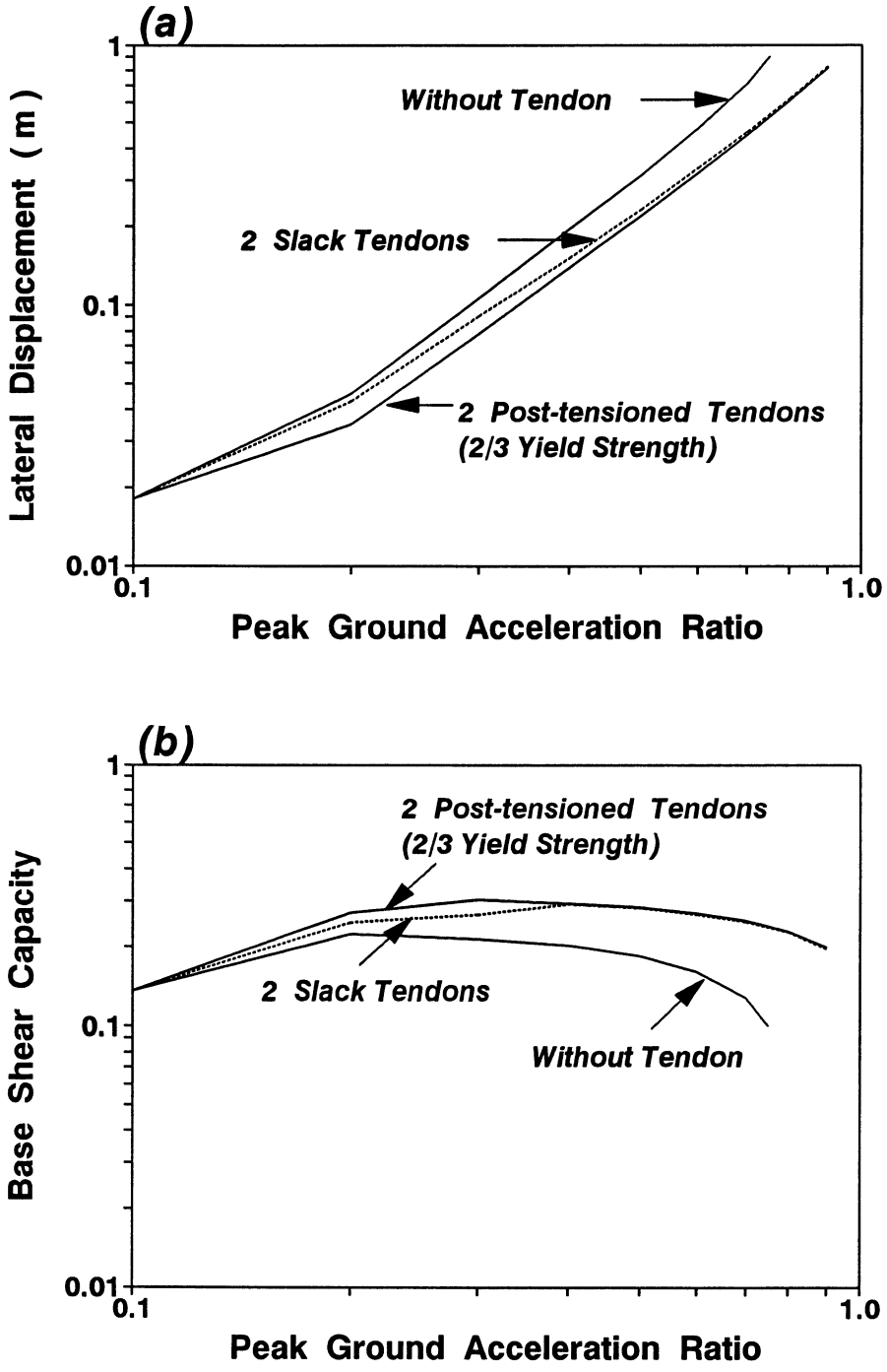

Figure 3-5 Comparison of (a) lateral displacement and (b) base shear capacity between various tendon applications in columns under ground excitations.

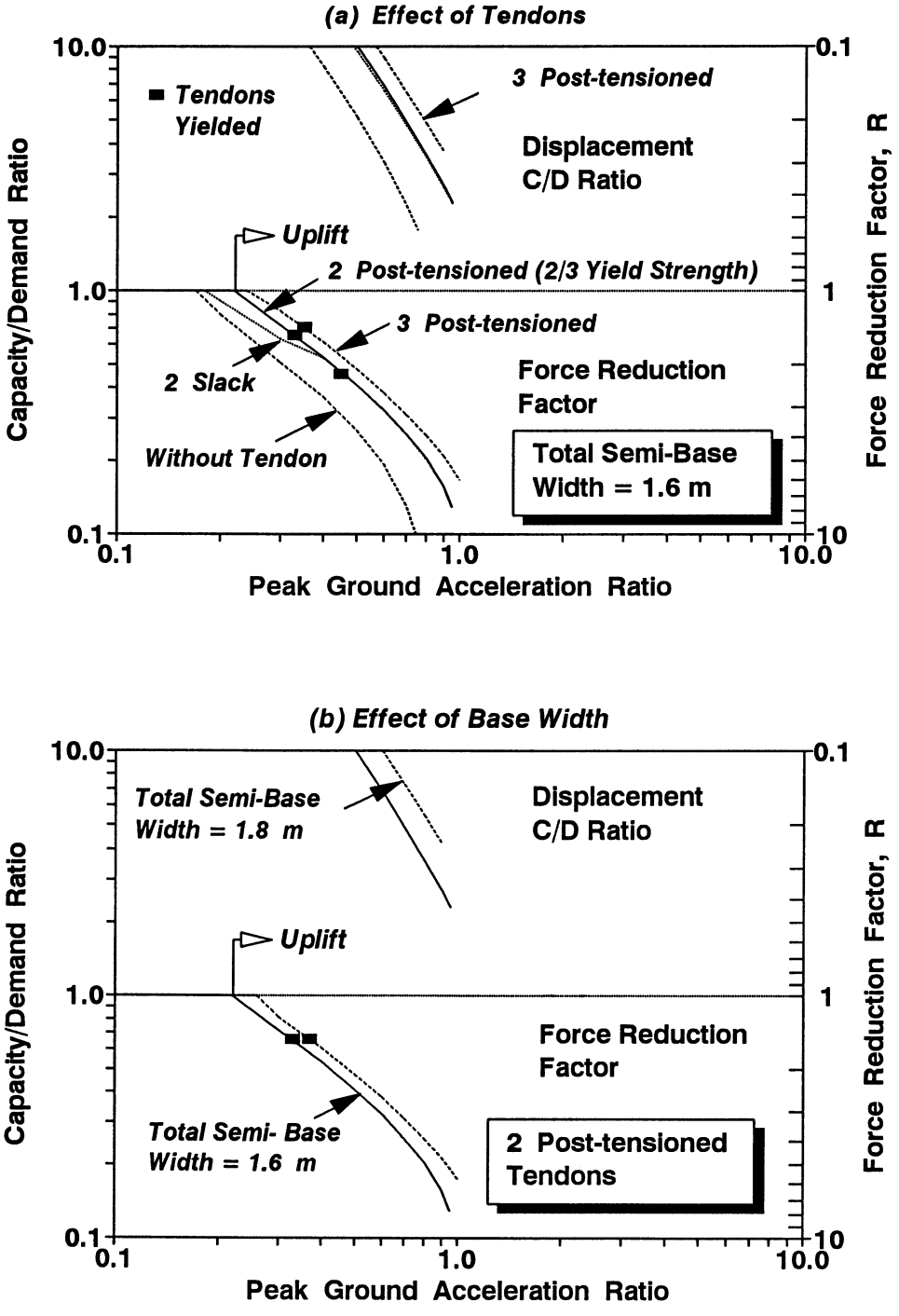

Figure 3-6 Capacity/demand evaluation for illustrative bridge pier example showing (a) the effect of tendons (b) the effect of base width.

in the columns proportionally increases the displacement capacity/demand ratio and reduces the force reduction factor. Moreover, the presence of tendons, especially when post-tensioned, raise the required ground shaking intensity to uplift the columns. This helps the bridge to remain firmly seated under small intensity earthquakes.

Figure 3-6(b) presents the effect of base width on the response. In this figure, the total semi-base width ($b_b + b_t$) is increased to 1.8 m for the case of two central post-tensioned tendons. As expected, the increase in base width increases the displacement capacity/demand ratio and reduces the force reduction factor. Therefore, it is possible to improve the overturning safety factor of the rocking columns by either increasing the base width or the amount of tendons, however, at the expense of higher moment demand at the rocking base.

Finally, the column centrally reinforced with two post-tensioned tendons which gives a displacement capacity factor of safety of two for a 1.0 g peak ground acceleration (as shown in figure 3-6) is chosen for design. The details of this design are described in what follows.

3.4 Column Design

The columns are designed with circular section (0.8 m dia.) in the middle 5 m with a square section at both ends. Both columns are centrally reinforced with two 25 mm unbonded high strength threadbars ($A_s = 0.001\ m^2$, $f_{su} = 1100\ MPa$ and $f_y = 825\ MPa$) which are post-tensioned up to two-third of yield strength.

(1) Required force and moment:

As shown in figure 3-7, if the tendons reach maximum strength, the maximum moment is given by

$$\phi M_u = \left(\frac{W_y + m_b g}{2} \right) (b_b + b_t) + A_s f_{su} \frac{(b_b + b_t)}{2} = 2.03 \times 1.6 + 0.001 \times 1100 \times 0.8 = 4.13\ MN\text{-}m$$

- Assuming $\phi = 0.9$ the required moment is given by

$$M_u = 4.59\ MN\text{-}m$$

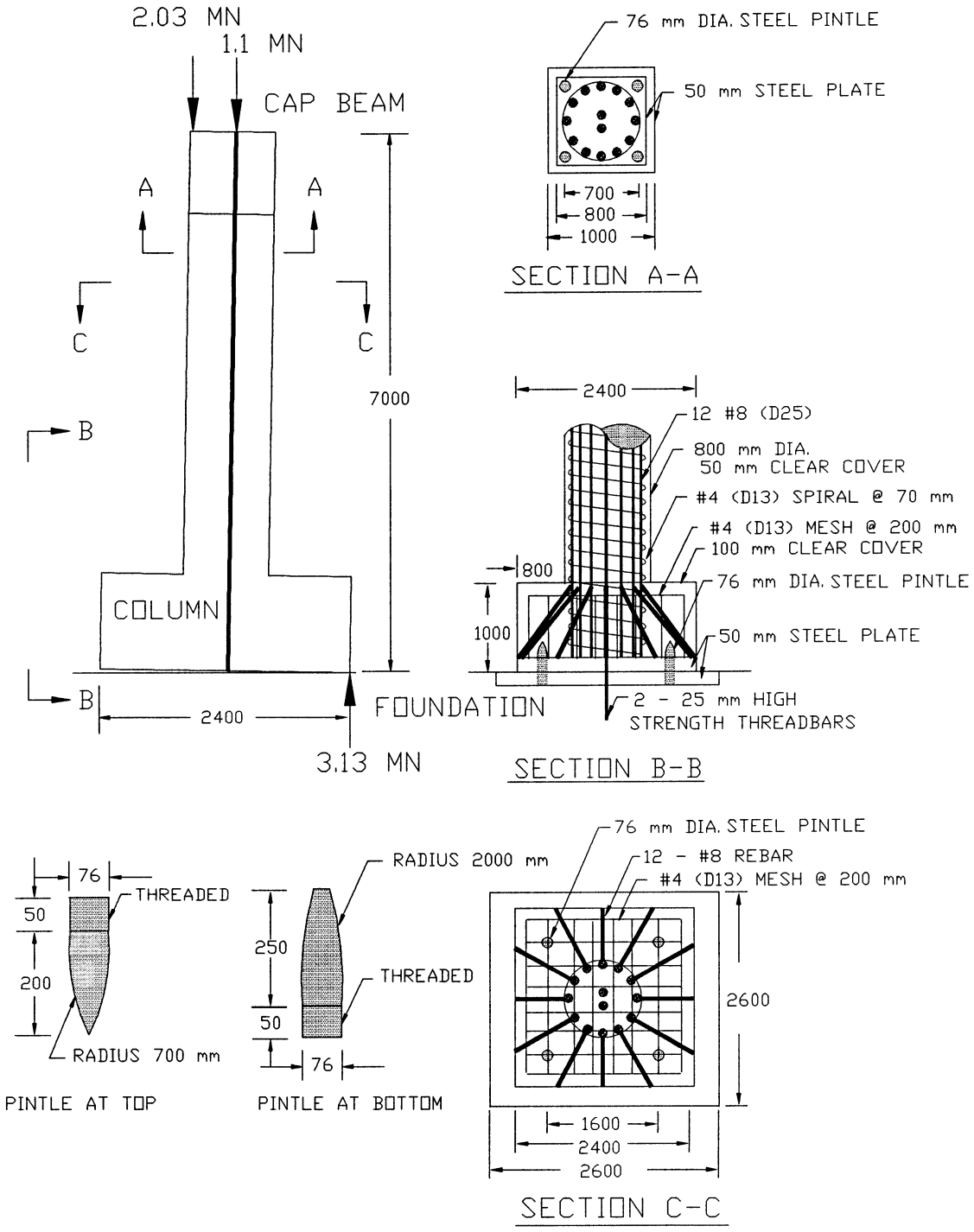

Figure 3-7 Force distribution and design details of rocking column.

- Maximum axial load ratio is $\dfrac{W_y/2 + m_b g/2 + A_s f_{su}}{f_c' A_g} = \dfrac{2.03 + 1.1}{40 \times 0.502} = 0.156$

- Lateral force in each column is $F = \dfrac{2M_u}{H_c} = \dfrac{2 \times 4.59}{7} = 1.31\ MN$

(2) Circular section

Longitudinal Reinforcement:

- Due to the uplift of the columns, the longitudinal reinforcement can be designed with the minimum requirement based on ACI 318-95 Code, that is

$$\rho_{min} = \frac{200}{f_y}\ (psi) = \frac{1.379}{f_y}\ (MPa) = \frac{1.379}{414} = 0.00333$$

- Use 12 - #8 ($A_s = 0.006\ m^2$, $f_y = 414\ MPa$) deformed rebar

$\rho_t = \dfrac{0.006}{0.502} = 0.012 > \rho_{min}$.

If post-tensioned tendons are added, total $\rho_t = 0.012 \times \dfrac{14}{12} = 0.014$.

Transverse Reinforcement:

- Use the less spacing of the following

(i) shear requirement:

- Concrete contribution

$$\phi V_c = \phi 0.167 \sqrt{f_c'\ (MPa)}\, 0.8 A_g = 0.85 \times 0.167 \times \sqrt{40} \times 0.8 \times 0.502 = 360\ kN$$

then $\dfrac{A_v}{s} = \dfrac{2}{\pi}\left(\dfrac{V_u - \phi V_c}{\phi f_{yh} d}\right) = \dfrac{2}{\pi}\left(\dfrac{(1150 - 360) \times 1000}{0.85 \times 414 \times (0.8 \times 800)}\right) = 2.23\ mm^2/mm$

If #4 spiral ($A_s = 127\ mm^2$) is used, $s = \frac{127}{2.23} = 56.9\ mm$.

(ii) Anti-buckling requirement: $s = 6 d_b = 6 \times 25 = 150\ mm$.

Use #4 spiral with a pitch of $50\ mm$.

(3) Rocking base

- To accommodate the high contact point forces at the rocking toe, steel-steel rocking interface is designed.
- A $2.4 \times 2.4 \times 0.05\ m$ steel plate ($f_y = 250\ MPa$) at bottom of the columns and a slightly larger plate ($2.6 \times 2.6 \times 0.05\ m$) on the opposite position (surface of foundation beam) are used for the bottom rocking base.
- For the top rocking interface, use a $0.8 \times 0.8 \times 0.05\ m$ steel plate at top of the columns and a slighter larger plate ($1.0 \times 1.0 \times 0.05\ m$) on the cap beam surface.

- To ensure proper force transfer between rocking toe and circular column for the bottom rocking base during uplift of the columns, a diagonal strut (#8 deformed rebar) is welded to each column longitudinal reinforcement and the edge of steel plate as shown in figure 3-7.

- Flexural moment capacity:

If upper layer of reinforcement is ignored, required steel area is

$$A_s = \frac{M_u}{\phi f_y (d - d')} = \frac{4.59}{0.9 \times 248 \times 0.85} = 0.024\ m^2$$

$$< A_s = 2.4 \times 0.05 = 0.12\ m^2$$

- To ensure the rocking base remains intact during rocking, use a minimum amount of reinforcement (M-shape mesh) at the upper layer of the rocking base.

$\therefore$ use #4 rebar with a spacing of $200\ mm$

- To prevent the columns from moving laterally during seismic excitation, use a 76 *mm* diameter steel bullet-shaped pintles at each of the four corners of the top and bottom rocking bases, as shown in figure 3-7.

  The shear capacity of four pintles is given by

$$\phi V_s = \phi \frac{f_y}{\sqrt{3}} A_s = 0.65 \times \frac{250}{\sqrt{3}} \times (4 \frac{\pi}{4} \times 0.076^2) = 1.7 \ MN > F = 1.31 \ MN$$

- Punching shear capacity: If capacity of bottom steel plate is ignored,

  based on ACI Code $V_c = 0.33\sqrt{f'_c \ (MPa)}\ b_0\ d$,

$$V_c = 0.33\sqrt{40} \times 2\pi \times 0.8 \times 0.9 = 9.6 \ MN > P_{max} = 2.79 \ MN$$

3.5 SUMMARY

In this section, an illustrative example based on the Damage Avoidance Design philosophy is demonstrated. Utilizing the proposed generic seismic analysis procedure, several solution schemes are evaluated through the capacity/demand assessment. Based on this evaluation, the column centrally reinforced with two post-tensioned tendons is designed which provides overturning safety of 2 under 1.0 g peak ground excitation (see figure 3-6). Finally, design details including circular cross section, square rocking base and steel-steel rocking interface are given.

SECTION 4
EXPERIMENTAL PERFORMANCE OF ROCKING PRE-CAST POST-TENSIONED COLUMN

4.1 INTRODUCTION

This section describes the design, construction, instrumentation, testing and data analysis of a pre-cast, post-tensioned concrete column with a rocking base-foundation connection.

Based on conceptual development presented in section 2 and the design example given in section 3, a near full-size rocking column specimen was constructed as shown in figure 4-1. The main part of the column was circular with $610\,mm$ in diameter. The upper $762\,mm$ and lower $305\,mm$ of the overall $3048\,mm$ length consisted of a $610\,mm$ square in cross section. The transverse reinforcement consisted of D10 (#3) spiral with a variable pitch along column height as shown in figure 4-1. In order to provide a better confinement for sustaining high post-tensioning forces at both ends of the column, a tighter pitch for the spiral reinforcement was used at each end. The column was longitudinally reinforced with twelve D19 (#6) grade $414\,MPa$ deformed rebars.

The steel-steel interface was designed to take the high contact pressure at the rocking toe by using three $410 \times 610 \times 76\,mm$ steel plates; one at the bottom of column and two plated embedded into beam and anchored to the longitudinal reinforcement of that beam. Two $25\,mm$ diameter post-tensioned unbonded tendons were installed to connect the column and foundation beam pre-cast elements together. The construction procedures for each element are described as follows.

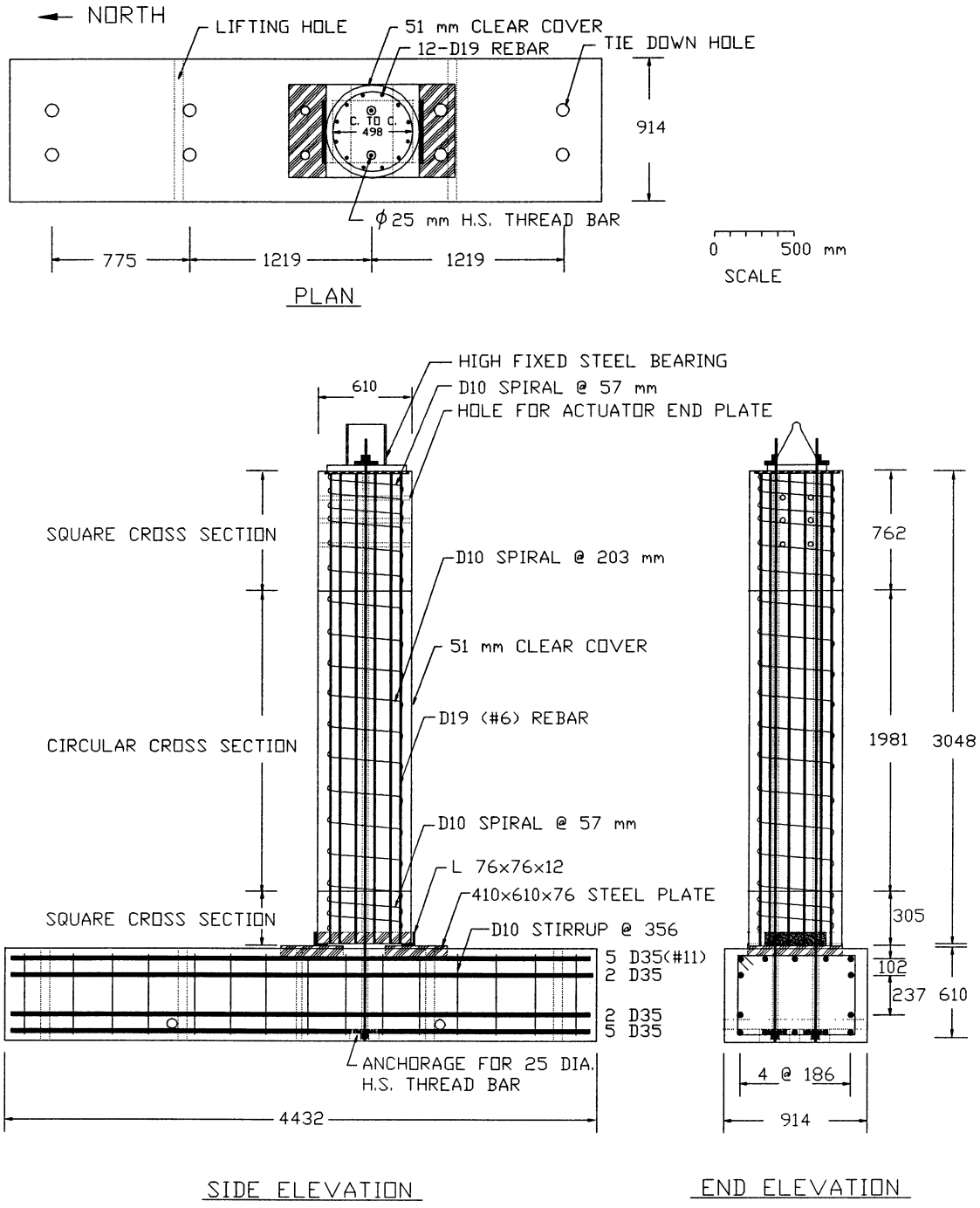

Figure 4-1 Construction details for the near full-size rocking column.

4.2 SPECIMEN CONSTRUCTION

4.2.1 The Foundation Beam

The foundation beam was first built for the test of another project and was modified for the present project. Two 38 *mm* diameter holes 305*mm* apart were drilled through the beam on the centerline of column to form ducts to pass and then anchor the two unbonded tendons (25*mm* high strength thread bars). The bottom end of holes were enlarged to 203 *mm* in diameter and 80 *mm* deep to seat the tendon anchorage.

Subsequently, on the top surface of foundation beam around column centerline, the cover concrete was removed by jack-hammering to expose the top layer of beam longitudinal reinforcement. Two 76 *mm* steel plates designed as the column-beam rocking interface were seated, leveled and welded to the beam reinforcement in the positions shown in figure 4-1. High performance high strength concrete (*EMARCO C77-CR* with water : mix ratio of 0.167) was poured into the cavity surrounding the steel plates to securely embed them. Finally, two steel angles designed as rocking guides/shear keys were welded on the top of the steel plates as shown in figure 4-1.

4.2.2 The Rocking Column

Longitudinal reinforcement evenly distributed around the perimeter was held in place by a steel plate on each end (top end with 13*mm* circular ring plate and bottom end with 76*mm* thick rectangular rocking base plate). After tying the transverse reinforcement, two 38 *mm* diameter plastic tubes were installed to form ducts for the two unbonded tendons parallel to the axis of the column, and also actuator holding bars (25*mm* high strength threadbars) passing through the top portion of the column.

Concrete for the column was poured in three stages. First, high strength concrete (mixed in the laboratory with a 7 day target strength of 48*MPa*) was poured into the square rocking base

(305*mm* in height). Next, the 610*mm* diameter cardboard tube form (1981*mm* in height) was fitted over the steel cage, plumbed and fastened to an external wooden falsework structure. Concrete provided by a local ready-mix supplier was then poured into the mold to providing the main portion of the circular column. After several days of curing, square plywood boxing (762*mm* in height) was fastened onto the top portion of the column. Finally, ready-mix concrete was poured into this box.

4.2.3 Beam-Column Assemblage

After one month of curing, the column was erected onto the steel plate seats on the foundation beam as shown in figure 4-1. Then, a high type fixed steel bearing was seated on top of the column for transferring the axial load from the lever beam. The bearing also served as an end-plate anchor for the two unbonded prestressing tendons. In order to monitor the stress state of tendons during testing, four strain gauges (two on each tendon wired as a half-bridge) were affixed on the tendon surface 25*mm* above the foundation beam. The two tendons were then stressed and anchored. Thus, the rocking pier specimen was completely assembled and ready for testing.

4.2.4 Materials

Ready-mix concrete for both the foundation beam and column was provided by a local supplier with a target 28 day strength 35*MPa*. Table 4-1 presents the measured compressive strength for each batch of concrete. Each value of compressive strength was obtained from the average of three compression tests on 152×305 *mm* cylinders. Stress-strain curves for the reinforcing steel are presented in figure 4-2 and values of the steel parameters are listed in table 4-2. The following symbols are used in table 4-2: f_c' = concrete compressive strength, d_b = nominal diameter of the bars, f_y = steel yield strength, f_{su} = ultimate stress of the steel, E_s = Young's modulus, ε_{su} = strain at ultimate stress, E_{sh} = strain hardening modulus, ε_{sh} = strain at onset of hardening.

Table 4-1 Compressive strength of concrete

Concrete		Compressive Strength f_c' (*MPa*)	
		28 days	**at time of testing**
Foundation beam		34	40
Column	Top	22	25
	Middle	26	30
	Base	43	46

Table 4-2 Steel properties

Steel	d_b (*mm*)	f_y (*MPa*)	E_s (*GPa*)	E_{sh} (*MPa*)	ϵ_{sh}	f_{su} (*MPa*)	ε_{su}
Threadbar	25	1025	200	3194	0.0170	1126	0.085
D19	19	437	199	8862	0.0070	687	0.100
D10	9.5	482	196	3679	0.0114	741	0.122

4.3 Experimental Apparatus

The experimental setup for testing the rocking column specimen is shown in figure 4-3. To prevent sliding of the specimen under lateral load, the foundation beam was anchored to the 457 *mm* thick laboratory strong floor by applying a prestress of 325 *kN* to four anchor bolts giving a total prestress 1300 *kN* to the strong-floor.

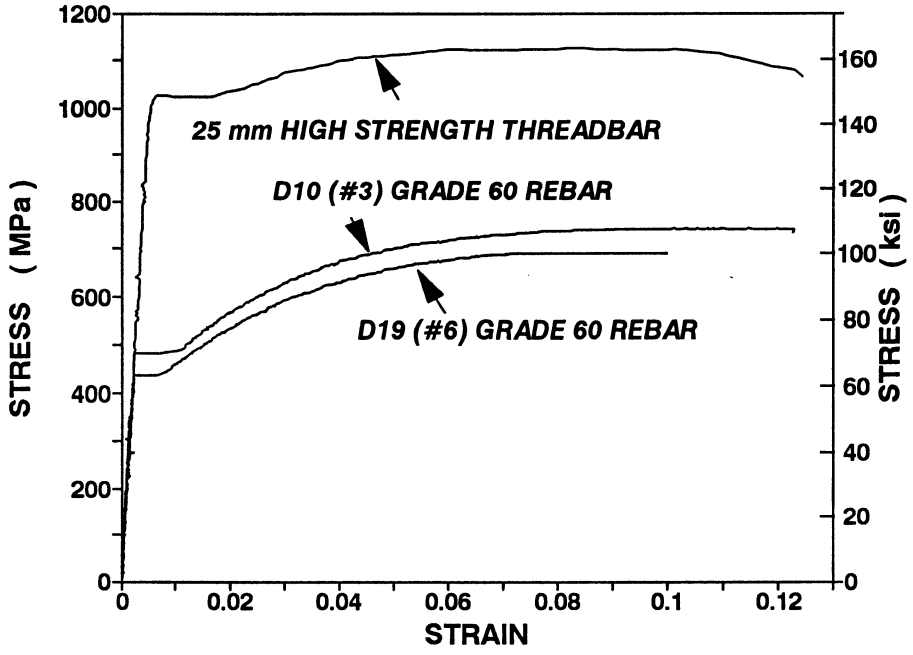

Figure 4-2 Stress-strain curve of reinforcing steel for the near full-size rocking column.

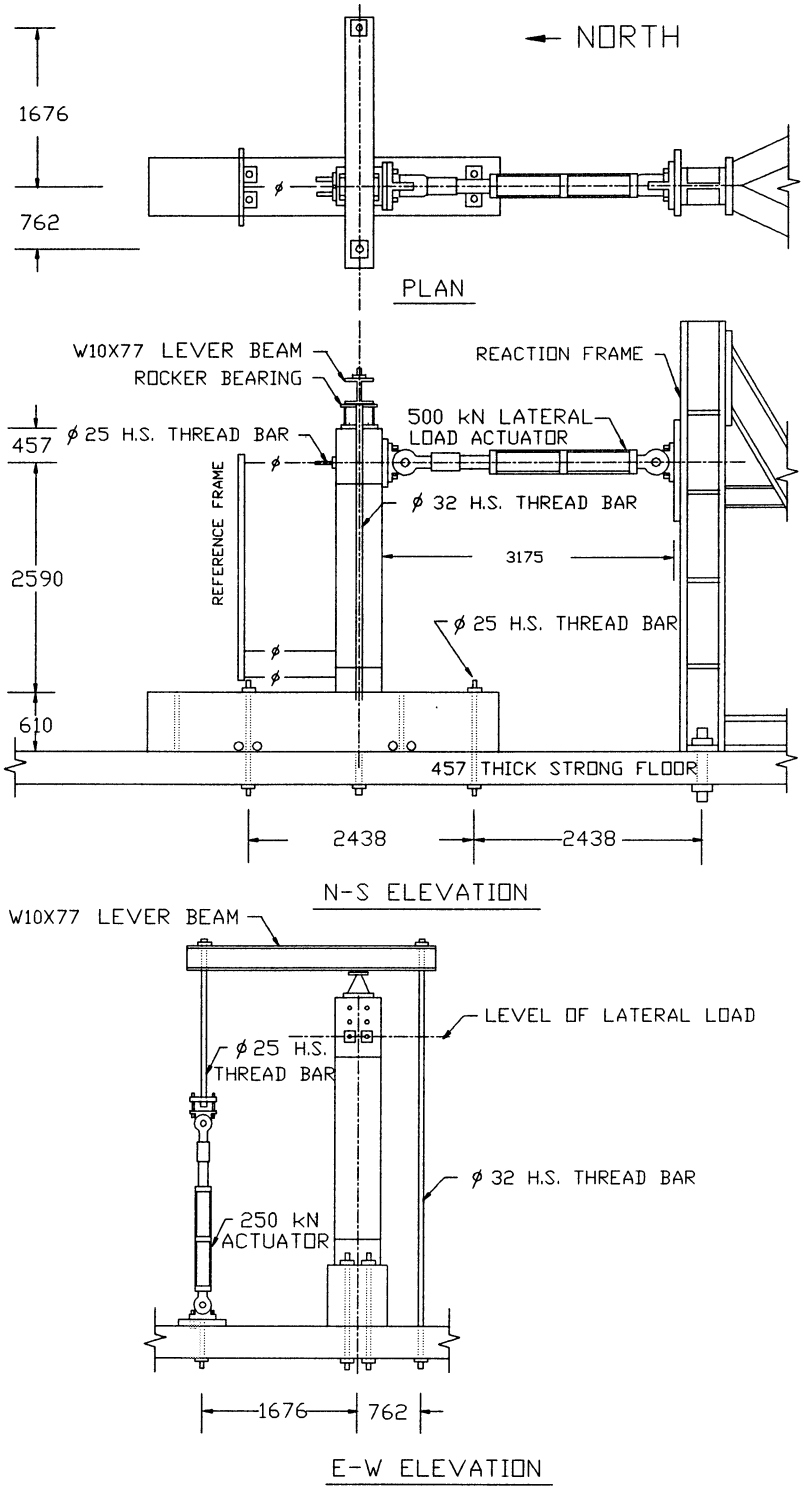

Figure 4-3 Test rig for the rocking column.

The lateral load was applied by a 500 *kN* servo-controlled MTS actuator at a height of 2590 *mm* above the base of the column, thus providing an aspect ratio of 4.25. The push load was directly transferred to the column through a 51*mm* thick steel adaptor plate, while the pull load was transferred by two 25 *mm* diameter high strength threadbars which were anchored on the opposite side of the column.

The gravity load was applied by a 250 *kN* hydraulic actuator through a *W10*×77 lever beam seated on a high type fixed steel bearing at the top of the column in a direction transverse to the axis of the lateral load. The lever beam system amplified the actuator load by a factor of 3.2, delivering a constant gravity load of 716 *kN* into the specimen.

4.4 Instrumentation and Data Acquisition

Forces, displacements, and column curvatures were measured by load cells, sonic and linear potentiometer displacement transducers, respectively. The arrangement of the transducers for the testing of the rocking column is presented in figure 4-4. Three sonic transducers were used to monitor the lateral displacements relative to foundation beam along the column height (*T1* to *T3*).

To measure the column rotations, four potentiometers (two on both sides) were used and mounted on two aluminum chassis (two potentiometers on one chassis); one covering an upper gauge length, the other covering the adjacent lower one. Each chassis was fixed to the end of a 13 *mm* threaded rod which had previously been cast into the concrete column during construction.

During testing, the output of all instruments was recorded by an Optim Megadac 5533A Data Acquisition system in an ASCII format. Data once captured cloud easily be ported to other computer systems for post-test analysis.

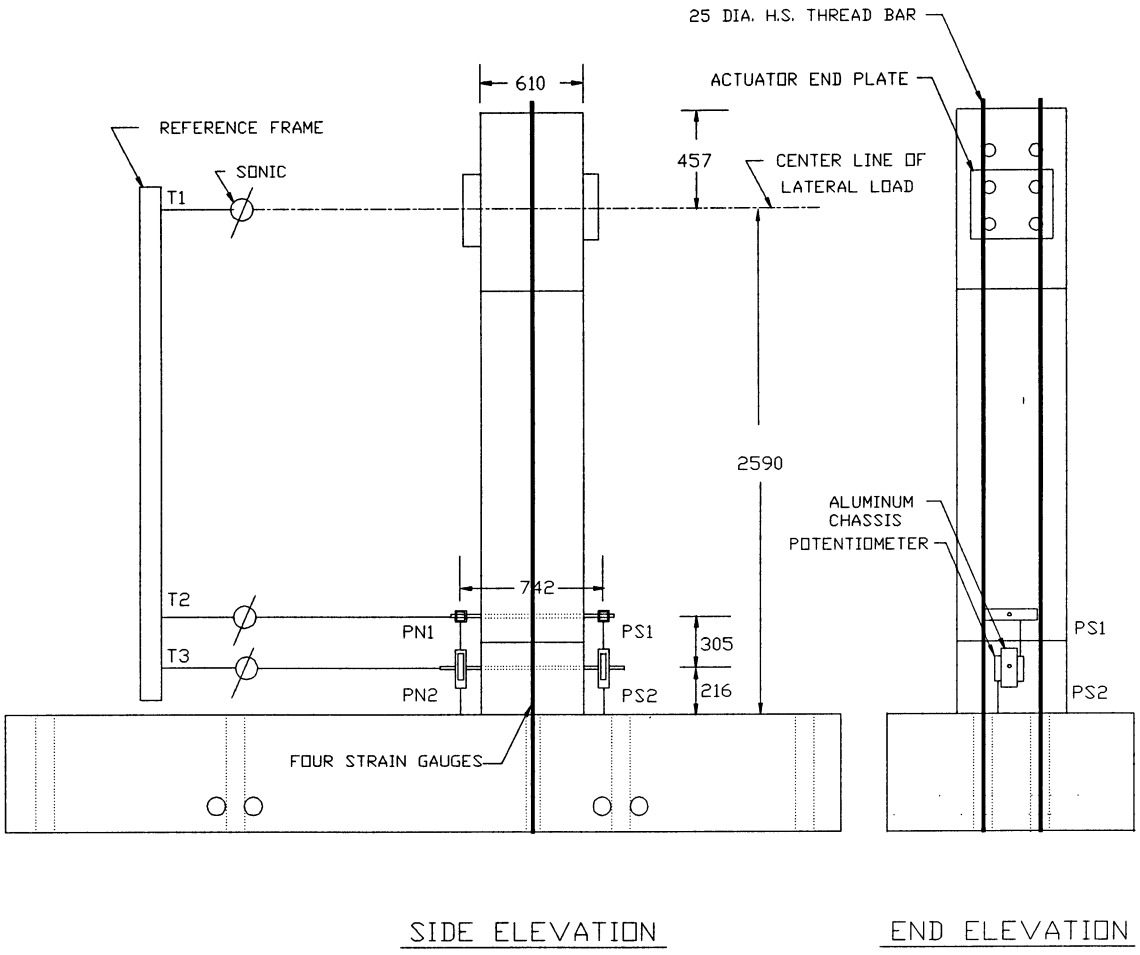

Figure 4-4 Instrumentation for the rocking column test.

4.5 DATA ANALYSIS

Column drifts θ were calculated by using the relation:

$$\theta = \frac{\Delta_1}{L} \tag{4-1}$$

where Δ_1 = displacement of top sonic transducer and L = clear column height.

Curvatures and strains (ϕ_i, ε_i) over the i-th gauge length were calculated from:

$$\phi_i = \frac{\Delta_{pi}}{L_{pi} L_{gi}} \tag{4-2}$$

and

$$\varepsilon_i = \frac{\Delta_{pi}}{L_{gi}} \tag{4-3}$$

in which Δ_{pi} = algebraic difference of readings from the potentiometer pairs, L_{pi} = center-to-center distance between the potentiometer pairs and L_{gi} = gage length.

Total displacements (Δ_t) of the column specimens were directly obtained from the readings of sonic transducers *T1* through *T6*. Flexural displacements Δ_f were calculated from the experimental curvatures using the moment area theorems as:

$$\Delta_f = \int_{y_A}^{y_B} \phi y \, dy \tag{4-4}$$

To evaluate this integral, the curvature diagram between points *A* and *B* was divided into n strips of height L_{gi} with curvature ϕ_i being measured at the center of each gauge length. Thus, equation (4-4) can be written in numerical form as:

$$\Delta_f = \sum_{i=1}^{n} (\phi_i L_{gi}) \, y_i \tag{4-5}$$

where y_i = moment arm of i^{th} strip about B.

If the flexural displacement is subtracted from the total displacement, then the remaining displacement is attributed to the effects of column shear as well as the component of displacement due to base rotation. Thus, for shear-rotation

$$\Delta_{sr} = \Delta_t - \Delta_f \tag{4-6}$$

By differentiating the shear and rotation displacements, the shear and rotation effects may be separated as shown in figure 4-5. Kim and Mander (1997) proposed a deformation model for shear and flexure in structural concrete members. The shear displacements were calculated based on a truss mechanism. The theoretical shear strain can thus be expressed as

$$\gamma = \frac{V}{K_{vs}} \tag{4-7}$$

where K_{vs} = cracked elastic shear stiffness. This cracked shear stiffness as a proportion of uncracked shear stiffness was therefore developed and shown in figure 4-6.

Hysteretic energy absorption (E_h) by the column per cycle is given by the area within the force-displacement loop. One cycle of loading is defined as one complete reversal between positive and negative drift amplitudes. The trapezoidal rule is used to find the hysteretical energy absorbed by the column resulting in

$$E_h = \sum_{i=1}^{n} \left(\frac{F_i + F_{i-1}}{2} \right) (x_i - x_{i-1}) \tag{4-8}$$

in which F_i = force in i^{th} step, and x_i = displacement of the same step.

The hysteretic energy absorption can be related to an Elasto-Perfectly-Plastic (EPP) material by: $E_h = \eta\ E_{EPP}$ where η = an efficiency factor, and E_{EPP} = the energy absorbed by a 100% perfect elasto-plastic system, defined as:

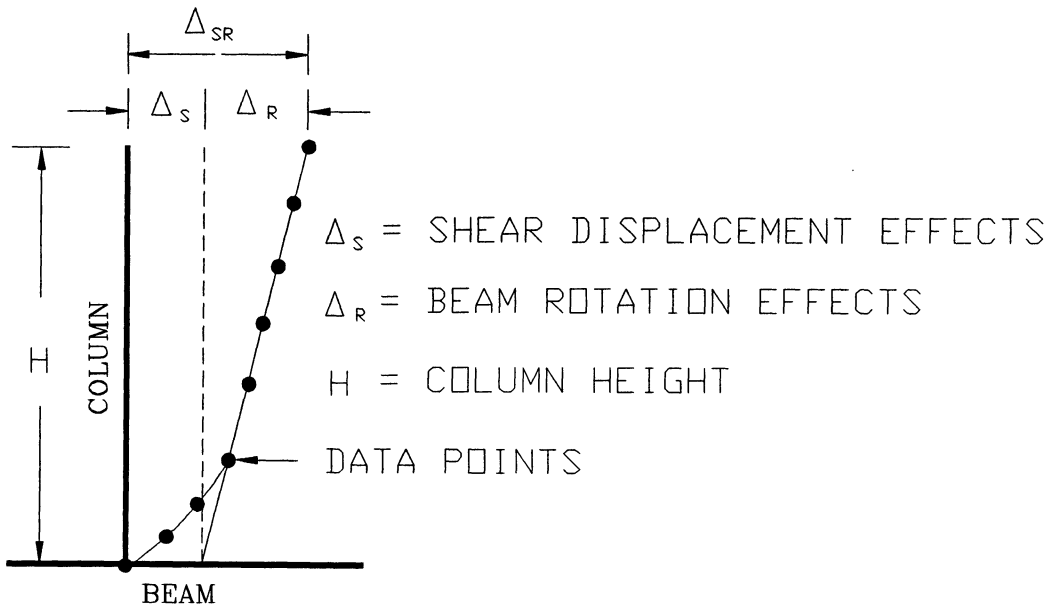

Figure 4-5 Separation of shear and rotation effects.

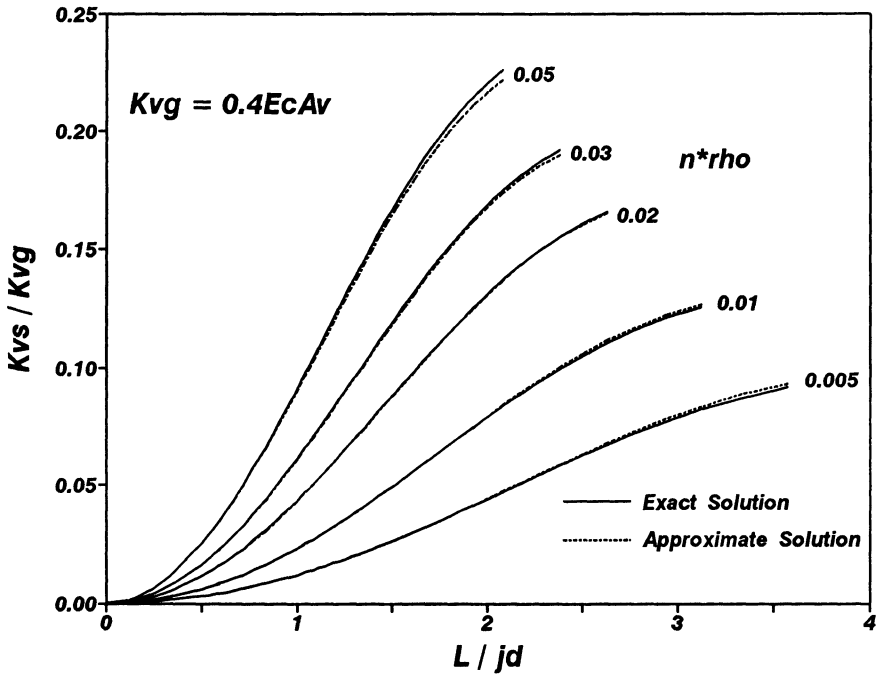

Figure 4-6 Theoretical cracked shear stiffness proposed by Kim and Mander (1997).

$$E_{EPP} = (M_n^+ + M_n^-)(\theta_p^+ + \theta_p^-) \quad \textbf{(4-9)}$$

where M_n^+ = the nominal moment capacity of column in the push direction, M_n^- = the corresponding value in the pull direction, θ_p^+ = the plastic component of the drift amplitude in the push direction, and θ_p^- = the corresponding value in the pull direction. The normalized energy is defined by dividing the energy in equation (4-8) by $(M_n^+ + M_n^-)$. Thus, by also dividing the E_{EPP} by $(M_n^+ + M_n^-)$ in equation (4-9), a comparison of the efficiency of energy absorbed by the column and a 100% EPP material can be obtained.

From the hysteretic energy absorbed by the column, two approaches for establishing the relationship between effective damping ratio and displacement ductility are proposed and described in what follows.

Cyclic Energy Absorption Efficiency (η).

One way to evaluate the equivalent damping ratio is by measuring the hysteretic performance using the concept of energy absorption efficiency with respect to an Elasto-Perfectly-Plastic (EPP) system. By dividing the real cumulative energy absorbed by the piers (that is the area under the load-displacement hysteretic loop) by equation (4-9), the efficiency of energy absorption along cumulative plastic drift can be obtained from

$$\eta = \frac{E_{cycle}}{E_{EPP}} \quad \textbf{(4-10)}$$

where E_{cycle} = energy absorbed in an entire pier system are one complete loading cycle (between drifts θ_p^- and θ_p^+). Generally, the values of η for a given loading cycle are initially constant until severe deterioration commences at the onset of either buckling of the longitudinal steel and/or spalling of the cover concrete.

Effective Viscous Damping Ratio (ξ_{eff})

One way to evaluate the effective damping ratio ξ_{eff} is directly calculating the equivalent damping ratio ξ_{eq} from the hysteretic area of column absorbed. Therefore, the effective damping ratio is defined as

$$\xi = \xi_o + \xi_{eq} = \xi_o + \frac{1}{2\pi} \frac{E_{cycle}}{F_{max} \Delta_{max}} \tag{4-11}$$

where ξ_o = ordinary structural damping (usually taken as 5% of critical), ξ_{eq} = equivalent damping ratio of column, F_{max} = average maximum strength in forward and reverse loading directions and Δ_{max} = average maximum displacements in both loading directions can be taken as $\mu \Delta_y$ where Δ_y is the yield displacement.

From the result of energy absorption efficiency for each bridge pier and assuming a bilinear hysteresis loop, the equivalent damping ratio ξ_{eq} for the bridge system can be derived as

$$\xi_{eq} = \frac{2\eta}{\pi} \frac{(1-\alpha)\left(1 - \frac{1}{\mu}\right)}{(1-\alpha+\mu\alpha)} \tag{4-12}$$

where, μ = displacement ductility factor and α = ratio between the post-yield stiffness and initial stiffness.

4.6 Experimental Procedures

Five distinctly different tests were conducted on the rocking column specimen. Each test was performed under displacement control where the command signal was provided by an analog function generator in the form of a positive sine wave (this loaded the specimen by firstly pushing and then pulling).

The first test (*RKG-GU*) was performed with a constant 716 *kN* gravity load and the presence of unbonded tendons throughout the test. The unbonded tendons were hand tight (snug) anchored without any pre-stress. The lateral load was applied by a series of variable drift amplitude sub-tests, each sub-test consisting of two cycles of loading at drift amplitudes of ±0.25%, ±1%, ±2%, ±3%, ±4% and ±5% with a 0.034 *Hz* (30 second period) frequency and a 6 *Hz* data acquisition sampling rate.

The second test (*RKG-G*) was performed with the same constant gravity load only and a loose anchorage for unbonded tendons at the top of column such that no lateral resistance by unbonded tendons during rocking was encountered. The lateral load was applied by a constant drift amplitude phase which consisted of two cycles at drift level ±5% with a 0.034 *Hz* cycling frequency and a 6 *Hz* data acquisition sampling rate.

The third test (*RKG-U*) was performed with the tendons being snug tight. The gravity load actuator was deactivated so no external axial load could be applied. The same lateral loading procedures as the previous test was applied to this test.

The fourth test (*RKG-RB*) was performed by the same procedures as the second test (*RKG-G*) except a 9.5*mm* thick rubber pad was installed at the base of the column and sandwiched between the column and steel angle rocking interface seats.

The fifth test (*RKG-PT*) was performed with post-tensioned tendons and the same constant gravity load. A post-tensioned force of 752 *kN* was applied to the two unbonded tendons, delivering a 742 *MPa* initial prestress in each tendon. After the bars were anchored, the strain gauges indicated that the prestress had relaxed to 696 *MPa*. Eventually after the application of the constant 716 *kN* gravity load through gravity load actuator, the stress in tendons further reduced to 669 *MPa* as a result of axial shortening. This gives an overall 10% loss of the initial prestress which is in the range expected for this class of prestressed concrete structure. The lateral load was applied in the form of a series of variable drift amplitude sub-tests, each sub-tests consisting of two cycles. Sub tests were performed at drift amplitudes of ±0.25%, ±0.5%, ±1%,

±2%, ±3%, ±4% and ±4.5% with a 0.017 *Hz* frequency (60 second period) and a 3 *Hz* data acquisition sampling rate (this approach gives 180 data pints per cycle of external loading).

4.7 Visual Observations

The rocking column specimen which was designed using the damage avoidance concepts (described previously in section 2) performed accordingly with absolutely no damage being observed. A few fine cracks were noticed for the test when the column was post-tensioned (test *RKG-PT*), but it should be emphasized that this was not damage, but rather regular flexural cracks that are to be expected as the cracking moment is exceeded. Figure 4-7(a) shows the extent of these fine flexural cracks. Figure 4-7(b) shows the uplift at the base when the column was rocking at a drift amplitude some 4%. From the figure, it is evident that the special detailing used at the foot of the column was effective in mitigating the high stress concentration when the column rocks back and forth from heel to toe.

4.8 Experimental Results

4.8.1 Force-Displacement Behavior

The lateral force-displacement behavior presented in terms of base shear capacity vs. drift angle for each test are plotted in figure 4-8. With the exception of test *RKG-U* (with the non-prestressed unbonded tendons only which performed linearly), all tests behaved in a bi-linear elastic fashion with little energy dissipation. Up to column drift angles of around 0.5%, when the uplift of column commenced and entered the second linear elastic range (rocking), the column behaved as a normal fixed base elastic structure.

Results from tests *RKG-GU*, *RKG-G* and *RKG-U* show that the lateral strength of column was basically resisted by two components: gravity load and restraint provided by the unbonded tendons. It was noted that a small hysteresis loop in the tests of *RKG-GU* and *RKG-G* was observed due to the slight variation of axial load. This resulted from the response lag of vertical

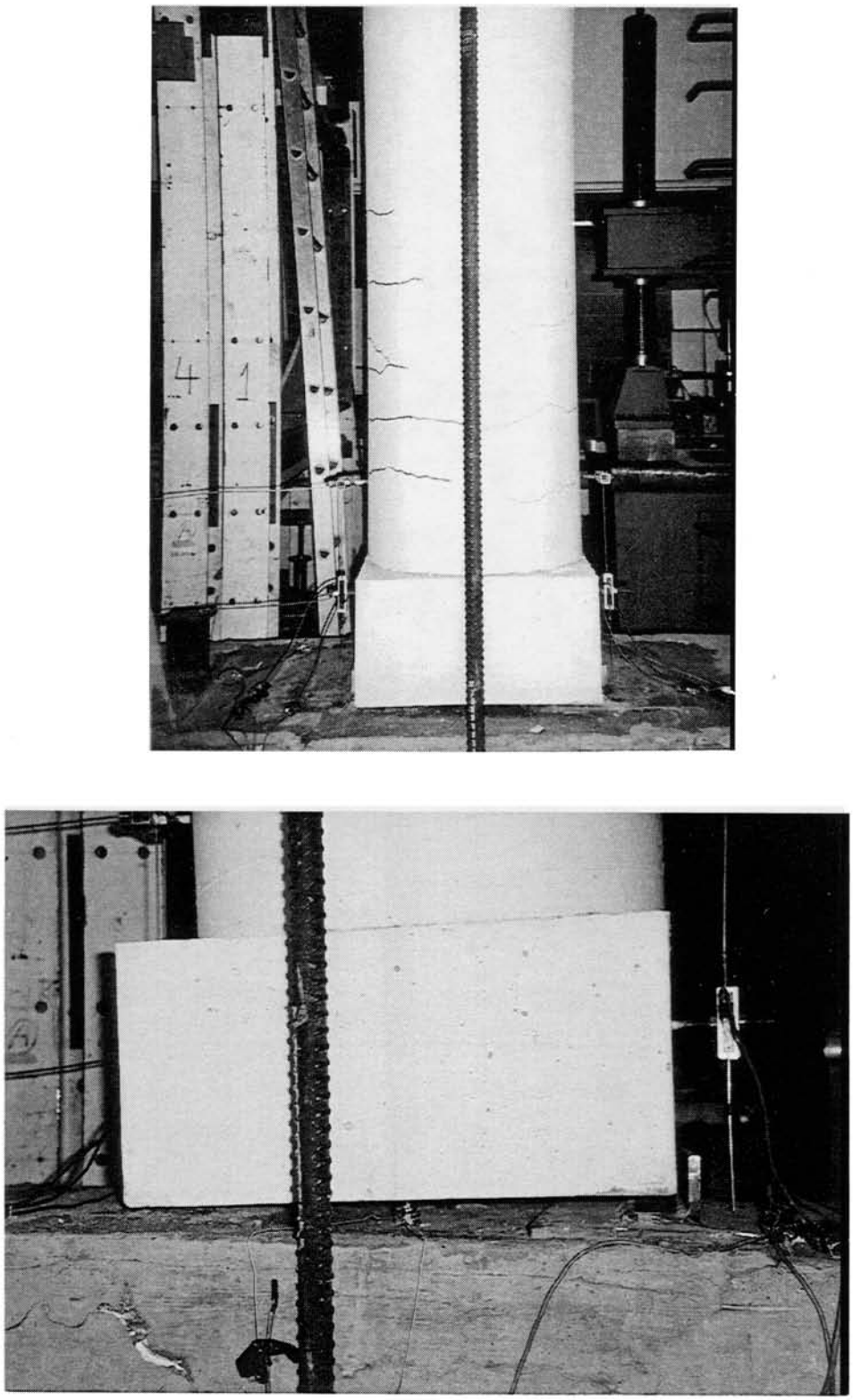

Figure 4-7 Photographs of rocking columns: top showing at the conclusion of 1% sub-test and bottom sowing the uplift of base during 4% sub-test.

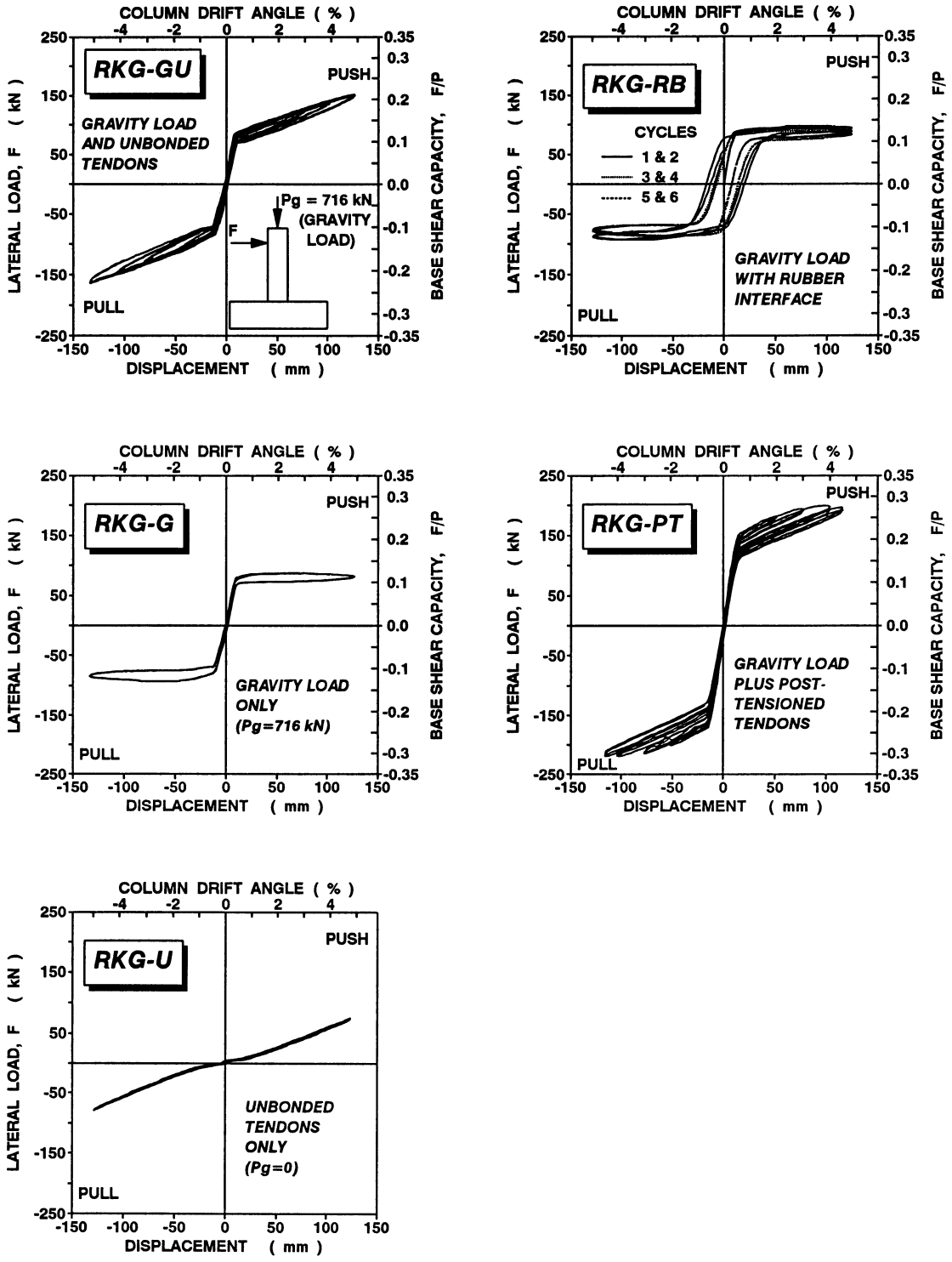

Figure 4-8 Hysteretic performance of the rocking columns.

load actuator to the command signal during loading and unloading. It may be observed that the faster the lateral loading was applied, the larger the variation of axial load. This is due to the inability of the vertical loading system to accurately follow the command signal under high speed lateral loading.

For the tests *RKG-RB* and *RKG-PT*, some energy was dissipated by the rubber seat during cyclic loading. However, due to progressive "cutting" of the rubber during rocking it was found the hysteretic energy absorption decreased as the number of cycles increased.

By applying prestress to the specimen increases of 40%, 70%, and 30% were observed in stiffness, uplift/rocking capacity and maximum lateral strength, respectively.

Under the same drift amplitude of 5%, the column with the gravity load only had a base shear capacity of around *0.1*. With the slack unbonded tendons, the column lateral resistance increased by *0.1* to give a total base shear capacity of *0.2*. The post-tension force resulting in the yielding of tendons during rocking also provided an increase in the base shear resistance by about *0.1* giving a total base shear capacity of *0.3*.

It is clearly evident that the performance of the post-tensioned rocking column is very satisfactory as good strength and deformation capacity may be attained——without damage. Finally, it should be emphasized that there was no residual drift observed at the end of each cycle of loading and hence re-centering is always ensured.

4.8.2 Total, Flexural and Rocking Displacements

When analyzing the behavior of conventionally constructed columns it is customary to examine the distribution of curvatures over the length of the member. However, it is a nonsense to examine curvatures of a rocking column that is in itself elastic at all times. For a rocking column, it is more important to examine the various contributions that make up the overall displacement, particularly the rotational component of rocking.

The various contributions of displacement (total, flexural, rocking, and foundation beam flexibility) that make up the overall displacement and distributed over the column height calculating using equation (4-4) and (4-6) are plotted in figures 4-9 and 4-10 for two contrasting tests. In figure 4-9 the results for the specimen seated on rubber pads (*RKG-RB*) are presented, showing a small but consistent contribution of displacement arising from apparent foundation flexibility and column flexure. In contrast to this, figure 4-10 shows the results for the post-tensioned specimen (*RKG-PT*). The apparent displacement due to flexibility and column flexure increases. Both increases are attributed to the high axial and lateral loads resulting from the post-tensioned tendon force.

4.8.3 Strength and Energy Dissipation

Envelopes of strength with respect to the total cumulative drift are shown for each test in figure 4-11(a). The largest strength envelop was observed for the test with the post-tensioned tendons (*RKG-PT*). The peak force reached a maximum level at the 4% drift amplitude; following this point the tendons yielded.

If the strength and displacement of the column at the onset of uplift are assumed to be equivalent to the "yield strength" and "yield displacement", then the energy dissipation can be normalized in accordance with equations (4-8) and (4-9). The normalized cumulative energy and cumulative plastic drift for the four tests is plotted in figure 4-11(b). In this graph, the dotted straight line represents an elasto-perfectly-plastic (EPP) material which has 100% efficiency, this is used as a reference to compare the efficiency of energy dissipation for each column. Due to the bi-linear elastic force-displacement behavior, the energy dissipation of the rocking column is relatively small when compared to the replaceable-hinge specimen tests. For each type of rocking column test, the energy absorption efficiency remains constant with respect to the drift amplitude.

The energy dissipated by the elastic unbonded tendons was very small and negligible. The average rates of energy absorption with respect to the 100% EPP material for the tests with

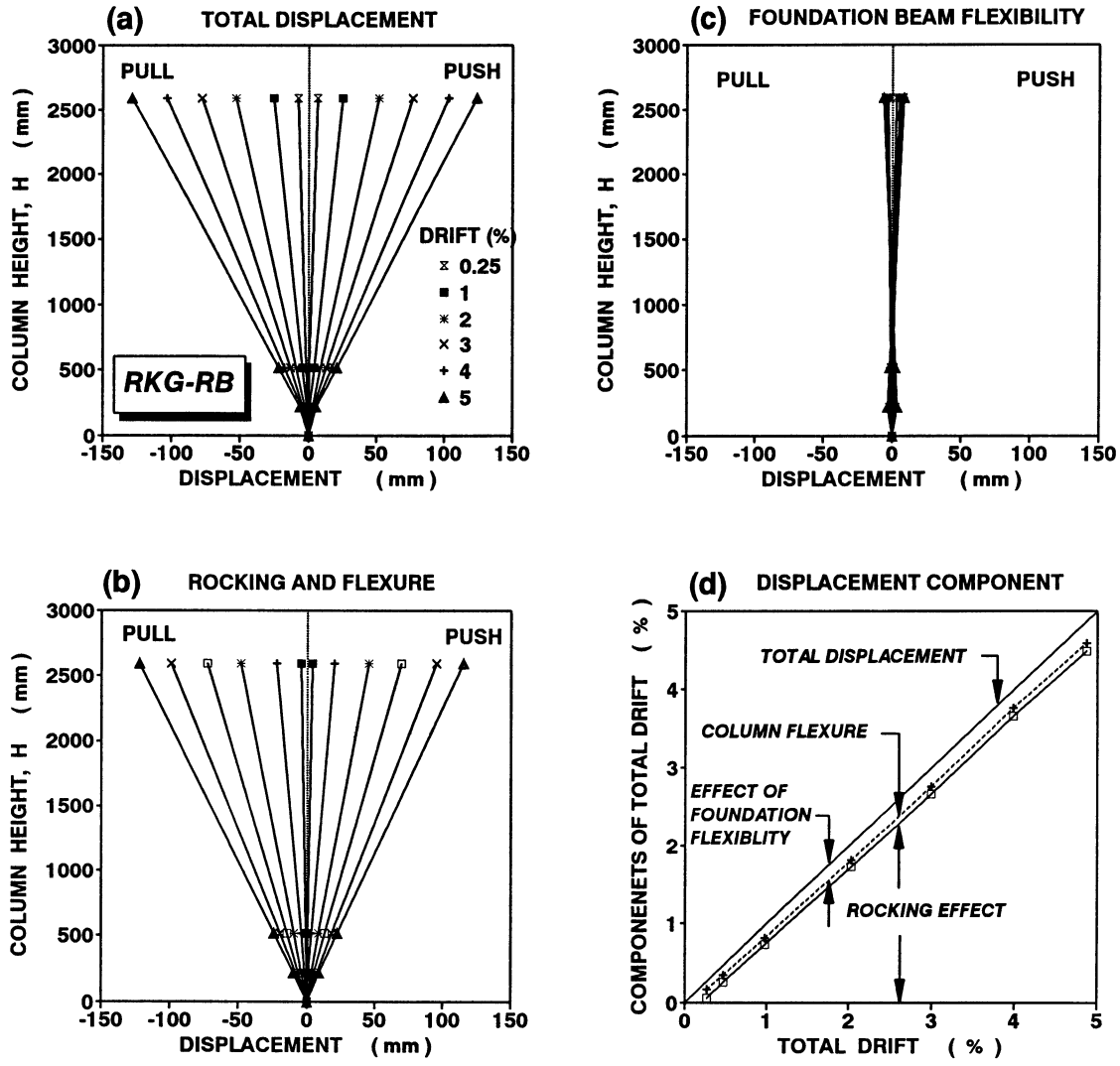

Figure 4-9 Distribution of experimental (total and flexure) and derived component of displacement for column *RKG-RB*.

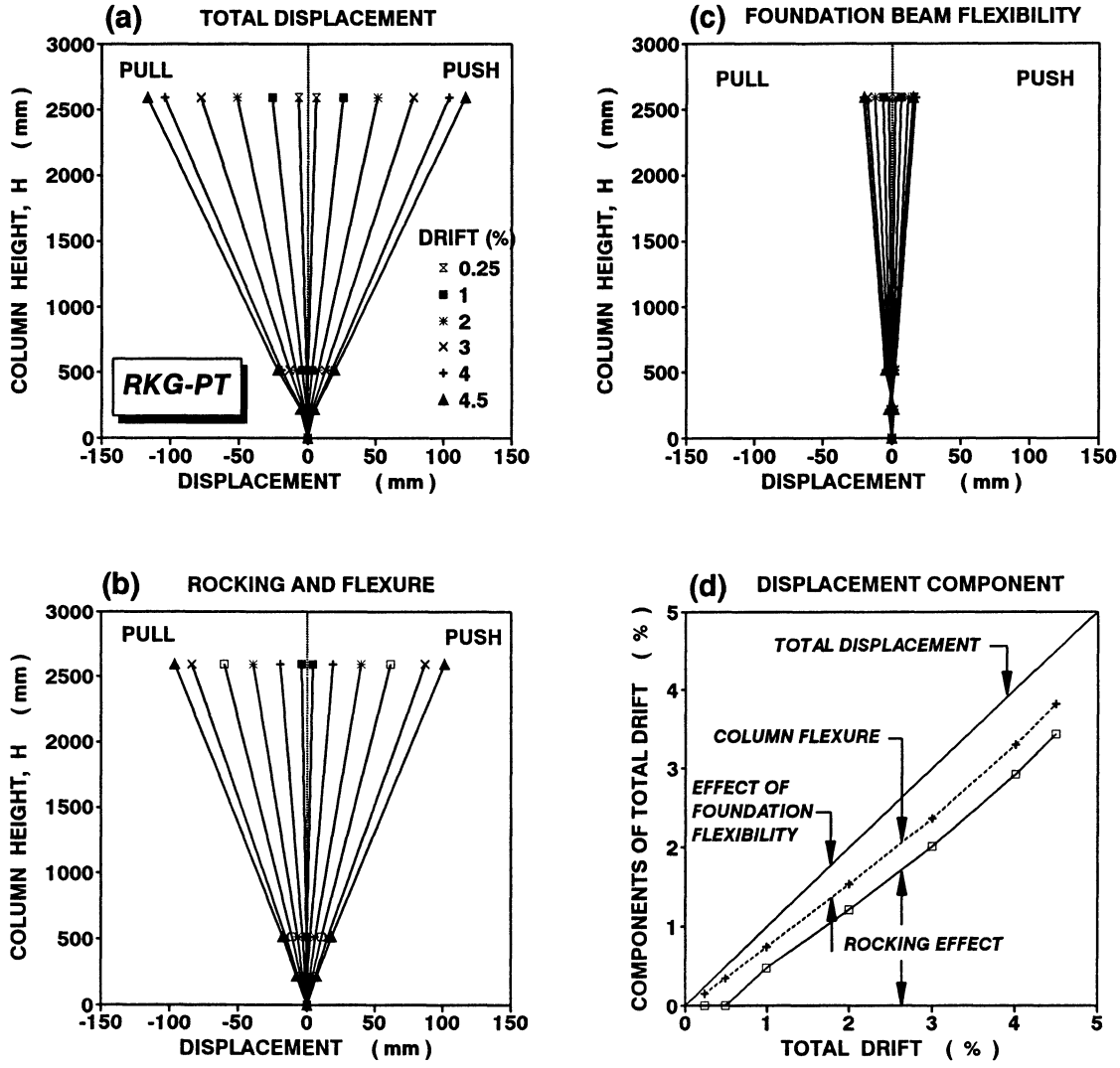

Figure 4-10 Distribution of experimental (total and flexure) and derived component of displacement for column *RKG-PT*.

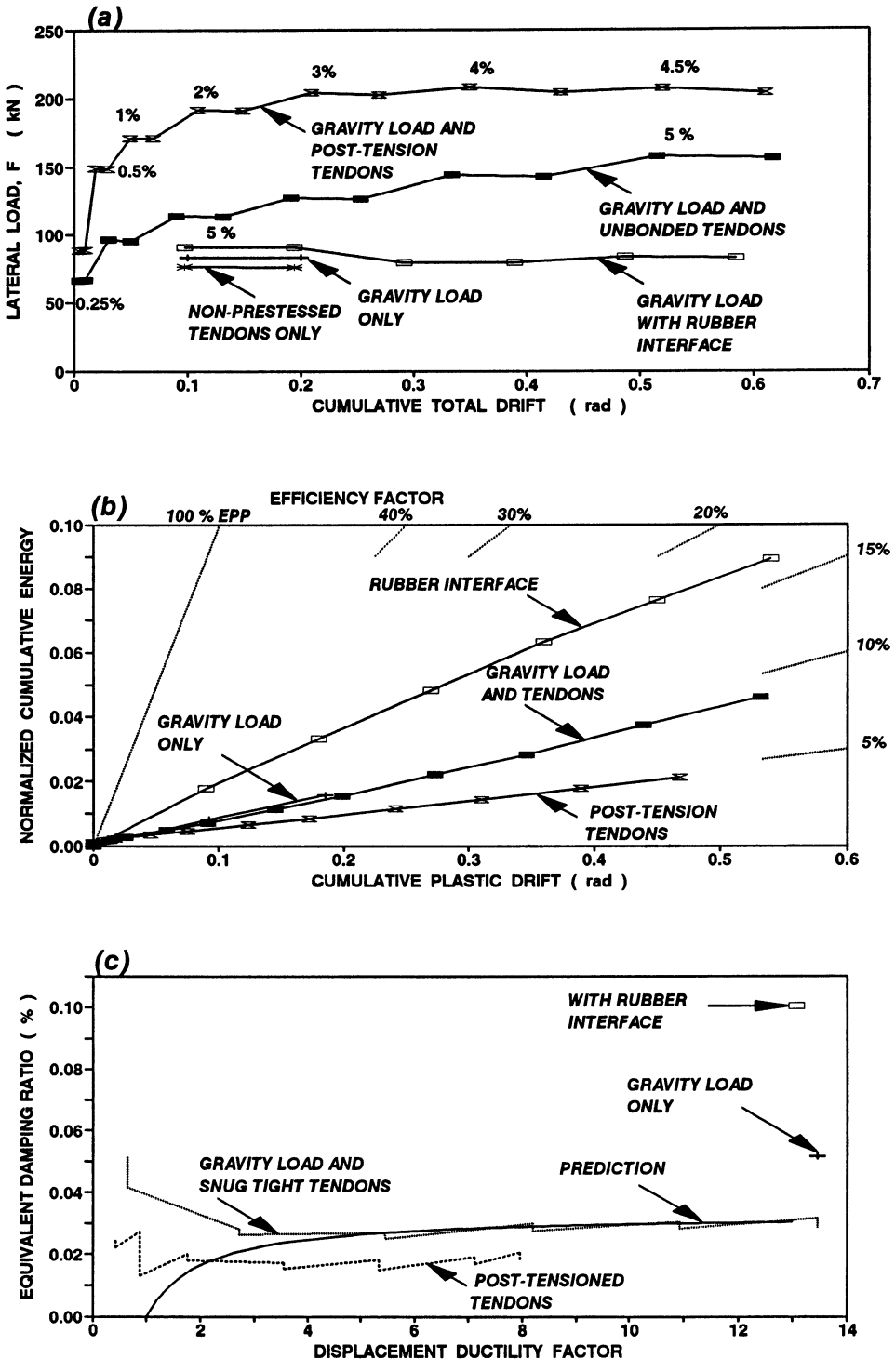

Figure 4-11 Cumulative performance of columns showing (a) peak lateral load versus cumulative total drift, (b) normalized cumulative energy versus cumulative plastic drift, and (c) equivalent damping ratio along μ_Δ.

the rubber interface, gravity load only, gravity load plus snug tight tendons, gravity load plus post-tension tendons are 17.9%, 8.6%, 8.1% and 5.2%, respectively. It is expected the test with post-tensioned tendons may have higher energy dissipation due to the yielding of tendons than the non-prestressed test. However, the post-tensioning evidently kept the nonlinear flexural (cracked) behavior to a minimum thus minimizing material nonlinear behavior and maximizing structural geometric (rocking) nonlinear response.

4.8.4 Equivalent Damping Ratio

Based on equation (4-11), the equivalent damping ratio in terms of the displacement ductility factor for each test is plotted in figure 4-11(c). Due to the low rate of energy absorption of rocking columns, corresponding low equivalent damping ratio of less 5% is in distinct contrast with 20% a rate typical of conventional construction as suggested by Priestley (1996b). With the rubber interface, the equivalent damping ratio increases to 10%, this is due to the material non-linearity of the rubbers.

Figure 4-11(c) shows that when equation (4-12) is used to predict the equivalent viscous damping reliable predictions can be made, but only when displacements exceed uplift. For small (pre-uplift) displacements usual assumptions relating to structural damping apply.

4.9 SUMMARY

The experimental performance of the rocking columns designed in accordance with the damage avoidance concept (DAD) was investigated. Test results showed that less lateral strength capacity in rocking columns is obtained than the traditional construction with ductile columns. However, more importantly, rocking columns can be designed, detailed and constructed to behave in an elastic fashion at all times. Although they possess a lower lateral strength, rocking piers can be easily tuned to the design requirement by simply altering the semi-base width, the axial load/prestress or both. It should be emphasized that rocking bridge piers not only adapt to large lateral deformations but also maintain their strength without any

deterioration in strength capacity under many cycles of loading.

Although yielding of the prestressing tendons may occur during a large seismic excitation, plastic strains in the tendons are expected to be very small. Therefore, after a strong earthquake, the tendons do not need to be replaced, but the prestress (if any) should be checked and retensioned, if necessary.

In summary, rocking bridge piers have certain distinct advantages: no earthquake induced structural damage, recentering of the structure, and therefore immediate post-earthquake serviceability. Further advantages can be realized in terms of economy of construction. As rocking bridge piers lend themselves to an assemblage of precast elements, considerable time savings can be made in the construction schedule. This is an especially important consideration for construction sites where the harsh winter climate necessitates cessation of all work activity for several months. This winter period can be utilized manufacturing and curing the precast elements under cover in controlled factory-like conditions.

SECTION 5
MODELING EXPERIMENTAL RESULTS

5.1 INTRODUCTION

This section presents the force-deformation modeling of the experimental results described in the previous section. This force-deformation model integrates four important aspects of behavior: rocking, structural flexibility, prestressing and friction. Based on this comprehensive force-deformation model, push over analyses are performed which consider real (experimental) p-delta effect. The predictive results are compared with the experimental observations.

5.2 FORCE-DISPLACEMENT MODELING

The use of unbounded tendons not only connects the column to the pier and/or pile cap beam, but also provides enhanced lateral resistance, shear resistance at a joint region, stability and ductility for the rocking column. As a consequence, the total lateral resistance of the pier results from a combination of gravity load, (provided by the superstructure) and additional axial load provided by the unbounded tendons within the column.

The force-displacement relation is expected to be bi-linear elastic. The first elastic range is governed by the structural flexibility of the rocking column until the commencement of uplift. Following uplift the force-displacement relation enters a second elastic range which is governed by the rocking of the column. The prestressing force will affect the column stiffness and strength in both the pre-rocking and post-rocking stages. By integrating these four aspects of behavior (rocking, structural flexibility, prestressing and friction), it is possible to develop theoretical force-displacement relationships.

Within the limitation of space in the laboratory, a typical bridge substructure (one-quarter of a twin-column pier bent) was assembled and tested, with results presented in section 4. Such a bridge substructure designed in accordance with the damage avoidance concepts was subjected to the axial and lateral load as plotted in figure 5-1(a). The force-displacement behavior is analyzed in the following subsections:

5.2.1 Pre-Rocking Behavior

Prior to uplift, the force-displacement relation of the system is governed by the elastic flexibility of the column and foundation and may be found from

$$\Delta_t = \Delta_f + \Delta_s + \Delta_\theta \tag{5-1}$$

where Δ_f = flexural displacement of the columns, Δ_s = shear displacement of the columns and Δ_θ = the rotational displacement of the column resulting from the deformation of the foundation beam. These three components of displacement are explained below.

The *flexural* displacement of a cantilever column is given by

$$\Delta_f = \frac{FL^3}{3EI_{eff}} \tag{5-2}$$

where L = length of the column, EI_{eff} = effective flexural rigidity of the column which may be taken as $0.5EI_g$ for the reinforced column and $0.7EI_g$ for the prestressed column (Priestley et al., 1996).

The *shear* displacement is given by

$$\Delta_s = \frac{F\alpha_f L}{GA_v} \tag{5-3}$$

where α_f = the form factor, $G = 0.4E_c$ for concrete and A_v = shear area.

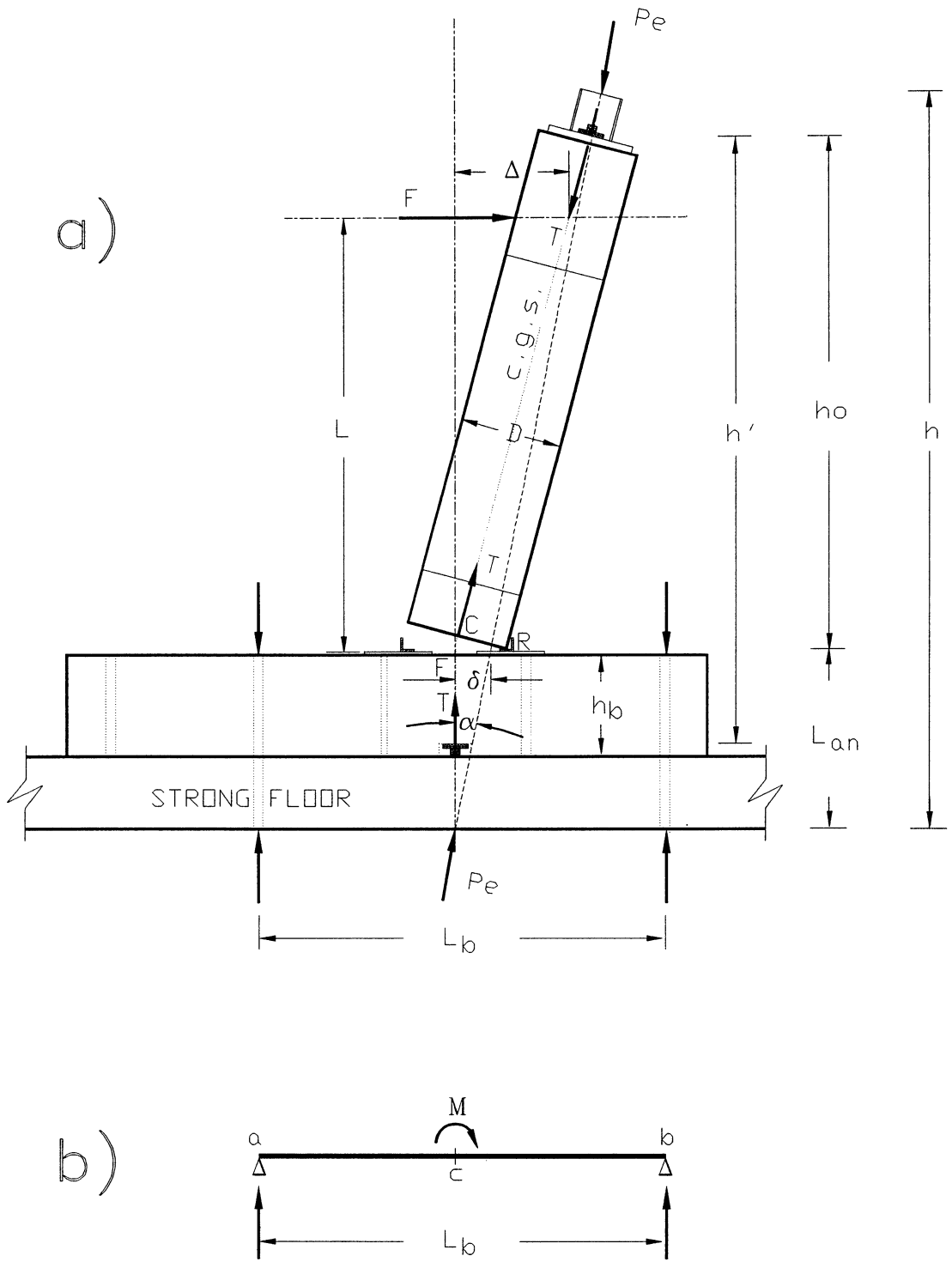

Figure 5-1 Schematic graphs showing (a) relations of forces in the rocking column and (b) forces in simple support foundation beam.

As shown in figure 5-1, the *rotational* contribution that arises from the flexibility of the foundation beam may be determined from

$$\Delta_\theta = \frac{F\left(1 + \frac{h_b}{2L}\right)L^2 L_b}{12EI_b} \tag{5-4}$$

in which h_b = beam depth, L_b = beam length between supported ends, EI_b = flexural rigidity of the foundation beam.

Combining component flexibilities, the total pre-uplift elastic stiffness of the column can be found from

$$\frac{1}{K_e} = \frac{L^3}{3EI_{eff}} + \frac{\alpha_f}{0.4EA_v} + \frac{\left(1 + \frac{h_b}{2L}\right)L^2 L_b}{12EI_b} \tag{5-5}$$

Inverting and rearranging such that $K_{col} = 3EI_{eff}/L^3$ gives

$$K_e = \frac{K_{col}}{1 + \frac{7.5\,\alpha_f}{L^2}\frac{I_{eff}}{A_v} + \frac{1}{4}\left(1 + \frac{h_s}{2L}\right)\frac{L_b}{L}\frac{I_{eff}}{I_b}} \tag{5-6}$$

5.2.2 Post-Rocking Behavior

If the column rocks on a rigid (steel-steel) foundation surface with a lateral displacement Δ (measured at the point of the application of the lateral force F), then by taking moments about the rocking toe as shown in the figure 5-1, moment equilibrium requires:

$$FL = P_e(B - \delta) + TB \tag{5-7}$$

where L = the lever arm of lateral load, P_e = the external axial load, B = semi-width of the column, δ = offset dimension of the line of the axial load to the column centroid at the rocking interface and T= total internal tendon force which can be calculated from a stress-strain relationship with an upper limit of the yielding force of the tendons given by

$$T = E_s A_s (\varepsilon + \varepsilon_o) \leq A_s f_y \tag{5-8}$$

in which E_s = Young's modulus of tendons, A_s = total area of tendons, ε = strain in tendons due to rocking, ε_o = strain in tendons due to post-tensioned prestress and f_y = yield stress of tendons.

From geometry, the strain in the tendons due to rocking ε and lever arm δ can be separately calculated as

$$\varepsilon = B\left(\frac{\Delta - \Delta_e}{L\,h'}\right) \tag{5-9}$$

and

$$\delta = L_{an}\,\alpha = L_{an}\,\frac{h_o\left(\frac{\Delta}{L}\right)}{h} \tag{5-10}$$

where h' = length of unbounded tendons between two anchorages, Δ_e = lateral elastic displacement at the onset of uplift and L_{an} = length from the soffit of strong floor to the foundation surface. Substituting equation (5-9) into (5-8), one can obtain

$$T = E_s A_s\left(\frac{B(\Delta - \Delta_e)}{L h'} + \varepsilon_o\right) \tag{5-11}$$

If the friction force resulting form the angle change of tendons during rocking is accounted for, the change in tendon force from point C (bottom of the column) to point F (top of the foundation beam) can be found as follows (Collins and Mitchell, 1990):

$$T_{FL} = T_{CL}\, e^{-(\mu_f \theta + kx)} \tag{5-12}$$

where T_{FL} and T_{CL} are the tendon forces at points F and C during uplift, respectively. The μ_f and k are respectively the friction and wobble friction coefficients between tendons and duct. Also, the θ and x are the total angle change and tendon length between points F and C, respectively. The value of T_{CL} can be directly substituted by equation (5-11). A friction coefficient μ_f = 0.5 between tendons and duct is adopted. Because the tendons within the

transition of angle change appear in the air without the duct during rocking, the wobble friction can be neglected. The tendon force at the point F becomes

$$T_{FL} = T\, e^{-\mu_f \theta} \tag{5-13}$$

During uplift, the tendons move upward and the friction force act downward so that the tendon force in the point C is greater than that of point F, and vice versa during unloading. When the unloading commences, the tendon force in the point C (bottom of the column) is given by

$$T_{CU} = T_{FU}\, e^{-\mu_f \theta} \tag{5-14}$$

where T_{CU} and T_{FU} are the tendon forces at the points F and C during unloading, respectively.

At the onset of unloading, the tendon force in the point F during loading and unloading should be the same. The tendon force at the point C during unloading is obtained by combining equations (5-13) and (5-14) as

$$T_{CU} = T\, e^{-2\mu_f \theta} \tag{5-15}$$

Because a small angle change of tendons is expected, the equation can be simplified by taking only the first term in a Taylor series expansion, thus

$$T_{CU} = T\,(1 - 2\mu_f \theta) \tag{5-16}$$

From geometry, the angle change is the uplift angle of the rocking base so that

$$T_{CU} = T\left[1 - 2\mu_f \frac{(\Delta - \Delta_e)}{L}\right] \tag{5-17}$$

Applying equations (5-10) and (5-11) into (5-7), the lateral force during loading case is given by

$$F_L = (P_e + T)\frac{B}{L} - P_e\frac{L_{an}h_o\theta}{hL} \tag{5-18}$$

Similarly, the lateral force during unloading case can be obtained by substituting the equations (5-10), (5-11) and (5-17) into (5-7), that is

$$F_U = (P_e + T_{CU})\frac{B}{L} - P_e\frac{L_{an}h_o\theta}{hL} \tag{5-19}$$

The differential friction force can be obtained by subtracting lateral force for unloading curve (equation (5-19)) by loading curve (equation (5-18))

$$\Delta F = (2\mu_f\theta)T \tag{5-20}$$

Therefore, lateral force for both loading and unloading curves can be expressed as

$$F = \left(P_e + T(1 + \mu_f\theta\, sgn\dot{\theta})\right)\frac{B}{L} - P_e\frac{L_{an}h_o\theta}{hL} \tag{5-21}$$

where $sgn\dot{\theta}$ is positive for loading and negative during unloading.

By using equations (5-6) and (5-21), a bilinear force-displacement behavior of the rocking column can thus be obtained.

5.3 Modeling Results

Figure 5-2 presents both the analytical and experimental results of three tests, including the test with the gravity load and non-prestressed unbounded tendons (*RKG-GU*), the test with the gravity load only (*RKG-G*) and the test with unbounded tendons only (*RKG-U*). The test of (*RKG-GU*) can be treated as the summation of the other two tests: *RKG-G* and *RKG-U*. Based on the experimental results stated in the section 5.7, the hysteresis energy of the gravity load test came from the various response of the vertical actuator during loading and unloading, and a small contribution from friction. For simulation, the analytical predictions are calculated by the experimentally variable axial load varied with displacement rather than a fixed axial load. The

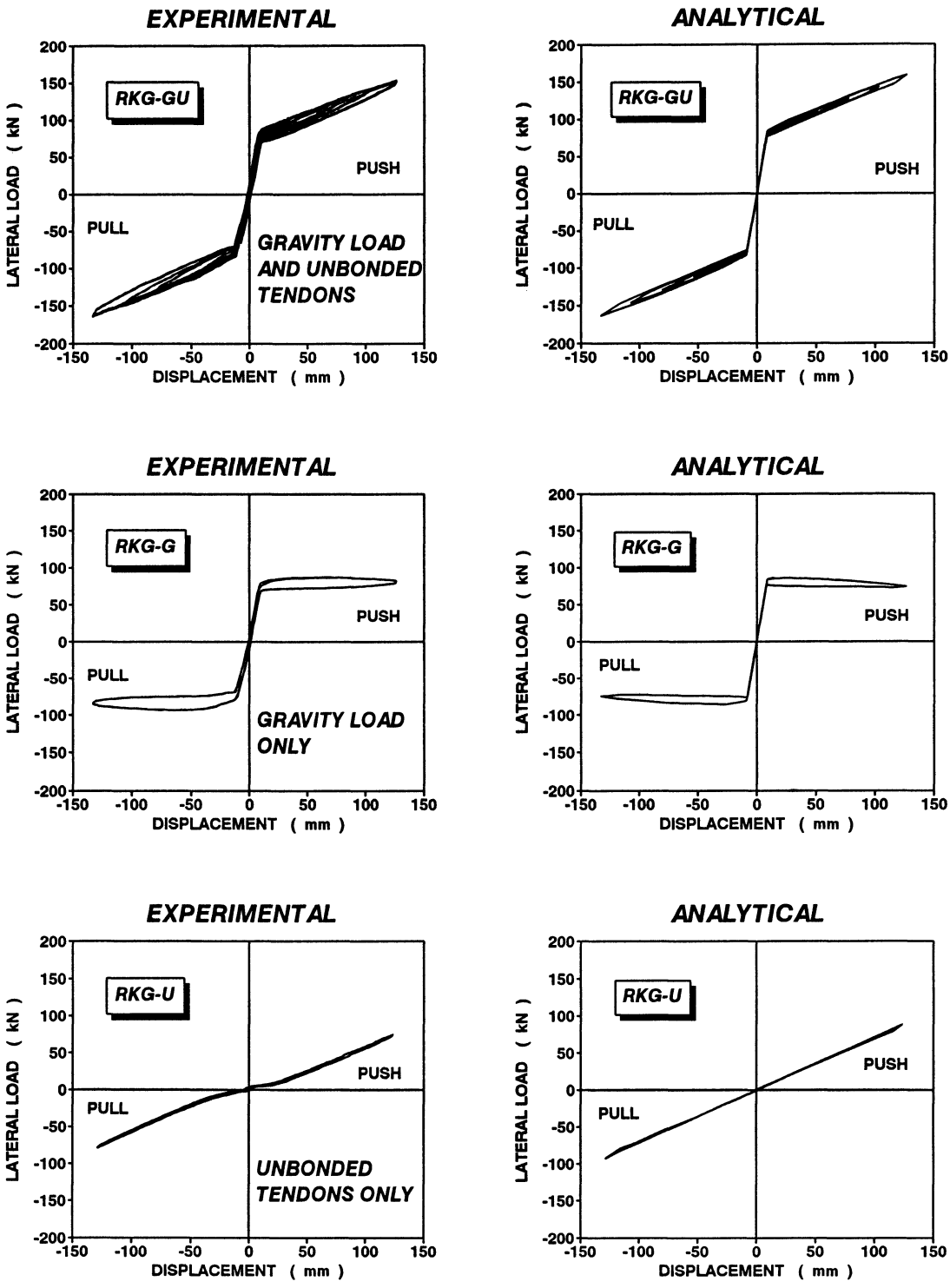

Figure 5-2 Comparison of hysteretic performance between experimental and analytical results for rocking column test *RKG-GU*, *RKG-G* and *RKG-U*.

difference is attributed to friction within the experimental apparatus. Analytical predictions show slightly less hysteresis energy than the experimental results. However, satisfactory agreement between the two for three tests was obtained, as seen in the figure 5-2.

The experimental results with rubber interfaces (*RKG-RB*) showed a larger energy absorption. During the test, the cutting and compressing of soft rubber by the steel rocking toe was visually observed. Therefore, instead of a distinct lever arm for the axial load, a varying lever arm (*B*) is assumed to occur during rocking. This is shown schematically in figure 5-3. Accordingly, the experimental and analytical results are plotted together in figure 5-4, where the result for the case with post-tensioned tendons is also presented. As shown in the figure, good agreement between the two for these cases is evident. Moreover, a relation of stress calculated from the prediction and strain measured form the strain gauges are also presented for the test with post-tensioned tendons. In the figure, a sudden elongation in tendons measured by strain gauges that was larger than the calculated strain took place when yielding of tendons commenced.

5.4 Push Over Analysis

Due to the test apparatus of the laboratory, the P-delta effect is expected to be less than that in the real situation in the field. Therefore, based on the model derived in the previous section, a pushover analysis using the real P-delta effect was performed with results presented in figure 5-5. Figure 5-5(a) shows the result with the presence of the axial load, whereas figure 5-5(b) shows the result without axial load. The later scenario is considered to be a critical situation that might occur in the presence of large vertical (downward) accelerations where the effect of gravity load is lost.

As seen in figure 5-5(a), the unbounded tendons greatly increase the drift level of overturning from 12% to 27%. This is in spite of whether the tendons are initially post-tensioned or just slack. The initial prestress force in the tendons increases the stiffness and lateral strength of the column only in the pre-yield range; in the post-yield range the strength

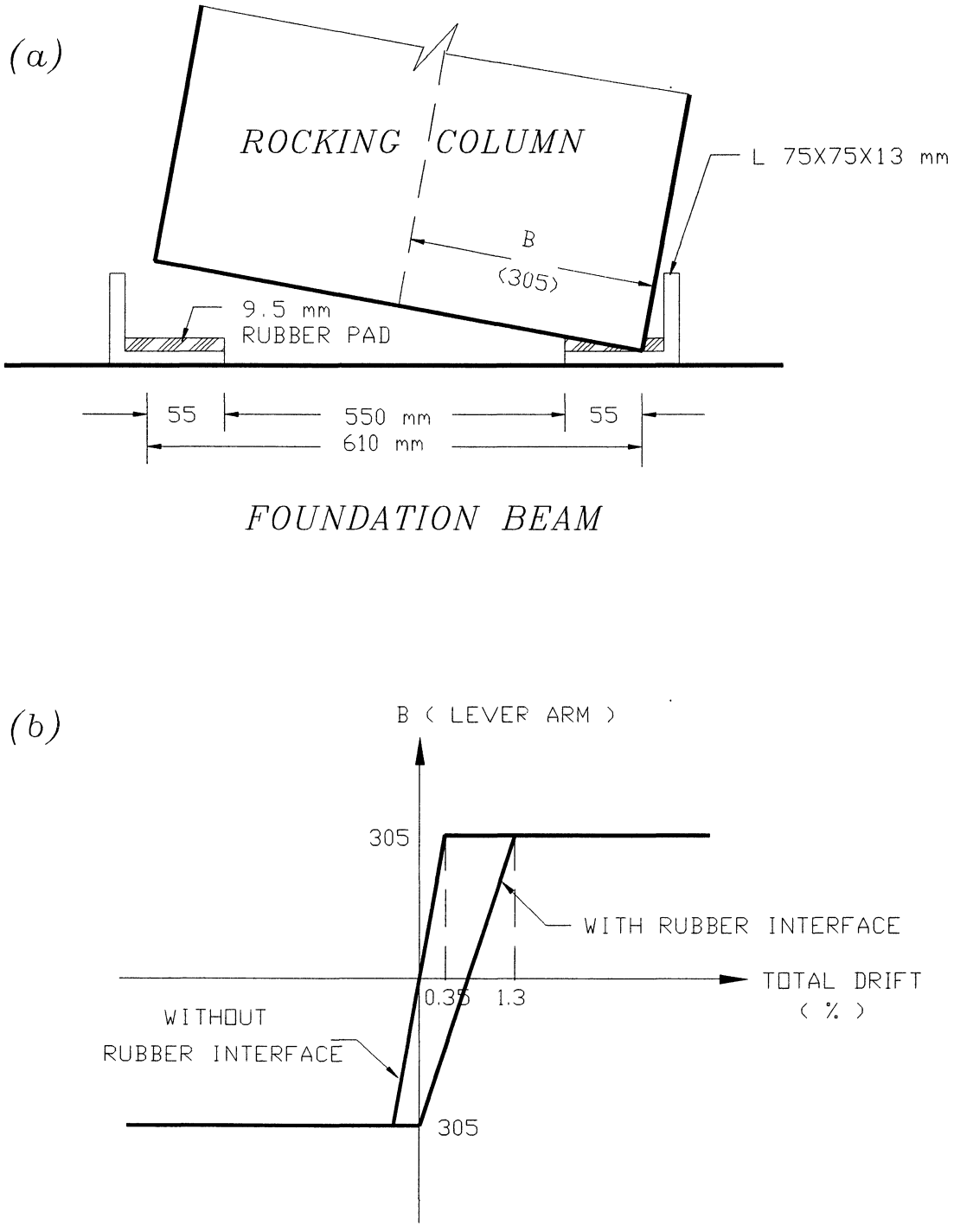

Figure 5-3 Schematic details showing (a) rocking base with rubber interface (b) variation of lever arm during cyclic rocking.

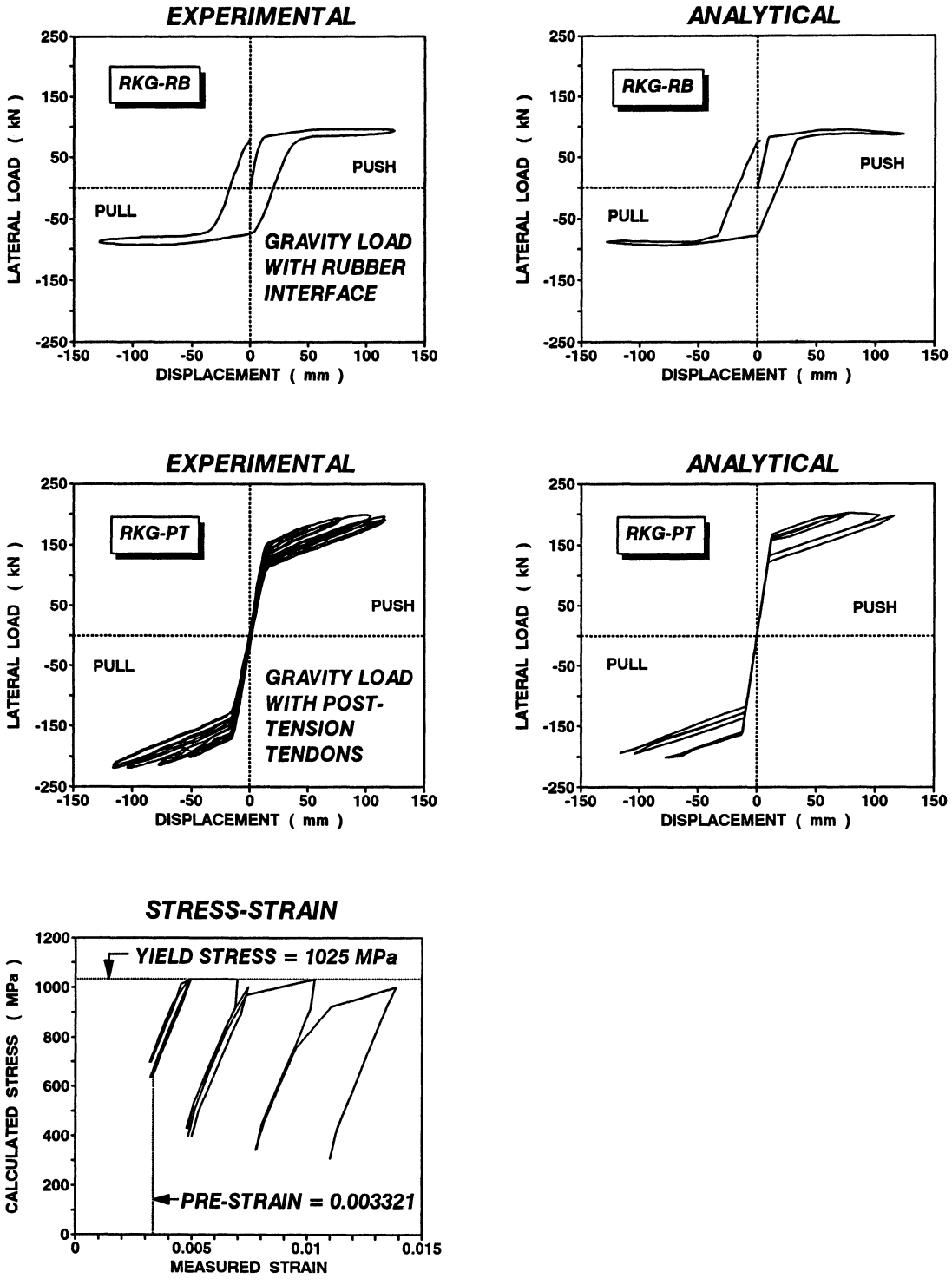

Figure 5-4 Comparison of hysteretic performance between experimental and analytical results for rocking column test *RKG-RB* and *RKG-PT*.

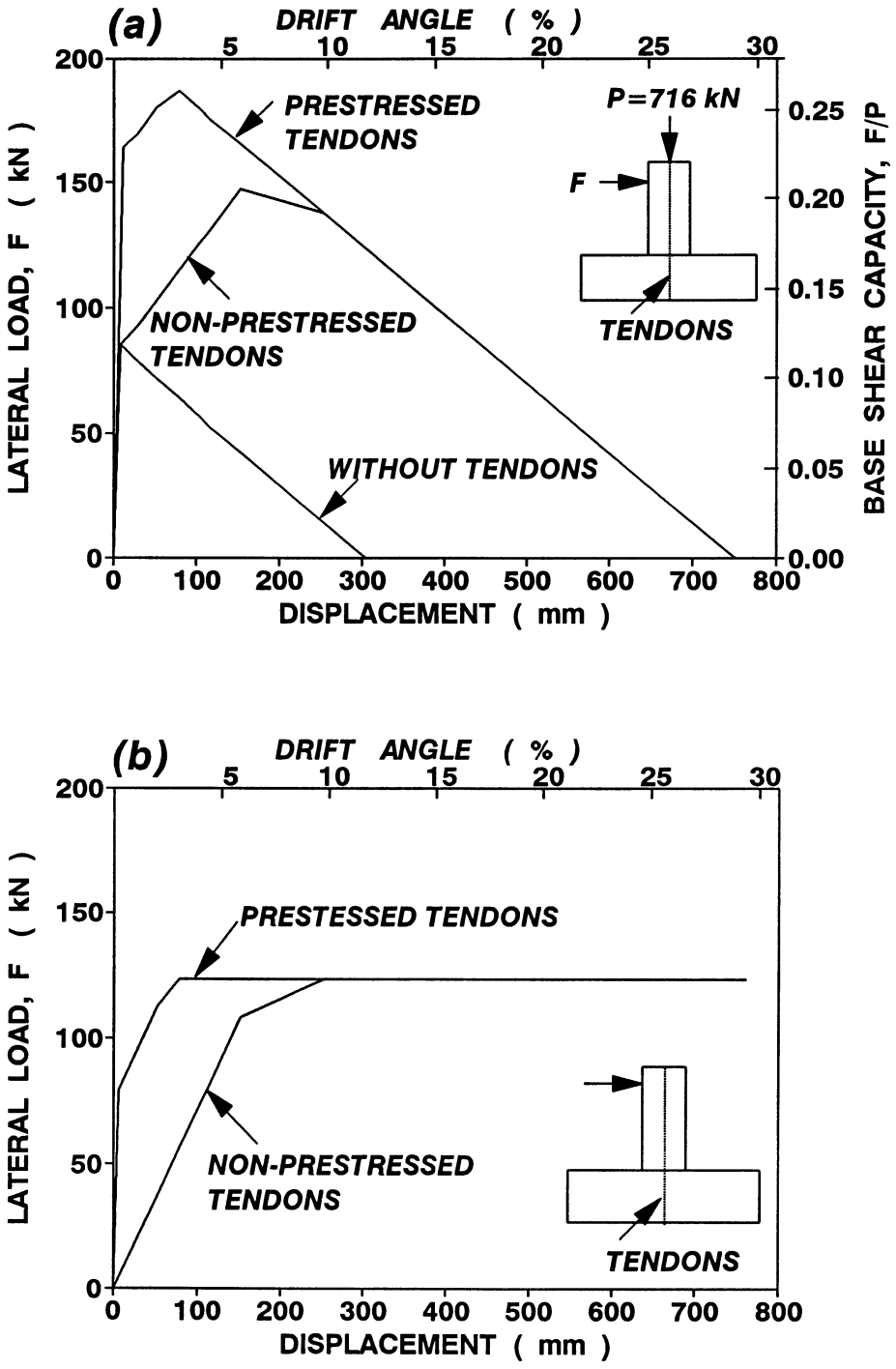

Figure 5-5 Push over analysis of rocking column (a) with the axial load (b) without the axial load.

and stiffness are essentially the same regardless of the level of prestress. This is also observed in the case with the absence of axial load, as shown in figure 5-5(b).

Compared the figure 5-5(a) and (b), the maximum lateral strength of the column is increased by the existence of the axial load. But the higher the drift levels, the more the P-delta effect. Unlike gravity axial load which nay be unreliable with vertical motions, the unbounded tendons are always acting in a positive fashion. Therefore, the presence of unbounded tendons is an important consideration in the dynamic stability of rocking bridge piers, especially if large vertical accelerations are to be expected.

5.5 SUMMARY

In this section, the non-linear force-deformation behavior of flexible rocking columns which may or may not be post-tensioned is presented. The force-displacement relation of rocking column is expected to behave in a bi-linear elastic fashion. A complete force-deformation model for the column accounting for structural flexibility (pre-rocking), rigid body kinematics (post-rocking), the prestressing action of the tendons and friction force between tendons and duct is proposed. Good agreement between the predictive theory and the experimentally observed force-deformation results was demonstrated.

Based on this complete force-deformation model, a pushover analysis of this type of column was also performed considering real P-delta effect that are expected to occur in the field. The restraint of unbounded tendons, whether they be post-tensioned or just slack, substantially increases the overturning displacement capacity of the column. Therefore, the restraint of unbounded tendons plays an important role in stabilizing rocking columns, especially when large vertical accelerations may be present.

SECTION 6
CONCLUSIONS AND RECOMMENDATIONS

6.1 SUMMARY

In this research, a new paradigm for the design of bridge piers referred to as *Damage Avoidance Design* (DAD) is proposed. In this approach, the columns that make up a bridge pier are designed to have discontinuous longitudinal reinforcement at column-beam interface enabling the columns to freely rock on specially detailed foundation/cap beams. Premature uplift can be restrained by the use of supplementary unbonded column prestressing. When equipped with a steel-steel rocking interface, the pier is expected to behave in a bilinear elastic fashion; neither permanent damage nor degradation in strength and stiffness are expected. The fact that the longitudinal reinforcement is discontinuous also provides flexibility for utilizing precast/prestressed construction. Structural elements can be factory-made, thus minimizing on-site construction time.

A complete cyclic loading modeling procedure is proposed which can be simplified for design procedures to give a bi-linear push over force-deformation analysis. Furthermore, the rocking amplitude and the associated energy radiated (lost) on impact is converted into an equivalent viscous damping constant. By comparing the push over capacity with the appropriate damped seismic design elastic (demand) spectra, the structure's maximum force and displacement can be determined. This proposed design approach is compatible with similar approaches used for seismic evaluation and design of isolated bridge structures (Buckle and Friedland, 1995), and the emerging displacement based design philosophy (Kowalsky et al., 1995, and Priestley 1996).

Based on the proposed theory, a design example of a twin-column bridge pier was presented. To validate the proposed design philosophy, a near full-size rocking column substructure was precast, erected, post-tensioned and tested. A complete force-deformation model for the rocking column is proposed to predict the experimentally observed force-

deformation behavior. This model accounts for the three important aspects of structural flexibility (pre-rocking), rigid body kinematics (post-rocking) and the prestressing action of the tendons

6.2 CONCLUSIONS

Based on this theoretical development and the experimental validation reported herein, the following specific conclusions can be drawn:

6.2.1 Theoretical Considerations of the DAD Concept

1. Seismic overturning moments are resisted by a combination of applied gravity load and supplementary internal prestressing forces. Column moments are a product of these internal forces times the semi-base width of the column foot. A complete force-deformation model for the column accounting for structural flexibility (pre-rocking), rigid body kinematics (post-rocking) and the prestressing action of the tendons is proposed. Good agreement between the predictive theory and the experimentally observed force-deformation results was demonstrated.

2. A generalized seismic design procedure is proposed for bridge structures with rocking piers based on a pushover analysis. Damping is assessed based on the energy radiated (lost) on impact and converted to equivalent viscous damping. For a given pushover curve and effective damping the expected seismic displacement may be predicted. It is shown that the proposed seismic displacement theory collapses to the classical rigid rocking block theory of Housner (1963).

6.2.2 Experimental Performance of Specimen Designed in Accordance with DAD Philosophy

1. Due to the discontinuous longitudinal reinforcement at the beam-column interface, it is necessary to provide special detailing to enable the column to rock. During the rocking motion very high point stresses are induced at the rocking toe. This concentration of stress was effectively mitigated by using a steel-steel rocking interface together with a high degree of confinement at the end region of the column. Due to the presence of the steel-steel rocking interface and resulting absence of damage, the rocking column behaved in a bilinear elastic fashion without inducing any permanent damage. Even after the completion of hundreds of rocking cycles neither strength nor stiffness deterioration was observed; the damage avoidance concept is thus considered validated.

2. When rubber was added between the steel-steel interface the capability of energy dissipation increased. This approach can only be used if the internal tendons are not prestressed; creep in the rubber over time may eventually lead to a significant loss in prestress.

3. With the post-tensioning in the unbonded tendons, the pre-rocking stiffness, pre-rocking elastic strength (uplift) and maximum lateral strength were increased 40%, 70% and 30% respectively above the case where tendons were just slack. If service load strength (pre-rocking uplift capacity) is important then the capacity can be increased either by enlarging the semi-base width of the column, prestressing the column, or both.

4. As the inherent energy dissipation capacity of a rocking mechanism is low, a rocking structure needs to rely on radiation damping that occurs on each impact. A strong foundation system is therefore essential.

6.3 Design Recommendations

1. The size of the rocking column is designed based on the axial load ratio. An axial load ratio of about 0.1 including gravity load and supplementary prestressing is preferred.

2. The longitudinal reinforcement of the columns should be disconnected at the rocking interfaces to allow column rocking and avoid damage. Unbonded prestressing steel is strongly recommended to provide improved lateral resistance, ductility, overturning protection, and stability under small ground excitations. A total volumetric ratio of longitudinal reinforcement of less than 0.02 (including unbonded tendons) is preferred.

3. The semi-base width of the pier system can be determined from standard strength design considerations that already exist. It is recommended that the maximum design displacement of a pier system be limited to 50% of the maximum displacement capacity.

4. A steel-steel rocking beam-column interface is recommended to accommodate large contact pressures that occur at the rocking toe during uplift of the columns. The thickness of rocking steel plate can be designed in a way to sustain the maximum moment acting at the rocking base during uplift. Special care should be taken to provide adequate force transfer between the rocking toe and the columns. Pintles or shear key are recommended for this purpose.

5. To maintain consistent quality and improve on-site construction scheduling, all elements of the bridge substructure can be shop fabricated and precast.

6.4 Recommendations for Future Research

Based on the study completed to date, the following topics are recommended for future research.

1. In this research a theoretical investigation on the seismic response of structures with rocking columns focused on uni-directional lateral ground excitation. The seismic response due to the bi-directional loading coupled with the effects of vertical ground shaking should be further studied both experimentally and theoretically.

2. The torsional resistance of skewed and irregular bridges designed with rocking columns is not at all well understood and should be investigated. This requires the development of computational tools that can undertake transient dynamic analysis. Particular care needs to be taken with the dynamic impact problem ensuring radiation damping is properly handled. Present computational software is unable to carry out such an analysis, and this fact may be the major impediment on implementing designs with rocking columns.

3. Due to less capability of energy dissipation in the rocking column, other energy dissipation devices such as supplementary dampers may be considered. The effect of such devices on the seismic response needs to be further studied.

4. The DAD design philosophy may be applied to the beam-column connections in building construction. Therefore, full design procedures and design criteria for rocking columns applied to both bridge and building structures need to be developed.

SECTION 7

REFERENCES

_____American Concrete Institute. (1989). *Building Code Requirements for Reinforced Concrete*. ACI 318-89, Detroit.

_____Applied Technology Council. (1995). "Guidelines and Commentary for the seismic Rehabilitation of Buildings," Project ATC-33, 75% complete draft, Redwood City, California, October.

Aslam, M. Goddon, W.G. and Scalise, D.T. (1980) "Earthquake Rocking Response of Rigid Blocks," *Journal of Structural Engineering, ASCE*, Vol. 106, No. 2, February 1980, pp. 377-392.

Blakeley, R.W.G. and Park, R. (1971). "Seismic Resistance of Prestressed Concrete Beam-Column Assemblies," *Journal of American Concrete Institute*, Vol. 68, No. 9, Sept. 1971, pp. 677-692.

Buckle, I.G. and Friedland, I.M. (1995). *Seismic Retrofitting Manual for Highway Bridges*, Report No. FHWA-RD-94-052, May 1995, Federal Highway Administration, Department of Transportation, Virginia.

Bull, D., Park, R., Elliott, D. and Park, A. (1995). "The Performance of Modular Precast Concrete Frames, that are not Part of the Primary Lateral Force Resisting System, under Simulated Seismic Loading," Pacific Conference on Earthquake Engineering, Australia, 20-22 November 1995, pp. 17-26.

Cormack, L.G. (1988). "The Design and Construction of the Major Bridges on the Mangaweka Rail Division," Transactions, Institution of Professional Engineers, New Zealand, 15, I/CE, pp. 16-23.

Constantinou, M.C., Soong, T.T. and Dargush, G.F. (1996). "Passive Energy Dissipation System for Structure Design and Retrofit," An NCEER Monograph, National centers for Earthquake Engineering Research, June, 1996.

Housner, G.W. (1963). "The Behavior of Inverted Pendulum Structures During Earthquake," Bulletin of the Seismological Society of America, Vol. 53, No.2, pp. 403-417.

Iyengar, R.N. and Roy, D. (1996). "Nonlinear Dynamics of a rigid Block on a Rigid Base," *Journal of Applied Mechanics*, Vol.63, No.1, March 1996, pp. 55-61.

Jones, N.P. and Shenton, H.W. (1992). "Generalized Slide-rocking Response of Rigid Blocks during Earthquake," Proc. of U.S. National Conference Earthquake Engineering, Vol. 3, pp.31-40.

Kadakal, U. (1994). "Rocking Response of Rigid Blocks," Technical Report 94-001, Dept. of Earthquake Engineering , Kandilli Observatory and Earthquake Research Institute, Bogazici University, Istanbul, Turkey.

Kim, J-H. and Mander, J.B. (1997). "A deformation model for shear and flexure in structural members," Technical Report, National Center for Earthquake Engineering Research (in process).

Kowalsky, M.J. Priestly, M.J.N. and MacRae, G.A. (1995). "Displacement-Based Design of RC Bridge Columns in Seismic Regions," *Earthquake Engineering and structural Dynamics*, Vol. 24, pp. 1623-1643, 1995.

Lin, H. and Yim, S.C.S. (1996). "Nonlinear Rocking Motions. I:Chaos under Noisy Period Excitations," *Journal of Mechanical Engineering, ASCE*, Vol 122, No.8, August 1996, pp. 719-727.

Lin, H. and Yim, S.C.S. (1996). "Nonlinear Rocking Motions. II:Overturning under Random Excitations," *Journal of Mechanical Engineering, ASCE*, Vol 122, No.8, August 1996, pp. 728-735.

McManus, K.J. Priestley, M.J.N. and Carr, A.J. (1980). "The Seismic Response of Bridge Structures Free to Rock on their Foundations," Research Report No. 80/4, Department of Civil Engineering, University of Canterbury, Christchurch, New Zealand.

Park, R. and Thompson, K.J. (1977). "Cyclic Load Tests on Prestressed and Partially Prestressed Beam-Column Joints," *PCI Journal*, Vol. 22, No. 5, September-October 1977, pp. 85-100.

Paulay, T. and Priestley, M.J.N. (1992). *Seismic Design of Reinforced Concrete and Masonry Building*, John Wiley and Sons, Inc., New York, N.Y..

Priestley, M.J.N., Evison, R.j. and Carr, A.J. (1978). "Seismic Response of Structures Free to Rock on Their Foundation," Bulletin of the New Zealand National Society for Earthquake Engineering, Vol. 20, No.3, September 1987, pp. 141-150.

Priestley, M.J.N. and Tao, J. (1993). "Seismic Response of Precast Prestressed Concrete Frames with Partially Debonded Tendons," *PCI Journal*, Vol. 38, No. 1, January-February 1993, pp. 58-69.

Priestley, M.J.N. and MacRae, G.A. (1996). "Seismic Testing of Precast Beam-to-Column Joint Assemblage with Unbonded Tendons," *PCI Journal*, Vol. 41, No.1, pp. 64-80.

Priestley, M.J.N. (1996a). "Seismic Design Philosophy for Precast Concrete Frames," *Structural Engineering International*, Vol. 6, No.1 February, pp. 25-31.

Priestley, M.J.N. (1996b). "The PRESSS Program – Current Status and Proposed Plan for Phase III," *PCI Journal*, Vol. 41, No.2, March-April 1996, pp. 22-40.

Priestley, M.J.N., Seible, F. and Calvi, G.M. (1996). *Seismic Design and Retrofit of Bridges*, John Wiley & Sons, New York.

Psycharis, I.N. and Jennings, P. C. (1983). "Rocking of Slender Rigid Bodies Allowed to Uplift," *Earthquake Engineering and Structural Dynamics*, Vol. 11, pp. 57-76.

Skinner, R.I., Tyler, R.G., Heine, A.J. and Robinson, W.H. (1979). "Hysteretic Dampers for the Protection of Structures from earthquake," The Second South Pacific Regional Conference on Earthquake Engineering, May 8-10, 1979, Victoria University, Wellington, New Zealand, pp. 643-664.

Skinner, R.I., Robinson, W.H. and McVerry G.H. (1993). *An Introduction to Seismic Isolation*, John Wiley & Sons Ltd., England, p. 10.

Shenton, H.W. and Jones, N.P. (1992). "Effect of Friction and Restitution on Rocking Response," Proc. Tenth World Conference Earthquake Engineering, pp. 1933-1938.

Yim, C-S., Chopra, A.K. and Penzien, J. (1980). "Rocking Response of Rigid Blocks to Earthquake," *Earthquake Engineering and Structural Dynamics*, Vol. 8, pp. 565-587.

NATIONAL CENTER FOR EARTHQUAKE ENGINEERING RESEARCH
LIST OF TECHNICAL REPORTS

The National Center for Earthquake Engineering Research (NCEER) publishes technical reports on a variety of subjects related to earthquake engineering written by authors funded through NCEER. These reports are available from both NCEER Publications and the National Technical Information Service (NTIS). Requests for reports should be directed to NCEER Publications, National Center for Earthquake Engineering Research, State University of New York at Buffalo, Red Jacket Quadrangle, Buffalo, New York 14261. Reports can also be requested through NTIS, 5285 Port Royal Road, Springfield, Virginia 22161. NTIS accession numbers are shown in parenthesis, if available.

NCEER-87-0001 "First-Year Program in Research, Education and Technology Transfer," 3/5/87, (PB88-134275, A04, MF-A01).

NCEER-87-0002 "Experimental Evaluation of Instantaneous Optimal Algorithms for Structural Control," by R.C. Lin, T.T. Soong and A.M. Reinhorn, 4/20/87, (PB88-134341, A04, MF-A01).

NCEER-87-0003 "Experimentation Using the Earthquake Simulation Facilities at University at Buffalo," by A.M. Reinhorn and R.L. Ketter, to be published.

NCEER-87-0004 "The System Characteristics and Performance of a Shaking Table," by J.S. Hwang, K.C. Chang and G.C. Lee, 6/1/87, (PB88-134259, A03, MF-A01). This report is available only through NTIS (see address given above).

NCEER-87-0005 "A Finite Element Formulation for Nonlinear Viscoplastic Material Using a Q Model," by O. Gyebi and G. Dasgupta, 11/2/87, (PB88-213764, A08, MF-A01).

NCEER-87-0006 "Symbolic Manipulation Program (SMP) - Algebraic Codes for Two and Three Dimensional Finite Element Formulations," by X. Lee and G. Dasgupta, 11/9/87, (PB88-218522, A05, MF-A01).

NCEER-87-0007 "Instantaneous Optimal Control Laws for Tall Buildings Under Seismic Excitations," by J.N. Yang, A. Akbarpour and P. Ghaemmaghami, 6/10/87, (PB88-134333, A06, MF-A01). This report is only available through NTIS (see address given above).

NCEER-87-0008 "IDARC: Inelastic Damage Analysis of Reinforced Concrete Frame - Shear-Wall Structures," by Y.J. Park, A.M. Reinhorn and S.K. Kunnath, 7/20/87, (PB88-134325, A09, MF-A01). This report is only available through NTIS (see address given above).

NCEER-87-0009 "Liquefaction Potential for New York State: A Preliminary Report on Sites in Manhattan and Buffalo," by M. Budhu, V. Vijayakumar, R.F. Giese and L. Baumgras, 8/31/87, (PB88-163704, A03, MF-A01). This report is available only through NTIS (see address given above).

NCEER-87-0010 "Vertical and Torsional Vibration of Foundations in Inhomogeneous Media," by A.S. Veletsos and K.W. Dotson, 6/1/87, (PB88-134291, A03, MF-A01). This report is only available through NTIS (see address given above).

NCEER-87-0011 "Seismic Probabilistic Risk Assessment and Seismic Margins Studies for Nuclear Power Plants," by Howard H.M. Hwang, 6/15/87, (PB88-134267, A03, MF-A01). This report is only available through NTIS (see address given above).

NCEER-87-0012 "Parametric Studies of Frequency Response of Secondary Systems Under Ground-Acceleration Excitations," by Y. Yong and Y.K. Lin, 6/10/87, (PB88-134309, A03, MF-A01). This report is only available through NTIS (see address given above).

NCEER-87-0013 "Frequency Response of Secondary Systems Under Seismic Excitation," by J.A. HoLung, J. Cai and Y.K. Lin, 7/31/87, (PB88-134317, A05, MF-A01). This report is only available through NTIS (see address given above).

NCEER-87-0014 "Modelling Earthquake Ground Motions in Seismically Active Regions Using Parametric Time Series Methods," by G.W. Ellis and A.S. Cakmak, 8/25/87, (PB88-134283, A08, MF-A01). This report is only available through NTIS (see address given above).

NCEER-87-0015 "Detection and Assessment of Seismic Structural Damage," by E. DiPasquale and A.S. Cakmak, 8/25/87, (PB88-163712, A05, MF-A01). This report is only available through NTIS (see address given above).

NCEER-87-0016 "Pipeline Experiment at Parkfield, California," by J. Isenberg and E. Richardson, 9/15/87, (PB88-163720, A03, MF-A01). This report is available only through NTIS (see address given above).

NCEER-87-0017 "Digital Simulation of Seismic Ground Motion," by M. Shinozuka, G. Deodatis and T. Harada, 8/31/87, (PB88-155197, A04, MF-A01). This report is available only through NTIS (see address given above).

NCEER-87-0018 "Practical Considerations for Structural Control: System Uncertainty, System Time Delay and Truncation of Small Control Forces," J.N. Yang and A. Akbarpour, 8/10/87, (PB88-163738, A08, MF-A01). This report is only available through NTIS (see address given above).

NCEER-87-0019 "Modal Analysis of Nonclassically Damped Structural Systems Using Canonical Transformation," by J.N. Yang, S. Sarkani and F.X. Long, 9/27/87, (PB88-187851, A04, MF-A01).

NCEER-87-0020 "A Nonstationary Solution in Random Vibration Theory," by J.R. Red-Horse and P.D. Spanos, 11/3/87, (PB88-163746, A03, MF-A01).

NCEER-87-0021 "Horizontal Impedances for Radially Inhomogeneous Viscoelastic Soil Layers," by A.S. Veletsos and K.W. Dotson, 10/15/87, (PB88-150859, A04, MF-A01).

NCEER-87-0022 "Seismic Damage Assessment of Reinforced Concrete Members," by Y.S. Chung, C. Meyer and M. Shinozuka, 10/9/87, (PB88-150867, A05, MF-A01). This report is available only through NTIS (see address given above).

NCEER-87-0023 "Active Structural Control in Civil Engineering," by T.T. Soong, 11/11/87, (PB88-187778, A03, MF-A01).

NCEER-87-0024 "Vertical and Torsional Impedances for Radially Inhomogeneous Viscoelastic Soil Layers," by K.W. Dotson and A.S. Veletsos, 12/87, (PB88-187786, A03, MF-A01).

NCEER-87-0025 "Proceedings from the Symposium on Seismic Hazards, Ground Motions, Soil-Liquefaction and Engineering Practice in Eastern North America," October 20-22, 1987, edited by K.H. Jacob, 12/87, (PB88-188115, A23, MF-A01).

NCEER-87-0026 "Report on the Whittier-Narrows, California, Earthquake of October 1, 1987," by J. Pantelic and A. Reinhorn, 11/87, (PB88-187752, A03, MF-A01). This report is available only through NTIS (see address given above).

NCEER-87-0027 "Design of a Modular Program for Transient Nonlinear Analysis of Large 3-D Building Structures," by S. Srivastav and J.F. Abel, 12/30/87, (PB88-187950, A05, MF-A01). This report is only available through NTIS (see address given above).

NCEER-87-0028 "Second-Year Program in Research, Education and Technology Transfer," 3/8/88, (PB88-219480, A04, MF-A01).

NCEER-88-0001 "Workshop on Seismic Computer Analysis and Design of Buildings With Interactive Graphics," by W. McGuire, J.F. Abel and C.H. Conley, 1/18/88, (PB88-187760, A03, MF-A01). This report is only available through NTIS (see address given above).

NCEER-88-0002 "Optimal Control of Nonlinear Flexible Structures," by J.N. Yang, F.X. Long and D. Wong, 1/22/88, (PB88-213772, A06, MF-A01).

NCEER-88-0003 "Substructuring Techniques in the Time Domain for Primary-Secondary Structural Systems," by G.D. Manolis and G. Juhn, 2/10/88, (PB88-213780, A04, MF-A01).

NCEER-88-0004 "Iterative Seismic Analysis of Primary-Secondary Systems," by A. Singhal, L.D. Lutes and P.D. Spanos, 2/23/88, (PB88-213798, A04, MF-A01).

NCEER-88-0005 "Stochastic Finite Element Expansion for Random Media," by P.D. Spanos and R. Ghanem, 3/14/88, (PB88-213806, A03, MF-A01).

NCEER-88-0006 "Combining Structural Optimization and Structural Control," by F.Y. Cheng and C.P. Pantelides, 1/10/88, (PB88-213814, A05, MF-A01).

NCEER-88-0007 "Seismic Performance Assessment of Code-Designed Structures," by H.H-M. Hwang, J-W. Jaw and H-J. Shau, 3/20/88, (PB88-219423, A04, MF-A01). This report is only available through NTIS (see address given above).

NCEER-88-0008 "Reliability Analysis of Code-Designed Structures Under Natural Hazards," by H.H-M. Hwang, H. Ushiba and M. Shinozuka, 2/29/88, (PB88-229471, A07, MF-A01). This report is only available through NTIS (see address given above).

NCEER-88-0009 "Seismic Fragility Analysis of Shear Wall Structures," by J-W Jaw and H.H-M. Hwang, 4/30/88, (PB89-102867, A04, MF-A01).

NCEER-88-0010 "Base Isolation of a Multi-Story Building Under a Harmonic Ground Motion - A Comparison of Performances of Various Systems," by F-G Fan, G. Ahmadi and I.G. Tadjbakhsh, 5/18/88, (PB89-122238, A06, MF-A01). This report is only available through NTIS (see address given above).

NCEER-88-0011 "Seismic Floor Response Spectra for a Combined System by Green's Functions," by F.M. Lavelle, L.A. Bergman and P.D. Spanos, 5/1/88, (PB89-102875, A03, MF-A01).

NCEER-88-0012 "A New Solution Technique for Randomly Excited Hysteretic Structures," by G.Q. Cai and Y.K. Lin, 5/16/88, (PB89-102883, A03, MF-A01).

NCEER-88-0013 "A Study of Radiation Damping and Soil-Structure Interaction Effects in the Centrifuge," by K. Weissman, supervised by J.H. Prevost, 5/24/88, (PB89-144703, A06, MF-A01).

NCEER-88-0014 "Parameter Identification and Implementation of a Kinematic Plasticity Model for Frictional Soils," by J.H. Prevost and D.V. Griffiths, to be published.

NCEER-88-0015 "Two- and Three- Dimensional Dynamic Finite Element Analyses of the Long Valley Dam," by D.V. Griffiths and J.H. Prevost, 6/17/88, (PB89-144711, A04, MF-A01).

NCEER-88-0016 "Damage Assessment of Reinforced Concrete Structures in Eastern United States," by A.M. Reinhorn, M.J. Seidel, S.K. Kunnath and Y.J. Park, 6/15/88, (PB89-122220, A04, MF-A01). This report is only available through NTIS (see address given above).

NCEER-88-0017 "Dynamic Compliance of Vertically Loaded Strip Foundations in Multilayered Viscoelastic Soils," by S. Ahmad and A.S.M. Israil, 6/17/88, (PB89-102891, A04, MF-A01).

NCEER-88-0018 "An Experimental Study of Seismic Structural Response With Added Viscoelastic Dampers," by R.C. Lin, Z. Liang, T.T. Soong and R.H. Zhang, 6/30/88, (PB89-122212, A05, MF-A01). This report is available only through NTIS (see address given above).

NCEER-88-0019 "Experimental Investigation of Primary - Secondary System Interaction," by G.D. Manolis, G. Juhn and A.M. Reinhorn, 5/27/88, (PB89-122204, A04, MF-A01).

NCEER-88-0020 "A Response Spectrum Approach For Analysis of Nonclassically Damped Structures," by J.N. Yang, S. Sarkani and F.X. Long, 4/22/88, (PB89-102909, A04, MF-A01).

NCEER-88-0021 "Seismic Interaction of Structures and Soils: Stochastic Approach," by A.S. Veletsos and A.M. Prasad, 7/21/88, (PB89-122196, A04, MF-A01). This report is only available through NTIS (see address given above).

NCEER-88-0022 "Identification of the Serviceability Limit State and Detection of Seismic Structural Damage," by E. DiPasquale and A.S. Cakmak, 6/15/88, (PB89-122188, A05, MF-A01). This report is available only through NTIS (see address given above).

NCEER-88-0023 "Multi-Hazard Risk Analysis: Case of a Simple Offshore Structure," by B.K. Bhartia and E.H. Vanmarcke, 7/21/88, (PB89-145213, A05, MF-A01).

NCEER-88-0024 "Automated Seismic Design of Reinforced Concrete Buildings," by Y.S. Chung, C. Meyer and M. Shinozuka, 7/5/88, (PB89-122170, A06, MF-A01). This report is available only through NTIS (see address given above).

NCEER-88-0025 "Experimental Study of Active Control of MDOF Structures Under Seismic Excitations," by L.L. Chung, R.C. Lin, T.T. Soong and A.M. Reinhorn, 7/10/88, (PB89-122600, A04, MF-A01).

NCEER-88-0026 "Earthquake Simulation Tests of a Low-Rise Metal Structure," by J.S. Hwang, K.C. Chang, G.C. Lee and R.L. Ketter, 8/1/88, (PB89-102917, A04, MF-A01).

NCEER-88-0027 "Systems Study of Urban Response and Reconstruction Due to Catastrophic Earthquakes," by F. Kozin and H.K. Zhou, 9/22/88, (PB90-162348, A04, MF-A01).

NCEER-88-0028 "Seismic Fragility Analysis of Plane Frame Structures," by H.H-M. Hwang and Y.K. Low, 7/31/88, (PB89-131445, A06, MF-A01).

NCEER-88-0029 "Response Analysis of Stochastic Structures," by A. Kardara, C. Bucher and M. Shinozuka, 9/22/88, (PB89-174429, A04, MF-A01).

NCEER-88-0030 "Nonnormal Accelerations Due to Yielding in a Primary Structure," by D.C.K. Chen and L.D. Lutes, 9/19/88, (PB89-131437, A04, MF-A01).

NCEER-88-0031 "Design Approaches for Soil-Structure Interaction," by A.S. Veletsos, A.M. Prasad and Y. Tang, 12/30/88, (PB89-174437, A03, MF-A01). This report is available only through NTIS (see address given above).

NCEER-88-0032 "A Re-evaluation of Design Spectra for Seismic Damage Control," by C.J. Turkstra and A.G. Tallin, 11/7/88, (PB89-145221, A05, MF-A01).

NCEER-88-0033 "The Behavior and Design of Noncontact Lap Splices Subjected to Repeated Inelastic Tensile Loading," by V.E. Sagan, P. Gergely and R.N. White, 12/8/88, (PB89-163737, A08, MF-A01).

NCEER-88-0034 "Seismic Response of Pile Foundations," by S.M. Mamoon, P.K. Banerjee and S. Ahmad, 11/1/88, (PB89-145239, A04, MF-A01).

NCEER-88-0035 "Modeling of R/C Building Structures With Flexible Floor Diaphragms (IDARC2)," by A.M. Reinhorn, S.K. Kunnath and N. Panahshahi, 9/7/88, (PB89-207153, A07, MF-A01).

NCEER-88-0036 "Solution of the Dam-Reservoir Interaction Problem Using a Combination of FEM, BEM with Particular Integrals, Modal Analysis, and Substructuring," by C-S. Tsai, G.C. Lee and R.L. Ketter, 12/31/88, (PB89-207146, A04, MF-A01).

NCEER-88-0037 "Optimal Placement of Actuators for Structural Control," by F.Y. Cheng and C.P. Pantelides, 8/15/88, (PB89-162846, A05, MF-A01).

NCEER-88-0038 "Teflon Bearings in Aseismic Base Isolation: Experimental Studies and Mathematical Modeling," by A. Mokha, M.C. Constantinou and A.M. Reinhorn, 12/5/88, (PB89-218457, A10, MF-A01). This report is available only through NTIS (see address given above).

NCEER-88-0039 "Seismic Behavior of Flat Slab High-Rise Buildings in the New York City Area," by P. Weidlinger and M. Ettouney, 10/15/88, (PB90-145681, A04, MF-A01).

NCEER-88-0040 "Evaluation of the Earthquake Resistance of Existing Buildings in New York City," by P. Weidlinger and M. Ettouney, 10/15/88, to be published.

NCEER-88-0041 "Small-Scale Modeling Techniques for Reinforced Concrete Structures Subjected to Seismic Loads," by W. Kim, A. El-Attar and R.N. White, 11/22/88, (PB89-189625, A05, MF-A01).

NCEER-88-0042 "Modeling Strong Ground Motion from Multiple Event Earthquakes," by G.W. Ellis and A.S. Cakmak, 10/15/88, (PB89-174445, A03, MF-A01).

NCEER-88-0043 "Nonstationary Models of Seismic Ground Acceleration," by M. Grigoriu, S.E. Ruiz and E. Rosenblueth, 7/15/88, (PB89-189617, A04, MF-A01).

NCEER-88-0044 "SARCF User's Guide: Seismic Analysis of Reinforced Concrete Frames," by Y.S. Chung, C. Meyer and M. Shinozuka, 11/9/88, (PB89-174452, A08, MF-A01).

NCEER-88-0045 "First Expert Panel Meeting on Disaster Research and Planning," edited by J. Pantelic and J. Stoyle, 9/15/88, (PB89-174460, A05, MF-A01). This report is only available through NTIS (see address given above).

NCEER-88-0046 "Preliminary Studies of the Effect of Degrading Infill Walls on the Nonlinear Seismic Response of Steel Frames," by C.Z. Chrysostomou, P. Gergely and J.F. Abel, 12/19/88, (PB89-208383, A05, MF-A01).

NCEER-88-0047 "Reinforced Concrete Frame Component Testing Facility - Design, Construction, Instrumentation and Operation," by S.P. Pessiki, C. Conley, T. Bond, P. Gergely and R.N. White, 12/16/88, (PB89-174478, A04, MF-A01).

NCEER-89-0001 "Effects of Protective Cushion and Soil Compliancy on the Response of Equipment Within a Seismically Excited Building," by J.A. HoLung, 2/16/89, (PB89-207179, A04, MF-A01).

NCEER-89-0002 "Statistical Evaluation of Response Modification Factors for Reinforced Concrete Structures," by H.H-M. Hwang and J-W. Jaw, 2/17/89, (PB89-207187, A05, MF-A01).

NCEER-89-0003 "Hysteretic Columns Under Random Excitation," by G-Q. Cai and Y.K. Lin, 1/9/89, (PB89-196513, A03, MF-A01).

NCEER-89-0004 "Experimental Study of `Elephant Foot Bulge' Instability of Thin-Walled Metal Tanks," by Z-H. Jia and R.L. Ketter, 2/22/89, (PB89-207195, A03, MF-A01).

NCEER-89-0005 "Experiment on Performance of Buried Pipelines Across San Andreas Fault," by J. Isenberg, E. Richardson and T.D. O'Rourke, 3/10/89, (PB89-218440, A04, MF-A01). This report is available only through NTIS (see address given above).

NCEER-89-0006 "A Knowledge-Based Approach to Structural Design of Earthquake-Resistant Buildings," by M. Subramani, P. Gergely, C.H. Conley, J.F. Abel and A.H. Zaghw, 1/15/89, (PB89-218465, A06, MF-A01).

NCEER-89-0007 "Liquefaction Hazards and Their Effects on Buried Pipelines," by T.D. O'Rourke and P.A. Lane, 2/1/89, (PB89-218481, A09, MF-A01).

NCEER-89-0008 "Fundamentals of System Identification in Structural Dynamics," by H. Imai, C-B. Yun, O. Maruyama and M. Shinozuka, 1/26/89, (PB89-207211, A04, MF-A01).

NCEER-89-0009 "Effects of the 1985 Michoacan Earthquake on Water Systems and Other Buried Lifelines in Mexico," by A.G. Ayala and M.J. O'Rourke, 3/8/89, (PB89-207229, A06, MF-A01).

NCEER-89-R010 "NCEER Bibliography of Earthquake Education Materials," by K.E.K. Ross, Second Revision, 9/1/89, (PB90-125352, A05, MF-A01). This report is replaced by NCEER-92-0018.

NCEER-89-0011 "Inelastic Three-Dimensional Response Analysis of Reinforced Concrete Building Structures (IDARC-3D), Part I - Modeling," by S.K. Kunnath and A.M. Reinhorn, 4/17/89, (PB90-114612, A07, MF-A01).

NCEER-89-0012 "Recommended Modifications to ATC-14," by C.D. Poland and J.O. Malley, 4/12/89, (PB90-108648, A15, MF-A01).

NCEER-89-0013 "Repair and Strengthening of Beam-to-Column Connections Subjected to Earthquake Loading," by M. Corazao and A.J. Durrani, 2/28/89, (PB90-109885, A06, MF-A01).

NCEER-89-0014 "Program EXKAL2 for Identification of Structural Dynamic Systems," by O. Maruyama, C-B. Yun, M. Hoshiya and M. Shinozuka, 5/19/89, (PB90-109877, A09, MF-A01).

NCEER-89-0015 "Response of Frames With Bolted Semi-Rigid Connections, Part I - Experimental Study and Analytical Predictions," by P.J. DiCorso, A.M. Reinhorn, J.R. Dickerson, J.B. Radziminski and W.L. Harper, 6/1/89, to be published.

NCEER-89-0016 "ARMA Monte Carlo Simulation in Probabilistic Structural Analysis," by P.D. Spanos and M.P. Mignolet, 7/10/89, (PB90-109893, A03, MF-A01).

NCEER-89-P017 "Preliminary Proceedings from the Conference on Disaster Preparedness - The Place of Earthquake Education in Our Schools," Edited by K.E.K. Ross, 6/23/89, (PB90-108606, A03, MF-A01).

NCEER-89-0017 "Proceedings from the Conference on Disaster Preparedness - The Place of Earthquake Education in Our Schools," Edited by K.E.K. Ross, 12/31/89, (PB90-207895, A012, MF-A02). This report is available only through NTIS (see address given above).

NCEER-89-0018 "Multidimensional Models of Hysteretic Material Behavior for Vibration Analysis of Shape Memory Energy Absorbing Devices, by E.J. Graesser and F.A. Cozzarelli, 6/7/89, (PB90-164146, A04, MF-A01).

NCEER-89-0019 "Nonlinear Dynamic Analysis of Three-Dimensional Base Isolated Structures (3D-BASIS)," by S. Nagarajaiah, A.M. Reinhorn and M.C. Constantinou, 8/3/89, (PB90-161936, A06, MF-A01). This report has been replaced by NCEER-93-0011.

NCEER-89-0020 "Structural Control Considering Time-Rate of Control Forces and Control Rate Constraints," by F.Y. Cheng and C.P. Pantelides, 8/3/89, (PB90-120445, A04, MF-A01).

NCEER-89-0021 "Subsurface Conditions of Memphis and Shelby County," by K.W. Ng, T-S. Chang and H-H.M. Hwang, 7/26/89, (PB90-120437, A03, MF-A01).

NCEER-89-0022 "Seismic Wave Propagation Effects on Straight Jointed Buried Pipelines," by K. Elhmadi and M.J. O'Rourke, 8/24/89, (PB90-162322, A10, MF-A02).

NCEER-89-0023 "Workshop on Serviceability Analysis of Water Delivery Systems," edited by M. Grigoriu, 3/6/89, (PB90-127424, A03, MF-A01).

NCEER-89-0024 "Shaking Table Study of a 1/5 Scale Steel Frame Composed of Tapered Members," by K.C. Chang, J.S. Hwang and G.C. Lee, 9/18/89, (PB90-160169, A04, MF-A01).

NCEER-89-0025 "DYNA1D: A Computer Program for Nonlinear Seismic Site Response Analysis - Technical Documentation," by Jean H. Prevost, 9/14/89, (PB90-161944, A07, MF-A01). This report is available only through NTIS (see address given above).

NCEER-89-0026 "1:4 Scale Model Studies of Active Tendon Systems and Active Mass Dampers for Aseismic Protection," by A.M. Reinhorn, T.T. Soong, R.C. Lin, Y.P. Yang, Y. Fukao, H. Abe and M. Nakai, 9/15/89, (PB90-173246, A10, MF-A02).

NCEER-89-0027 "Scattering of Waves by Inclusions in a Nonhomogeneous Elastic Half Space Solved by Boundary Element Methods," by P.K. Hadley, A. Askar and A.S. Cakmak, 6/15/89, (PB90-145699, A07, MF-A01).

NCEER-89-0028 "Statistical Evaluation of Deflection Amplification Factors for Reinforced Concrete Structures," by H.H.M. Hwang, J-W. Jaw and A.L. Ch'ng, 8/31/89, (PB90-164633, A05, MF-A01).

NCEER-89-0029 "Bedrock Accelerations in Memphis Area Due to Large New Madrid Earthquakes," by H.H.M. Hwang, C.H.S. Chen and G. Yu, 11/7/89, (PB90-162330, A04, MF-A01).

NCEER-89-0030 "Seismic Behavior and Response Sensitivity of Secondary Structural Systems," by Y.Q. Chen and T.T. Soong, 10/23/89, (PB90-164658, A08, MF-A01).

NCEER-89-0031 "Random Vibration and Reliability Analysis of Primary-Secondary Structural Systems," by Y. Ibrahim, M. Grigoriu and T.T. Soong, 11/10/89, (PB90-161951, A04, MF-A01).

NCEER-89-0032 "Proceedings from the Second U.S. - Japan Workshop on Liquefaction, Large Ground Deformation and Their Effects on Lifelines, September 26-29, 1989," Edited by T.D. O'Rourke and M. Hamada, 12/1/89, (PB90-209388, A22, MF-A03).

NCEER-89-0033 "Deterministic Model for Seismic Damage Evaluation of Reinforced Concrete Structures," by J.M. Bracci, A.M. Reinhorn, J.B. Mander and S.K. Kunnath, 9/27/89, (PB91-108803, A06, MF-A01).

NCEER-89-0034 "On the Relation Between Local and Global Damage Indices," by E. DiPasquale and A.S. Cakmak, 8/15/89, (PB90-173865, A05, MF-A01).

NCEER-89-0035 "Cyclic Undrained Behavior of Nonplastic and Low Plasticity Silts," by A.J. Walker and H.E. Stewart, 7/26/89, (PB90-183518, A10, MF-A01).

NCEER-89-0036 "Liquefaction Potential of Surficial Deposits in the City of Buffalo, New York," by M. Budhu, R. Giese and L. Baumgrass, 1/17/89, (PB90-208455, A04, MF-A01).

NCEER-89-0037 "A Deterministic Assessment of Effects of Ground Motion Incoherence," by A.S. Veletsos and Y. Tang, 7/15/89, (PB90-164294, A03, MF-A01).

NCEER-89-0038 "Workshop on Ground Motion Parameters for Seismic Hazard Mapping," July 17-18, 1989, edited by R.V. Whitman, 12/1/89, (PB90-173923, A04, MF-A01).

NCEER-89-0039 "Seismic Effects on Elevated Transit Lines of the New York City Transit Authority," by C.J. Costantino, C.A. Miller and E. Heymsfield, 12/26/89, (PB90-207887, A06, MF-A01).

NCEER-89-0040 "Centrifugal Modeling of Dynamic Soil-Structure Interaction," by K. Weissman, Supervised by J.H. Prevost, 5/10/89, (PB90-207879, A07, MF-A01).

NCEER-89-0041 "Linearized Identification of Buildings With Cores for Seismic Vulnerability Assessment," by I-K. Ho and A.E. Aktan, 11/1/89, (PB90-251943, A07, MF-A01).

NCEER-90-0001 "Geotechnical and Lifeline Aspects of the October 17, 1989 Loma Prieta Earthquake in San Francisco," by T.D. O'Rourke, H.E. Stewart, F.T. Blackburn and T.S. Dickerman, 1/90, (PB90-208596, A05, MF-A01).

NCEER-90-0002 "Nonnormal Secondary Response Due to Yielding in a Primary Structure," by D.C.K. Chen and L.D. Lutes, 2/28/90, (PB90-251976, A07, MF-A01).

NCEER-90-0003 "Earthquake Education Materials for Grades K-12," by K.E.K. Ross, 4/16/90, (PB91-251984, A05, MF-A05). This report has been replaced by NCEER-92-0018.

NCEER-90-0004 "Catalog of Strong Motion Stations in Eastern North America," by R.W. Busby, 4/3/90, (PB90-251984, A05, MF-A01).

NCEER-90-0005 "NCEER Strong-Motion Data Base: A User Manual for the GeoBase Release (Version 1.0 for the Sun3)," by P. Friberg and K. Jacob, 3/31/90 (PB90-258062, A04, MF-A01).

NCEER-90-0006 "Seismic Hazard Along a Crude Oil Pipeline in the Event of an 1811-1812 Type New Madrid Earthquake," by H.H.M. Hwang and C-H.S. Chen, 4/16/90, (PB90-258054, A04, MF-A01).

NCEER-90-0007 "Site-Specific Response Spectra for Memphis Sheahan Pumping Station," by H.H.M. Hwang and C.S. Lee, 5/15/90, (PB91-108811, A05, MF-A01).

NCEER-90-0008 "Pilot Study on Seismic Vulnerability of Crude Oil Transmission Systems," by T. Ariman, R. Dobry, M. Grigoriu, F. Kozin, M. O'Rourke, T. O'Rourke and M. Shinozuka, 5/25/90, (PB91-108837, A06, MF-A01).

NCEER-90-0009 "A Program to Generate Site Dependent Time Histories: EQGEN," by G.W. Ellis, M. Srinivasan and A.S. Cakmak, 1/30/90, (PB91-108829, A04, MF-A01).

NCEER-90-0010 "Active Isolation for Seismic Protection of Operating Rooms," by M.E. Talbott, Supervised by M. Shinozuka, 6/8/9, (PB91-110205, A05, MF-A01).

NCEER-90-0011 "Program LINEARID for Identification of Linear Structural Dynamic Systems," by C-B. Yun and M. Shinozuka, 6/25/90, (PB91-110312, A08, MF-A01).

NCEER-90-0012 "Two-Dimensional Two-Phase Elasto-Plastic Seismic Response of Earth Dams," by A.N. Yiagos, Supervised by J.H. Prevost, 6/20/90, (PB91-110197, A13, MF-A02).

NCEER-90-0013 "Secondary Systems in Base-Isolated Structures: Experimental Investigation, Stochastic Response and Stochastic Sensitivity," by G.D. Manolis, G. Juhn, M.C. Constantinou and A.M. Reinhorn, 7/1/90, (PB91-110320, A08, MF-A01).

NCEER-90-0014 "Seismic Behavior of Lightly-Reinforced Concrete Column and Beam-Column Joint Details," by S.P. Pessiki, C.H. Conley, P. Gergely and R.N. White, 8/22/90, (PB91-108795, A11, MF-A02).

NCEER-90-0015 "Two Hybrid Control Systems for Building Structures Under Strong Earthquakes," by J.N. Yang and A. Danielians, 6/29/90, (PB91-125393, A04, MF-A01).

NCEER-90-0016 "Instantaneous Optimal Control with Acceleration and Velocity Feedback," by J.N. Yang and Z. Li, 6/29/90, (PB91-125401, A03, MF-A01).

NCEER-90-0017 "Reconnaissance Report on the Northern Iran Earthquake of June 21, 1990," by M. Mehrain, 10/4/90, (PB91-125377, A03, MF-A01).

NCEER-90-0018 "Evaluation of Liquefaction Potential in Memphis and Shelby County," by T.S. Chang, P.S. Tang, C.S. Lee and H. Hwang, 8/10/90, (PB91-125427, A09, MF-A01).

NCEER-90-0019 "Experimental and Analytical Study of a Combined Sliding Disc Bearing and Helical Steel Spring Isolation System," by M.C. Constantinou, A.S. Mokha and A.M. Reinhorn, 10/4/90, (PB91-125385, A06, MF-A01). This report is available only through NTIS (see address given above).

NCEER-90-0020 "Experimental Study and Analytical Prediction of Earthquake Response of a Sliding Isolation System with a Spherical Surface," by A.S. Mokha, M.C. Constantinou and A.M. Reinhorn, 10/11/90, (PB91-125419, A05, MF-A01).

NCEER-90-0021 "Dynamic Interaction Factors for Floating Pile Groups," by G. Gazetas, K. Fan, A. Kaynia and E. Kausel, 9/10/90, (PB91-170381, A05, MF-A01).

NCEER-90-0022 "Evaluation of Seismic Damage Indices for Reinforced Concrete Structures," by S. Rodriguez-Gomez and A.S. Cakmak, 9/30/90, PB91-171322, A06, MF-A01).

NCEER-90-0023 "Study of Site Response at a Selected Memphis Site," by H. Desai, S. Ahmad, E.S. Gazetas and M.R. Oh, 10/11/90, (PB91-196857, A03, MF-A01).

NCEER-90-0024 "A User's Guide to Strongmo: Version 1.0 of NCEER's Strong-Motion Data Access Tool for PCs and Terminals," by P.A. Friberg and C.A.T. Susch, 11/15/90, (PB91-171272, A03, MF-A01).

NCEER-90-0025 "A Three-Dimensional Analytical Study of Spatial Variability of Seismic Ground Motions," by L-L. Hong and A.H.-S. Ang, 10/30/90, (PB91-170399, A09, MF-A01).

NCEER-90-0026 "MUMOID User's Guide - A Program for the Identification of Modal Parameters," by S. Rodriguez-Gomez and E. DiPasquale, 9/30/90, (PB91-171298, A04, MF-A01).

NCEER-90-0027 "SARCF-II User's Guide - Seismic Analysis of Reinforced Concrete Frames," by S. Rodriguez-Gomez, Y.S. Chung and C. Meyer, 9/30/90, (PB91-171280, A05, MF-A01).

NCEER-90-0028 "Viscous Dampers: Testing, Modeling and Application in Vibration and Seismic Isolation," by N. Makris and M.C. Constantinou, 12/20/90 (PB91-190561, A06, MF-A01).

NCEER-90-0029 "Soil Effects on Earthquake Ground Motions in the Memphis Area," by H. Hwang, C.S. Lee, K.W. Ng and T.S. Chang, 8/2/90, (PB91-190751, A05, MF-A01).

NCEER-91-0001 "Proceedings from the Third Japan-U.S. Workshop on Earthquake Resistant Design of Lifeline Facilities and Countermeasures for Soil Liquefaction, December 17-19, 1990," edited by T.D. O'Rourke and M. Hamada, 2/1/91, (PB91-179259, A99, MF-A04).

NCEER-91-0002 "Physical Space Solutions of Non-Proportionally Damped Systems," by M. Tong, Z. Liang and G.C. Lee, 1/15/91, (PB91-179242, A04, MF-A01).

NCEER-91-0003 "Seismic Response of Single Piles and Pile Groups," by K. Fan and G. Gazetas, 1/10/91, (PB92-174994, A04, MF-A01).

NCEER-91-0004 "Damping of Structures: Part 1 - Theory of Complex Damping," by Z. Liang and G. Lee, 10/10/91, (PB92-197235, A12, MF-A03).

NCEER-91-0005 "3D-BASIS - Nonlinear Dynamic Analysis of Three Dimensional Base Isolated Structures: Part II," by S. Nagarajaiah, A.M. Reinhorn and M.C. Constantinou, 2/28/91, (PB91-190553, A07, MF-A01). This report has been replaced by NCEER-93-0011.

NCEER-91-0006 "A Multidimensional Hysteretic Model for Plasticity Deforming Metals in Energy Absorbing Devices," by E.J. Graesser and F.A. Cozzarelli, 4/9/91, (PB92-108364, A04, MF-A01).

NCEER-91-0007 "A Framework for Customizable Knowledge-Based Expert Systems with an Application to a KBES for Evaluating the Seismic Resistance of Existing Buildings," by E.G. Ibarra-Anaya and S.J. Fenves, 4/9/91, (PB91-210930, A08, MF-A01).

NCEER-91-0008 "Nonlinear Analysis of Steel Frames with Semi-Rigid Connections Using the Capacity Spectrum Method," by G.G. Deierlein, S-H. Hsieh, Y-J. Shen and J.F. Abel, 7/2/91, (PB92-113828, A05, MF-A01).

NCEER-91-0009 "Earthquake Education Materials for Grades K-12," by K.E.K. Ross, 4/30/91, (PB91-212142, A06, MF-A01). This report has been replaced by NCEER-92-0018.

NCEER-91-0010 "Phase Wave Velocities and Displacement Phase Differences in a Harmonically Oscillating Pile," by N. Makris and G. Gazetas, 7/8/91, (PB92-108356, A04, MF-A01).

NCEER-91-0011 "Dynamic Characteristics of a Full-Size Five-Story Steel Structure and a 2/5 Scale Model," by K.C. Chang, G.C. Yao, G.C. Lee, D.S. Hao and Y.C. Yeh," 7/2/91, (PB93-116648, A06, MF-A02).

NCEER-91-0012 "Seismic Response of a 2/5 Scale Steel Structure with Added Viscoelastic Dampers," by K.C. Chang, T.T. Soong, S-T. Oh and M.L. Lai, 5/17/91, (PB92-110816, A05, MF-A01).

NCEER-91-0013 "Earthquake Response of Retaining Walls; Full-Scale Testing and Computational Modeling," by S. Alampalli and A-W.M. Elgamal, 6/20/91, to be published.

NCEER-91-0014 "3D-BASIS-M: Nonlinear Dynamic Analysis of Multiple Building Base Isolated Structures," by P.C. Tsopelas, S. Nagarajaiah, M.C. Constantinou and A.M. Reinhorn, 5/28/91, (PB92-113885, A09, MF-A02).

NCEER-91-0015 "Evaluation of SEAOC Design Requirements for Sliding Isolated Structures," by D. Theodossiou and M.C. Constantinou, 6/10/91, (PB92-114602, A11, MF-A03).

NCEER-91-0016 "Closed-Loop Modal Testing of a 27-Story Reinforced Concrete Flat Plate-Core Building," by H.R. Somaprasad, T. Toksoy, H. Yoshiyuki and A.E. Aktan, 7/15/91, (PB92-129980, A07, MF-A02).

NCEER-91-0017 "Shake Table Test of a 1/6 Scale Two-Story Lightly Reinforced Concrete Building," by A.G. El-Attar, R.N. White and P. Gergely, 2/28/91, (PB92-222447, A06, MF-A02).

NCEER-91-0018 "Shake Table Test of a 1/8 Scale Three-Story Lightly Reinforced Concrete Building," by A.G. El-Attar, R.N. White and P. Gergely, 2/28/91, (PB93-116630, A08, MF-A02).

NCEER-91-0019 "Transfer Functions for Rigid Rectangular Foundations," by A.S. Veletsos, A.M. Prasad and W.H. Wu, 7/31/91, to be published.

NCEER-91-0020 "Hybrid Control of Seismic-Excited Nonlinear and Inelastic Structural Systems," by J.N. Yang, Z. Li and A. Danielians, 8/1/91, (PB92-143171, A06, MF-A02).

NCEER-91-0021 "The NCEER-91 Earthquake Catalog: Improved Intensity-Based Magnitudes and Recurrence Relations for U.S. Earthquakes East of New Madrid," by L. Seeber and J.G. Armbruster, 8/28/91, (PB92-176742, A06, MF-A02).

NCEER-91-0022 "Proceedings from the Implementation of Earthquake Planning and Education in Schools: The Need for Change - The Roles of the Changemakers," by K.E.K. Ross and F. Winslow, 7/23/91, (PB92-129998, A12, MF-A03).

NCEER-91-0023 "A Study of Reliability-Based Criteria for Seismic Design of Reinforced Concrete Frame Buildings," by H.H.M. Hwang and H-M. Hsu, 8/10/91, (PB92-140235, A09, MF-A02).

NCEER-91-0024 "Experimental Verification of a Number of Structural System Identification Algorithms," by R.G. Ghanem, H. Gavin and M. Shinozuka, 9/18/91, (PB92-176577, A18, MF-A04).

NCEER-91-0025 "Probabilistic Evaluation of Liquefaction Potential," by H.H.M. Hwang and C.S. Lee," 11/25/91, (PB92-143429, A05, MF-A01).

NCEER-91-0026 "Instantaneous Optimal Control for Linear, Nonlinear and Hysteretic Structures - Stable Controllers," by J.N. Yang and Z. Li, 11/15/91, (PB92-163807, A04, MF-A01).

NCEER-91-0027 "Experimental and Theoretical Study of a Sliding Isolation System for Bridges," by M.C. Constantinou, A. Kartoum, A.M. Reinhorn and P. Bradford, 11/15/91, (PB92-176973, A10, MF-A03).

NCEER-92-0001 "Case Studies of Liquefaction and Lifeline Performance During Past Earthquakes, Volume 1: Japanese Case Studies," Edited by M. Hamada and T. O'Rourke, 2/17/92, (PB92-197243, A18, MF-A04).

NCEER-92-0002 "Case Studies of Liquefaction and Lifeline Performance During Past Earthquakes, Volume 2: United States Case Studies," Edited by T. O'Rourke and M. Hamada, 2/17/92, (PB92-197250, A20, MF-A04).

NCEER-92-0003 "Issues in Earthquake Education," Edited by K. Ross, 2/3/92, (PB92-222389, A07, MF-A02).

NCEER-92-0004 "Proceedings from the First U.S. - Japan Workshop on Earthquake Protective Systems for Bridges," Edited by I.G. Buckle, 2/4/92, (PB94-142239, A99, MF-A06).

NCEER-92-0005 "Seismic Ground Motion from a Haskell-Type Source in a Multiple-Layered Half-Space," A.P. Theoharis, G. Deodatis and M. Shinozuka, 1/2/92, to be published.

NCEER-92-0006 "Proceedings from the Site Effects Workshop," Edited by R. Whitman, 2/29/92, (PB92-197201, A04, MF-A01).

NCEER-92-0007 "Engineering Evaluation of Permanent Ground Deformations Due to Seismically-Induced Liquefaction," by M.H. Baziar, R. Dobry and A-W.M. Elgamal, 3/24/92, (PB92-222421, A13, MF-A03).

NCEER-92-0008 "A Procedure for the Seismic Evaluation of Buildings in the Central and Eastern United States," by C.D. Poland and J.O. Malley, 4/2/92, (PB92-222439, A20, MF-A04).

NCEER-92-0009 "Experimental and Analytical Study of a Hybrid Isolation System Using Friction Controllable Sliding Bearings," by M.Q. Feng, S. Fujii and M. Shinozuka, 5/15/92, (PB93-150282, A06, MF-A02).

NCEER-92-0010 "Seismic Resistance of Slab-Column Connections in Existing Non-Ductile Flat-Plate Buildings," by A.J. Durrani and Y. Du, 5/18/92, (PB93-116812, A06, MF-A02).

NCEER-92-0011 "The Hysteretic and Dynamic Behavior of Brick Masonry Walls Upgraded by Ferrocement Coatings Under Cyclic Loading and Strong Simulated Ground Motion," by H. Lee and S.P. Prawel, 5/11/92, to be published.

NCEER-92-0012 "Study of Wire Rope Systems for Seismic Protection of Equipment in Buildings," by G.F. Demetriades, M.C. Constantinou and A.M. Reinhorn, 5/20/92, (PB93-116655, A08, MF-A02).

NCEER-92-0013 "Shape Memory Structural Dampers: Material Properties, Design and Seismic Testing," by P.R. Witting and F.A. Cozzarelli, 5/26/92, (PB93-116663, A05, MF-A01).

NCEER-92-0014 "Longitudinal Permanent Ground Deformation Effects on Buried Continuous Pipelines," by M.J. O'Rourke, and C. Nordberg, 6/15/92, (PB93-116671, A08, MF-A02).

NCEER-92-0015 "A Simulation Method for Stationary Gaussian Random Functions Based on the Sampling Theorem," by M. Grigoriu and S. Balopoulou, 6/11/92, (PB93-127496, A05, MF-A01).

NCEER-92-0016 "Gravity-Load-Designed Reinforced Concrete Buildings: Seismic Evaluation of Existing Construction and Detailing Strategies for Improved Seismic Resistance," by G.W. Hoffmann, S.K. Kunnath, A.M. Reinhorn and J.B. Mander, 7/15/92, (PB94-142007, A08, MF-A02).

NCEER-92-0017 "Observations on Water System and Pipeline Performance in the Limón Area of Costa Rica Due to the April 22, 1991 Earthquake," by M. O'Rourke and D. Ballantyne, 6/30/92, (PB93-126811, A06, MF-A02).

NCEER-92-0018 "Fourth Edition of Earthquake Education Materials for Grades K-12," Edited by K.E.K. Ross, 8/10/92, (PB93-114023, A07, MF-A02).

NCEER-92-0019 "Proceedings from the Fourth Japan-U.S. Workshop on Earthquake Resistant Design of Lifeline Facilities and Countermeasures for Soil Liquefaction," Edited by M. Hamada and T.D. O'Rourke, 8/12/92, (PB93-163939, A99, MF-E11).

NCEER-92-0020 "Active Bracing System: A Full Scale Implementation of Active Control," by A.M. Reinhorn, T.T. Soong, R.C. Lin, M.A. Riley, Y.P. Wang, S. Aizawa and M. Higashino, 8/14/92, (PB93-127512, A06, MF-A02).

NCEER-92-0021 "Empirical Analysis of Horizontal Ground Displacement Generated by Liquefaction-Induced Lateral Spreads," by S.F. Bartlett and T.L. Youd, 8/17/92, (PB93-188241, A06, MF-A02).

NCEER-92-0022 "IDARC Version 3.0: Inelastic Damage Analysis of Reinforced Concrete Structures," by S.K. Kunnath, A.M. Reinhorn and R.F. Lobo, 8/31/92, (PB93-227502, A07, MF-A02).

NCEER-92-0023 "A Semi-Empirical Analysis of Strong-Motion Peaks in Terms of Seismic Source, Propagation Path and Local Site Conditions, by M. Kamiyama, M.J. O'Rourke and R. Flores-Berrones, 9/9/92, (PB93-150266, A08, MF-A02).

NCEER-92-0024 "Seismic Behavior of Reinforced Concrete Frame Structures with Nonductile Details, Part I: Summary of Experimental Findings of Full Scale Beam-Column Joint Tests," by A. Beres, R.N. White and P. Gergely, 9/30/92, (PB93-227783, A05, MF-A01).

NCEER-92-0025 "Experimental Results of Repaired and Retrofitted Beam-Column Joint Tests in Lightly Reinforced Concrete Frame Buildings," by A. Beres, S. El-Borgi, R.N. White and P. Gergely, 10/29/92, (PB93-227791, A05, MF-A01).

NCEER-92-0026 "A Generalization of Optimal Control Theory: Linear and Nonlinear Structures," by J.N. Yang, Z. Li and S. Vongchavalitkul, 11/2/92, (PB93-188621, A05, MF-A01).

NCEER-92-0027 "Seismic Resistance of Reinforced Concrete Frame Structures Designed Only for Gravity Loads: Part I - Design and Properties of a One-Third Scale Model Structure," by J.M. Bracci, A.M. Reinhorn and J.B. Mander, 12/1/92, (PB94-104502, A08, MF-A02).

NCEER-92-0028 "Seismic Resistance of Reinforced Concrete Frame Structures Designed Only for Gravity Loads: Part II - Experimental Performance of Subassemblages," by L.E. Aycardi, J.B. Mander and A.M. Reinhorn, 12/1/92, (PB94-104510, A08, MF-A02).

NCEER-92-0029 "Seismic Resistance of Reinforced Concrete Frame Structures Designed Only for Gravity Loads: Part III - Experimental Performance and Analytical Study of a Structural Model," by J.M. Bracci, A.M. Reinhorn and J.B. Mander, 12/1/92, (PB93-227528, A09, MF-A01).

NCEER-92-0030 "Evaluation of Seismic Retrofit of Reinforced Concrete Frame Structures: Part I - Experimental Performance of Retrofitted Subassemblages," by D. Choudhuri, J.B. Mander and A.M. Reinhorn, 12/8/92, (PB93-198307, A07, MF-A02).

NCEER-92-0031 "Evaluation of Seismic Retrofit of Reinforced Concrete Frame Structures: Part II - Experimental Performance and Analytical Study of a Retrofitted Structural Model," by J.M. Bracci, A.M. Reinhorn and J.B. Mander, 12/8/92, (PB93-198315, A09, MF-A03).

NCEER-92-0032 "Experimental and Analytical Investigation of Seismic Response of Structures with Supplemental Fluid Viscous Dampers," by M.C. Constantinou and M.D. Symans, 12/21/92, (PB93-191435, A10, MF-A03).

NCEER-92-0033 "Reconnaissance Report on the Cairo, Egypt Earthquake of October 12, 1992," by M. Khater, 12/23/92, (PB93-188621, A03, MF-A01).

NCEER-92-0034 "Low-Level Dynamic Characteristics of Four Tall Flat-Plate Buildings in New York City," by H. Gavin, S. Yuan, J. Grossman, E. Pekelis and K. Jacob, 12/28/92, (PB93-188217, A07, MF-A02).

NCEER-93-0001 "An Experimental Study on the Seismic Performance of Brick-Infilled Steel Frames With and Without Retrofit," by J.B. Mander, B. Nair, K. Wojtkowski and J. Ma, 1/29/93, (PB93-227510, A07, MF-A02).

NCEER-93-0002 "Social Accounting for Disaster Preparedness and Recovery Planning," by S. Cole, E. Pantoja and V. Razak, 2/22/93, (PB94-142114, A12, MF-A03).

NCEER-93-0003 "Assessment of 1991 NEHRP Provisions for Nonstructural Components and Recommended Revisions," by T.T. Soong, G. Chen, Z. Wu, R-H. Zhang and M. Grigoriu, 3/1/93, (PB93-188639, A06, MF-A02).

NCEER-93-0004 "Evaluation of Static and Response Spectrum Analysis Procedures of SEAOC/UBC for Seismic Isolated Structures," by C.W. Winters and M.C. Constantinou, 3/23/93, (PB93-198299, A10, MF-A03).

NCEER-93-0005 "Earthquakes in the Northeast - Are We Ignoring the Hazard? A Workshop on Earthquake Science and Safety for Educators," edited by K.E.K. Ross, 4/2/93, (PB94-103066, A09, MF-A02).

NCEER-93-0006 "Inelastic Response of Reinforced Concrete Structures with Viscoelastic Braces," by R.F. Lobo, J.M. Bracci, K.L. Shen, A.M. Reinhorn and T.T. Soong, 4/5/93, (PB93-227486, A05, MF-A02).

NCEER-93-0007 "Seismic Testing of Installation Methods for Computers and Data Processing Equipment," by K. Kosar, T.T. Soong, K.L. Shen, J.A. HoLung and Y.K. Lin, 4/12/93, (PB93-198299, A07, MF-A02).

NCEER-93-0008 "Retrofit of Reinforced Concrete Frames Using Added Dampers," by A. Reinhorn, M. Constantinou and C. Li, to be published.

NCEER-93-0009 "Seismic Behavior and Design Guidelines for Steel Frame Structures with Added Viscoelastic Dampers," by K.C. Chang, M.L. Lai, T.T. Soong, D.S. Hao and Y.C. Yeh, 5/1/93, (PB94-141959, A07, MF-A02).

NCEER-93-0010 "Seismic Performance of Shear-Critical Reinforced Concrete Bridge Piers," by J.B. Mander, S.M. Waheed, M.T.A. Chaudhary and S.S. Chen, 5/12/93, (PB93-227494, A08, MF-A02).

NCEER-93-0011 "3D-BASIS-TABS: Computer Program for Nonlinear Dynamic Analysis of Three Dimensional Base Isolated Structures," by S. Nagarajaiah, C. Li, A.M. Reinhorn and M.C. Constantinou, 8/2/93, (PB94-141819, A09, MF-A02).

NCEER-93-0012 "Effects of Hydrocarbon Spills from an Oil Pipeline Break on Ground Water," by O.J. Helweg and H.H.M. Hwang, 8/3/93, (PB94-141942, A06, MF-A02).

NCEER-93-0013 "Simplified Procedures for Seismic Design of Nonstructural Components and Assessment of Current Code Provisions," by M.P. Singh, L.E. Suarez, E.E. Matheu and G.O. Maldonado, 8/4/93, (PB94-141827, A09, MF-A02).

NCEER-93-0014 "An Energy Approach to Seismic Analysis and Design of Secondary Systems," by G. Chen and T.T. Soong, 8/6/93, (PB94-142767, A11, MF-A03).

NCEER-93-0015 "Proceedings from School Sites: Becoming Prepared for Earthquakes - Commemorating the Third Anniversary of the Loma Prieta Earthquake," Edited by F.E. Winslow and K.E.K. Ross, 8/16/93, (PB94-154275, A16, MF-A02).

NCEER-93-0016 "Reconnaissance Report of Damage to Historic Monuments in Cairo, Egypt Following the October 12, 1992 Dahshur Earthquake," by D. Sykora, D. Look, G. Croci, E. Karaesmen and E. Karaesmen, 8/19/93, (PB94-142221, A08, MF-A02).

NCEER-93-0017 "The Island of Guam Earthquake of August 8, 1993," by S.W. Swan and S.K. Harris, 9/30/93, (PB94-141843, A04, MF-A01).

NCEER-93-0018 "Engineering Aspects of the October 12, 1992 Egyptian Earthquake," by A.W. Elgamal, M. Amer, K. Adalier and A. Abul-Fadl, 10/7/93, (PB94-141983, A05, MF-A01).

NCEER-93-0019 "Development of an Earthquake Motion Simulator and its Application in Dynamic Centrifuge Testing," by I. Krstelj, Supervised by J.H. Prevost, 10/23/93, (PB94-181773, A-10, MF-A03).

NCEER-93-0020 "NCEER-Taisei Corporation Research Program on Sliding Seismic Isolation Systems for Bridges: Experimental and Analytical Study of a Friction Pendulum System (FPS)," by M.C. Constantinou, P. Tsopelas, Y-S. Kim and S. Okamoto, 11/1/93, (PB94-142775, A08, MF-A02).

NCEER-93-0021 "Finite Element Modeling of Elastomeric Seismic Isolation Bearings," by L.J. Billings, Supervised by R. Shepherd, 11/8/93, to be published.

NCEER-93-0022 "Seismic Vulnerability of Equipment in Critical Facilities: Life-Safety and Operational Consequences," by K. Porter, G.S. Johnson, M.M. Zadeh, C. Scawthorn and S. Eder, 11/24/93, (PB94-181765, A16, MF-A03).

NCEER-93-0023 "Hokkaido Nansei-oki, Japan Earthquake of July 12, 1993, by P.I. Yanev and C.R. Scawthorn, 12/23/93, (PB94-181500, A07, MF-A01).

NCEER-94-0001 "An Evaluation of Seismic Serviceability of Water Supply Networks with Application to the San Francisco Auxiliary Water Supply System," by I. Markov, Supervised by M. Grigoriu and T. O'Rourke, 1/21/94, (PB94-204013, A07, MF-A02).

NCEER-94-0002 "NCEER-Taisei Corporation Research Program on Sliding Seismic Isolation Systems for Bridges: Experimental and Analytical Study of Systems Consisting of Sliding Bearings, Rubber Restoring Force Devices and Fluid Dampers," Volumes I and II, by P. Tsopelas, S. Okamoto, M.C. Constantinou, D. Ozaki and S. Fujii, 2/4/94, (PB94-181740, A09, MF-A02 and PB94-181757, A12, MF-A03).

NCEER-94-0003 "A Markov Model for Local and Global Damage Indices in Seismic Analysis," by S. Rahman and M. Grigoriu, 2/18/94, (PB94-206000, A12, MF-A03).

NCEER-94-0004 "Proceedings from the NCEER Workshop on Seismic Response of Masonry Infills," edited by D.P. Abrams, 3/1/94, (PB94-180783, A07, MF-A02).

NCEER-94-0005 "The Northridge, California Earthquake of January 17, 1994: General Reconnaissance Report," edited by J.D. Goltz, 3/11/94, (PB193943, A10, MF-A03).

NCEER-94-0006 "Seismic Energy Based Fatigue Damage Analysis of Bridge Columns: Part I - Evaluation of Seismic Capacity," by G.A. Chang and J.B. Mander, 3/14/94, (PB94-219185, A11, MF-A03).

NCEER-94-0007 "Seismic Isolation of Multi-Story Frame Structures Using Spherical Sliding Isolation Systems," by T.M. Al-Hussaini, V.A. Zayas and M.C. Constantinou, 3/17/94, (PB193745, A09, MF-A02).

NCEER-94-0008 "The Northridge, California Earthquake of January 17, 1994: Performance of Highway Bridges," edited by I.G. Buckle, 3/24/94, (PB94-193851, A06, MF-A02).

NCEER-94-0009 "Proceedings of the Third U.S.-Japan Workshop on Earthquake Protective Systems for Bridges," edited by I.G. Buckle and I. Friedland, 3/31/94, (PB94-195815, A99, MF-A06).

NCEER-94-0010 "3D-BASIS-ME: Computer Program for Nonlinear Dynamic Analysis of Seismically Isolated Single and Multiple Structures and Liquid Storage Tanks," by P.C. Tsopelas, M.C. Constantinou and A.M. Reinhorn, 4/12/94, (PB94-204922, A09, MF-A02).

NCEER-94-0011 "The Northridge, California Earthquake of January 17, 1994: Performance of Gas Transmission Pipelines," by T.D. O'Rourke and M.C. Palmer, 5/16/94, (PB94-204989, A05, MF-A01).

NCEER-94-0012 "Feasibility Study of Replacement Procedures and Earthquake Performance Related to Gas Transmission Pipelines," by T.D. O'Rourke and M.C. Palmer, 5/25/94, (PB94-206638, A09, MF-A02).

NCEER-94-0013 "Seismic Energy Based Fatigue Damage Analysis of Bridge Columns: Part II - Evaluation of Seismic Demand," by G.A. Chang and J.B. Mander, 6/1/94, (PB95-18106, A08, MF-A02).

NCEER-94-0014 "NCEER-Taisei Corporation Research Program on Sliding Seismic Isolation Systems for Bridges: Experimental and Analytical Study of a System Consisting of Sliding Bearings and Fluid Restoring Force/Damping Devices," by P. Tsopelas and M.C. Constantinou, 6/13/94, (PB94-219144, A10, MF-A03).

NCEER-94-0015 "Generation of Hazard-Consistent Fragility Curves for Seismic Loss Estimation Studies," by H. Hwang and J-R. Huo, 6/14/94, (PB95-181996, A09, MF-A02).

NCEER-94-0016 "Seismic Study of Building Frames with Added Energy-Absorbing Devices," by W.S. Pong, C.S. Tsai and G.C. Lee, 6/20/94, (PB94-219136, A10, A03).

NCEER-94-0017 "Sliding Mode Control for Seismic-Excited Linear and Nonlinear Civil Engineering Structures," by J. Yang, J. Wu, A. Agrawal and Z. Li, 6/21/94, (PB95-138483, A06, MF-A02).

NCEER-94-0018 "3D-BASIS-TABS Version 2.0: Computer Program for Nonlinear Dynamic Analysis of Three Dimensional Base Isolated Structures," by A.M. Reinhorn, S. Nagarajaiah, M.C. Constantinou, P. Tsopelas and R. Li, 6/22/94, (PB95-182176, A08, MF-A02).

NCEER-94-0019 "Proceedings of the International Workshop on Civil Infrastructure Systems: Application of Intelligent Systems and Advanced Materials on Bridge Systems," Edited by G.C. Lee and K.C. Chang, 7/18/94, (PB95-252474, A20, MF-A04).

NCEER-94-0020 "Study of Seismic Isolation Systems for Computer Floors," by V. Lambrou and M.C. Constantinou, 7/19/94, (PB95-138533, A10, MF-A03).

NCEER-94-0021 "Proceedings of the U.S.-Italian Workshop on Guidelines for Seismic Evaluation and Rehabilitation of Unreinforced Masonry Buildings," Edited by D.P. Abrams and G.M. Calvi, 7/20/94, (PB95-138749, A13, MF-A03).

NCEER-94-0022 "NCEER-Taisei Corporation Research Program on Sliding Seismic Isolation Systems for Bridges: Experimental and Analytical Study of a System Consisting of Lubricated PTFE Sliding Bearings and Mild Steel Dampers," by P. Tsopelas and M.C. Constantinou, 7/22/94, (PB95-182184, A08, MF-A02).

NCEER-94-0023 "Development of Reliability-Based Design Criteria for Buildings Under Seismic Load," by Y.K. Wen, H. Hwang and M. Shinozuka, 8/1/94, (PB95-211934, A08, MF-A02).

NCEER-94-0024 "Experimental Verification of Acceleration Feedback Control Strategies for an Active Tendon System," by S.J. Dyke, B.F. Spencer, Jr., P. Quast, M.K. Sain, D.C. Kaspari, Jr. and T.T. Soong, 8/29/94, (PB95-212320, A05, MF-A01).

NCEER-94-0025 "Seismic Retrofitting Manual for Highway Bridges," Edited by I.G. Buckle and I.F. Friedland, published by the Federal Highway Administration (PB95-212676, A15, MF-A03).

NCEER-94-0026 "Proceedings from the Fifth U.S.-Japan Workshop on Earthquake Resistant Design of Lifeline Facilities and Countermeasures Against Soil Liquefaction," Edited by T.D. O'Rourke and M. Hamada, 11/7/94, (PB95-220802, A99, MF-E08).

NCEER-95-0001 "Experimental and Analytical Investigation of Seismic Retrofit of Structures with Supplemental Damping: Part 1 - Fluid Viscous Damping Devices," by A.M. Reinhorn, C. Li and M.C. Constantinou, 1/3/95, (PB95-266599, A09, MF-A02).

NCEER-95-0002 "Experimental and Analytical Study of Low-Cycle Fatigue Behavior of Semi-Rigid Top-And-Seat Angle Connections," by G. Pekcan, J.B. Mander and S.S. Chen, 1/5/95, (PB95-220042, A07, MF-A02).

NCEER-95-0003 "NCEER-ATC Joint Study on Fragility of Buildings," by T. Anagnos, C. Rojahn and A.S. Kiremidjian, 1/20/95, (PB95-220026, A06, MF-A02).

NCEER-95-0004 "Nonlinear Control Algorithms for Peak Response Reduction," by Z. Wu, T.T. Soong, V. Gattulli and R.C. Lin, 2/16/95, (PB95-220349, A05, MF-A01).

NCEER-95-0005 "Pipeline Replacement Feasibility Study: A Methodology for Minimizing Seismic and Corrosion Risks to Underground Natural Gas Pipelines," by R.T. Eguchi, H.A. Seligson and D.G. Honegger, 3/2/95, (PB95-252326, A06, MF-A02).

NCEER-95-0006 "Evaluation of Seismic Performance of an 11-Story Frame Building During the 1994 Northridge Earthquake," by F. Naeim, R. DiSulio, K. Benuska, A. Reinhorn and C. Li, to be published.

NCEER-95-0007 "Prioritization of Bridges for Seismic Retrofitting," by N. Basöz and A.S. Kiremidjian, 4/24/95, (PB95-252300, A08, MF-A02).

NCEER-95-0008 "Method for Developing Motion Damage Relationships for Reinforced Concrete Frames," by A. Singhal and A.S. Kiremidjian, 5/11/95, (PB95-266607, A06, MF-A02).

NCEER-95-0009 "Experimental and Analytical Investigation of Seismic Retrofit of Structures with Supplemental Damping: Part II - Friction Devices," by C. Li and A.M. Reinhorn, 7/6/95, (PB96-128087, A11, MF-A03).

NCEER-95-0010 "Experimental Performance and Analytical Study of a Non-Ductile Reinforced Concrete Frame Structure Retrofitted with Elastomeric Spring Dampers," by G. Pekcan, J.B. Mander and S.S. Chen, 7/14/95, (PB96-137161, A08, MF-A02).

NCEER-95-0011 "Development and Experimental Study of Semi-Active Fluid Damping Devices for Seismic Protection of Structures," by M.D. Symans and M.C. Constantinou, 8/3/95, (PB96-136940, A23, MF-A04).

NCEER-95-0012 "Real-Time Structural Parameter Modification (RSPM): Development of Innervated Structures," by Z. Liang, M. Tong and G.C. Lee, 4/11/95, (PB96-137153, A06, MF-A01).

NCEER-95-0013 "Experimental and Analytical Investigation of Seismic Retrofit of Structures with Supplemental Damping: Part III - Viscous Damping Walls," by A.M. Reinhorn and C. Li, 10/1/95, (PB96-176409, A11, MF-A03).

NCEER-95-0014 "Seismic Fragility Analysis of Equipment and Structures in a Memphis Electric Substation," by J-R. Huo and H.H.M. Hwang, (PB96-128087, A09, MF-A02), 8/10/95.

NCEER-95-0015 "The Hanshin-Awaji Earthquake of January 17, 1995: Performance of Lifelines," Edited by M. Shinozuka, 11/3/95, (PB96-176383, A15, MF-A03).

NCEER-95-0016 "Highway Culvert Performance During Earthquakes," by T.L. Youd and C.J. Beckman, available as NCEER-96-0015.

NCEER-95-0017 "The Hanshin-Awaji Earthquake of January 17, 1995: Performance of Highway Bridges," Edited by I.G. Buckle, 12/1/95, to be published.

NCEER-95-0018 "Modeling of Masonry Infill Panels for Structural Analysis," by A.M. Reinhorn, A. Madan, R.E. Valles, Y. Reichmann and J.B. Mander, 12/8/95.

NCEER-95-0019 "Optimal Polynomial Control for Linear and Nonlinear Structures," by A.K. Agrawal and J.N. Yang, 12/11/95, (PB96-168737, A07, MF-A02).

NCEER-95-0020 "Retrofit of Non-Ductile Reinforced Concrete Frames Using Friction Dampers," by R.S. Rao, P. Gergely and R.N. White, 12/22/95, (PB97-133508, A10, MF-A02).

NCEER-95-0021 "Parametric Results for Seismic Response of Pile-Supported Bridge Bents," by G. Mylonakis, A. Nikolaou and G. Gazetas, 12/22/95, (PB97-100242, A12, MF-A03).

NCEER-95-0022 "Kinematic Bending Moments in Seismically Stressed Piles," by A. Nikolaou, G. Mylonakis and G. Gazetas, 12/23/95.

NCEER-96-0001 "Dynamic Response of Unreinforced Masonry Buildings with Flexible Diaphragms," by A.C. Costley and D.P. Abrams," 10/10/96.

NCEER-96-0002 "State of the Art Review: Foundations and Retaining Structures," by I. Po Lam, to be published.

NCEER-96-0003 "Ductility of Rectangular Reinforced Concrete Bridge Columns with Moderate Confinement," by N. Wehbe, M. Saiidi, D. Sanders and B. Douglas, 11/7/96, (PB97-133557, A06, MF-A02).

NCEER-96-0004 "Proceedings of the Long-Span Bridge Seismic Research Workshop," edited by I.G. Buckle and I.M. Friedland, to be published.

NCEER-96-0005 "Establish Representative Pier Types for Comprehensive Study: Eastern United States," by J. Kulicki and Z. Prucz, 5/28/96.

NCEER-96-0006 "Establish Representative Pier Types for Comprehensive Study: Western United States," by R. Imbsen, R.A. Schamber and T.A. Osterkamp, 5/28/96.

NCEER-96-0007 "Nonlinear Control Techniques for Dynamical Systems with Uncertain Parameters," by R.G. Ghanem and M.I. Bujakov, 5/27/96, (PB97-100259, A17, MF-A03).

NCEER-96-0008 "Seismic Evaluation of a 30-Year Old Non-Ductile Highway Bridge Pier and Its Retrofit," by J.B. Mander, B. Mahmoodzadegan, S. Bhadra and S.S. Chen, 5/31/96.

NCEER-96-0009 "Seismic Performance of a Model Reinforced Concrete Bridge Pier Before and After Retrofit," by J.B. Mander, J.H. Kim and C.A. Ligozio, 5/31/96.

NCEER-96-0010 "IDARC2D Version 4.0: A Computer Program for the Inelastic Damage Analysis of Buildings," by R.E. Valles, A.M. Reinhorn, S.K. Kunnath, C. Li and A. Madan, 6/3/96, (PB97-100234, A17, MF-A03).

NCEER-96-0011 "Estimation of the Economic Impact of Multiple Lifeline Disruption: Memphis Light, Gas and Water Division Case Study," by S.E. Chang, H.A. Seligson and R.T. Eguchi, 8/16/96, (PB97-133490, A11, MF-A03).

NCEER-96-0012 "Proceedings from the Sixth Japan-U.S. Workshop on Earthquake Resistant Design of Lifeline Facilities and Countermeasures Against Soil Liquefaction, Edited by M. Hamada and T. O'Rourke, 9/11/96, (PB97-133581, A99, MF-A06).

NCEER-96-0013 "Chemical Hazards, Mitigation and Preparedness in Areas of High Seismic Risk: A Methodology for Estimating the Risk of Post-Earthquake Hazardous Materials Release," by H.A. Seligson, R.T. Eguchi, K.J. Tierney and K. Richmond, 11/7/96.

NCEER-96-0014 "Response of Steel Bridge Bearings to Reversed Cyclic Loading," by J.B. Mander, D-K. Kim, S.S. Chen and G.J. Premus, 11/13/96, (PB97-140735, A12, MF-A03).

NCEER-96-0015 "Highway Culvert Performance During Past Earthquakes," by T.L. Youd and C.J. Beckman, 11/25/96, (PB97-133532, A06, MF-A01).

NCEER-97-0001 "Evaluation, Prevention and Mitigation of Pounding Effects in Building Structures," by R.E. Valles and A.M. Reinhorn, 2/20/97, (PB97-159552, A14, MF-A03).

NCEER-97-0002 "Seismic Design Criteria for Bridges and Other Highway Structures," by C. Rojahn, R. Mayes, D.G. Anderson, J. Clark, J.H. Hom, R.V. Nutt and M.J. O'Rourke, 4/30/97, (PB97-194658, A06, MF-A03).

NCEER-97-0003 "Proceedings of the U.S.-Italian Workshop on Seismic Evaluation and Retrofit," Edited by D.P. Abrams and G.M. Calvi, 3/19/97, (PB97-194666, A13, MF-A03).

NCEER-97-0004 "Investigation of Seismic Response of Buildings with Linear and Nonlinear Fluid Viscous Dampers," by A.A. Seleemah and M.C. Constantinou, 5/21/97, (PB98-109002, A15, MF-A03).

NCEER-97-0005 "Proceedings of the Workshop on Earthquake Engineering Frontiers in Transportation Facilities," edited by G.C. Lee and I.M. Friedland, 8/29/97.

NCEER-97-0006 "Cumulative Seismic Damage of Reinforced Concrete Bridge Piers," by S.K. Kunnath, A. El-Bahy, A. Taylor and W. Stone, 9/2/97, (PB98-108814, A11, MF-A03).

NCEER-97-0007 "Structural Details to Accommodate Seismic Movements of Highway Bridges and Retaining Walls," by R.A. Imbsen, R.A. Schamber, E. Thorkildsen, A. Kartoum, B.T. Martin, T.N. Rosser and J.M. Kulicki, 9/3/97.

NCEER-97-0008 "A Method for Earthquake Motion-Damage Relationships with Application to Reinforced Concrete Frames," by A. Singhal and A.S. Kiremidjian, 9/10/97, (PB98-108988, A13, MF-A03).

NCEER-97-0009 "Seismic Analysis and Design of Bridge Abutments Considering Sliding and Rotation," by K. Fishman and R. Richards, Jr., 9/15/97, (PB98-108897, A06, MF-A02).

NCEER-97-0010 "Proceedings of the FHWA/NCEER Workshop on the National Representation of Seismic Ground Motion for New and Existing Highway Facilities," edited by I.M. Friedland, M.S. Power and R.L. Mayes, 9/22/97.

NCEER-97-0011 "Seismic Analysis for Design or Retrofit of Gravity Bridge Abutments," by K.L. Fishman, R. Richards, Jr. and R.C. Divito, 10/2/97.

NCEER-97-0012 "Evaluation of Simplified Methods of Analysis for Yielding Structures," by P. Tsopelas, M.C. Constantinou, C.A. Kircher and A.S. Whittaker, 10/31/97.

NCEER-97-0013 "Seismic Design of Bridge Columns Based on Control and Repairability of Damage," by C-T. Cheng and J.B. Mander, 12/8/97.

NCEER-97-0014 "Seismic Resistance of Bridge Piers Based on Damage Avoidance Design," by J.B. Mander and C-T. Cheng, 12/10/97.

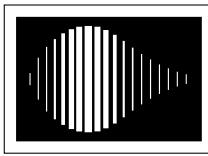

NATIONAL CENTER FOR EARTHQUAKE ENGINEERING RESEARCH

Headquartered at the State University of New York at Buffalo

State University of New York at Buffalo
Red Jacket Quadrangle
Buffalo, New York 14261
Telephone: 716/645-3391
FAX: 716/645-3399

ISSN 1088-3800